



UNIVERSIDAD NACIONAL AUTÓNOMA DE MÉXICO

PROGRAMA DE MAESTRÍA Y DOCTORADO EN INGENIERÍA

INGENIERÍA AMBIENTAL – RESIDUOS SÓLIDOS

IDENTIFICATION OF MICROBIAL INDICATORS FOR MONITORING ANAEROBIC
DIGESTION PROCESSES FED WITH ORGANIC SOLID WASTE

TESIS

QUE PARA OPTAR POR EL GRADO DE:

DOCTOR EN INGENIERÍA

PRESENTA:

M.I. JONATHAN FRANCISCO CORTEZ CERVANTES

DIRECTORES DE TESIS

DR. JULIÁN CARRILLO REYES, INSTITUTO DE INGENIERÍA

DR. IVÁN MORENO ANDRADE, INSTITUTO DE INGENIERÍA

COMITÉ TUTORAL

DRA. ANA ELENA ESCALANTE HERNÁNDEZ, INSTITUTO DE ECOLOGÍA

DR. DANIEL DE LOS COBOS VASCONCELOS, INSTITUTO DE INGENIERÍA

SANTIAGO DE QUERÉTARO, QUERÉTARO, ENERO 2025



Universidad Nacional
Autónoma de México

Dirección General de Bibliotecas de la UNAM

Biblioteca Central



UNAM – Dirección General de Bibliotecas
Tesis Digitales
Restricciones de uso

DERECHOS RESERVADOS ©
PROHIBIDA SU REPRODUCCIÓN TOTAL O PARCIAL

Todo el material contenido en esta tesis esta protegido por la Ley Federal del Derecho de Autor (LFDA) de los Estados Unidos Mexicanos (México).

El uso de imágenes, fragmentos de videos, y demás material que sea objeto de protección de los derechos de autor, será exclusivamente para fines educativos e informativos y deberá citar la fuente donde la obtuvo mencionando el autor o autores. Cualquier uso distinto como el lucro, reproducción, edición o modificación, será perseguido y sancionado por el respectivo titular de los Derechos de Autor.

PROTESTA UNIVERSITARIA DE INTEGRIDAD Y HONESTIDAD
ACADÉMICA Y PROFESIONAL

De conformidad con lo dispuesto en los artículos 87, fracción V, del Estatuto General, 68, primer párrafo, del Reglamento General de Estudios Universitarios y 26, fracción 1, y 35 del Reglamento General de Exámenes, me comprometo en todo tiempo a honrar a la Institución y a cumplir con los principios establecidos en el Código de Ética de la Universidad Nacional Autónoma de México, especialmente con los de integridad y honestidad académica.

De acuerdo con lo anterior, manifiesto que el trabajo escrito titulado "*Identification of microbial indicators for monitoring anaerobic processes fed with organic solid waste*" que presenté para obtener el grado de Doctorado es original, de mi autoría y lo realicé con el rigor metodológico exigido por mi programa de posgrado, citando las fuentes de ideas, textos, imágenes, gráficos u otro tipo de obras empleadas para su desarrollo.

En consecuencia, acepto que la falta de cumplimiento de las disposiciones reglamentarias y normativas de la Universidad, en particular las ya referidas en el Código de Ética, llevará a la nulidad de los actos de carácter académico administrativo del proceso de graduación.

Atentamente



FIRMA

Jonathan Francisco Cortez Cervantes
No. Cuenta UNAM 518002615.

JURADO ASIGNADO:

Presidente: Dra. Ana Elena Escalante Hernández

Secretario: Dr. Daniel de los Cobos Vasconcelos

1^{er}. Vocal: Dra. Claudia Etchebehere Arenas

2^{do}. Vocal: Dr. Iván Moreno Andrade

3^{er}. Vocal: Dr. Julián Carrillo Reyes

LUGAR DONDE SE REALIZÓ LA TESIS:

Laboratorio de Investigación en Procesos Avanzados de Tratamiento de Aguas (LIPATA).

Unidad Académica Juriquilla, Instituto de Ingeniería, Universidad Nacional Autónoma de México,
Campus Juriquilla, Blvd. Juriquilla 3001, 76230 Querétaro, México.

TUTORES DE TESIS:

DR. JULIÁN CARRILLO REYES



FIRMA

DR. IVÁN MORENO ANDRADE



FIRMA

Institutional Acknowledgments

This work was developed in the Laboratory for Research in Advanced Water Treatment Processes at the Juriquilla Academic Unit of the Institute of Engineering of the National Autonomous University of Mexico under the direction of Dr. Julián Carrillo Reyes and Dr. Iván Moreno Andrade.

The financial support of the DGAPA-UNAM is gratefully acknowledged through the PAPIIT IN105423 and IN102722 projects is acknowledged. We acknowledge the scholarship from the National Council of Science and Technology (CONAHCYT, Mexico) for doctoral studies.

The technical support of the M. in C. Gloria Moreno Rodríguez, L.I. Angel Avizua Hernández Huerta and M. in B. Jaime Pérez Trevilla in the physicochemical parameters quantification techniques, computational systems and laboratory equipment of this thesis is also acknowledged.

The author acknowledges the financial support of the Interdisciplinary Research Group at the UNAM Engineering Institute (Grupo Interdisciplinario de Investigación del Instituto de Ingeniería de la UNAM), under the project "Cambio de paradigma: residuos como materia prima para conciliar el eje agua-energía-ambiente-seguridad alimentaria" and we thank for its support.



AGRADECIMIENTOS

Quisiera expresar mi más sincero agradecimiento a todos quienes conforman la estructura académica y organizativa de la comunidad de LIPATA. Mis agradecimientos al Lic. Javier, responsable del área administrativa; al Lic. Ángel, en el área computacional; al Mtro. Jaime, encargado de la instrumentación del equipo de laboratorio; a los investigadores, Dra. Idania, Dr. Francisco, Dr. Alejandro, Dr. Germán, Dr. Miguel, y Dra. Karla; y a la Mtra. Gloria, quien coordina el laboratorio. También, extendiendo mi especial gratitud a mis tutores principales, Dr. Iván y Dr. Julián, por sus valiosos consejos y observaciones. Todos ustedes fueron pilares fundamentales que permitieron que completara esta tesis de posgrado en tiempo y forma.

También dar gracias por el apoyo emocional e incondicional que aportaron mis familiares, principalmente mi mamá Edith y mi papá Ramiro. Ellos fueron una fuente de luz en un camino que tal vez habría sido más complejo y oscuro. Quizá no habría descubierto que un posgrado doctoral puede ser un trayecto relativamente sencillo y cómodo, cuando se cuenta con el apoyo incondicional de un núcleo cercano a la persona.

Asimismo, quiero expresar mi agradecimiento a todos mis compañeros de la comunidad estudiantil de la Unidad Académica Juriquilla. Cada uno de ustedes tiene una historia única y maravillosa que contar, y generosamente me la compartieron, brindándome experiencias valiosas que contribuyeron tanto a mi desarrollo profesional como personal. En especial a la comunidad de LIPATA, personas tan abiertas que te permiten incrustarse fácilmente en una gama de experiencias tan diversas, que hicieron por 7 años, un lapso de aprendizaje y de los más disfrutables de mi vida (hasta el momento). Sigamos adelante

Por último, un agradecimiento a él todo, que hace posible este proceso de transformación personal, que me permite mantener una visión de vida desde una perspectiva de disfrute, aprendizaje y sencillez, apreciando cada momento sin etiquetas ni conceptos. Gracias vida.

SUMMARY	1
CHAPTER 1. Theoretical Framework	13
1.1. Anaerobic digestion process of organic solid waste	13
1.2. Key challenges during OFMSW and FW digestion	15
1.2.1. Ammonia inhibition	15
1.2.2. Over-acidification	17
1.2.3. Foaming	19
1.2.4. H ₂ S generation	20
1.3. Microbial indicators.....	20
1.3.1. Diversity indices	21
1.3.2. Key taxa and genes	23
1.4. Attributes of microbial indicators	27
1.4.1. Universality.....	29
1.4.2. Significant changes	29
1.4.3. Keystones.....	30
1.4.4. Early warning signs.....	31
1.4.5. Key metabolic roles	32
1.5. Hypotheses and objectives.....	34
1.5.1. Hypotheses.....	34
1.5.2. General objective	34
1.5.3. Specific objectives	34
CHAPTER 2. Research design	35
CHAPTER 3. Identifying reliable microbial indicators in anaerobic digestion of organic solid waste: Insights from a meta-analysis	38
3.1. Abstract.....	38
3.2. Introduction.....	39
3.3. Material and methods.....	42
3.3.1. Data collection	42
3.3.2. 16S rRNA sequencing datasets processing	42
3.3.3. Categorization of samples according to CH ₄ yield.	43
3.3.4. Diversity analysis.....	44
3.3.5. Selecting the core microbiome.....	44
3.3.6. Statistical analysis.....	48
3.3.6.1. Key diversity indexes	48
3.3.6.2. Universality	48
3.3.6.3. Robust fold change	49
3.3.6.4. Predictive capability	50
3.3.6.5. Relevant roles in inhibition.....	50
3.4. Results and discussion	52
3.4.1. Sample selection, processing, and categorization	52
3.4.2. Microbial community diversity in response to the methane yield categories	53
3.4.3. The Core Microbiome: Key Players in AD.....	56
3.4.4. Association between differentially abundant taxa and methane yield categories	57

3.4.5. Key alpha indices and key taxa can predict the CH ₄ yield.....	59
3.4.6. Correlations between key taxa and AD by-products.....	59
3.4.6.1. Key taxa from the core microbiome	59
3.4.6.2 Key taxa from the whole microbial community	60
3.4.7. Applications of reliable MI: Detecting key challenges	61
3.5. Conclusions.....	64
CHAPTER 4. Ammonia as a key inhibitory compound in food waste digestion: Challenges of heterogeneous feedstock composition.....	65
4.1. Abstract.....	65
4.2. Introduction.....	66
4.3. Material and Methods	67
4.3.1. Inoculum and feedstock	67
4.3.2. Experimental design.....	67
4.3.3. Batch assays.....	68
4.3.4. Stastitcal analysis	68
4.4. Results and discussion	69
4.4.1. The effects of ammonia, greases and sulfates on CH ₄ yield	69
4.5 Conclusions.....	72
CHAPTER 5. Suitable microbial indicators for detecting ammonia inhibition in anaerobic digestion of food wastes.....	73
5.1. Abstract.....	73
5.2. Introduction.....	74
5.3. Material and methods.....	77
5.3.1. Batch assay for identifying ammonia inhibition levels	77
5.3.1.1. Inoculum and substrate	77
5.3.1.3 Determination ammonia inhibitory levels	78
5.3.2. DNA collection and metagenomic analysis	79
5.3.3. Diversity analysis.....	80
5.3.4. Statistical framework to identify MIs attributes.....	80
5.3.4.1. Keystone	81
5.3.4.2. Significant abundance changes.....	81
5.3.4.3. Potential early warnings signs	86
5.3.4.4. Metabolic roles	86
5.3.5. Analytic methods	88
5.4. Results and discussion	89
5.4.1. Definition of ammonia inhibitory levels	89
5.4.2. Variation in microbiome diversity across ammonia inhibitory levels.....	91
5.4.3. Significant abundance change using a dual approach	93
5.4.3.1. NIC level vs inhibition level.....	94
5.4.3.2. NIC level vs MIC level.....	94
5.4.4. Potential early warning attribute	97
5.4.5. Key metabolic role attribute.....	99
5.4.6. Future applications of suitable MIs.....	106
5.5. Conclusion	107

CHAPTER 6. Evaluation of microbial indicators for ammonia inhibition detection in anaerobic sequencing batch reactors	108
6.1. Abstract.....	108
6.2. Introduction.....	109
6.3. Material and methods.....	111
6.3.1. Feedstocks sources and activated inoculum.....	111
6.3.2. Operation of the AnSBR system	111
6.3.3. Determination of ammonia inhibitory levels	113
6.3.4. DNA extraction and full-length 16S amplicon sequencing analysis	115
6.3.5. Diversity analysis.....	116
6.3.6. Statistical analysis for evaluation of MIs	117
6.3.7. Analytic methods	118
6.4. Results and discussion	119
6.4.1. Physicochemical characterization of ammonia inhibitory levels	119
6.4.2. Physicochemical characterization of operating cycles	121
6.4.3. Microbial diversity across ammonia inhibitory levels	124
6.4.4. Response of MIs to ammonia inhibitory levels.....	125
6.4.5. MI profiles in the AnSBR processes	128
6.5. Conclusion	130
CHAPTER 7. General conclusions and future perspectives.....	131
7.1. Retrospective management: Key challenges detection	132
7.2. Prospective management: Process monitoring.....	133
7.3. Proactive management: Countermeasures feasibility	134
7.4. Integration of microbial management into the design of new control strategies	134
PRODUCTS DERIVED FROM THIS THESIS	137
REFERENCES.....	139

LIST OF FIGURES

Figure 1.1. The main microorganisms and metabolic activities during the AD of OFMSW and FW.....	14
Figure 1.2. Key challenges in FW digesters influenced by feedstock composition, microbiome changes, and metabolites concentration.....	16
Figure 1.3. Response of alpha and beta diversity indices in FW digesters. a) Alpha diversity may show conflicting responses, potentially defining process performance.	23
Figure 1.4. Criteria for determining key taxa and genes as suitable MI.	28
Figure 2.1. Research design for identifying suitable microbial indicators for FW digesters.....	35
Figure 3.1. Distribution of physicochemical parameters across methane yield categories.....	53
Figure 3.2. Distribution of significant alpha diversity indices grouped by methane yield categories identified by different colors (C1-C6) at both the a) sOTUs and b) genus levels.....	54
Figure 3.3. Principal coordinate analysis (PCoA) depicts microbial community dynamics through methane yield categories (C1-C6) at both the a) sOTUs and b) genus levels..	55
Figure 3.4. Principal coordinate analysis (PCoA) depicts microbial community dynamics through a case study at both the a) sOTUs and b) genus levels.	55
Figure 3.5. The boxplots display the median, quartiles, and extreme values of data, with significance determined using the Kruskal-Wallis h test ($p < 0.10$)..	57
Figure 3.6. The average absolute abundances of key taxa selected from differential abundances within the entire microbial community are depicted.....	58
Figure 3.7. A Venn diagram illustrates the number of genera obtained and shared between differential analysis methods (EdgeR, LefSe, DESeq2, and ALDEx2).	58
Figure 3.8. The heatmap illustrates the correlations between the key taxa and AD by-products..	61
Figure 4.1. The CH ₄ yields for each condition evaluated.....	70
Figure 4.2. The distribution of metabolites in the different conditions evaluated.	70
Figure 4.3. Half-normal (a) and main effects (b) plots..	71
Figure 5.1. The validated Hill Model determined NIC and MIC, defining ammonia inhibitory levels....	89
Figure 5.2. The bar plot illustrates the concentration of AD by-products within each determined ammonia inhibition level.	90
Figure 5.3. Distribution of key alpha indices through ammonia inhibitory levels based on q1 and Pielou at a) genera and b) genes level.....	91
Figure 5.4. NMDS plots showing sample distributions based on Bray-Curtis and Jaccard dissimilarity indices at the (a) genus and (b) gene levels.	92
Figure 5.5. Venn diagrams illustrate the number of genera and genes shared between differential analyses.	93
Figure 5.6. The plots show the distribution of genera and genes based on their topological properties within a microbial network determined in NIC level.....	95
Figure 5.7. The bar plots show genera and genes with significant differences in ammonia inhibitory levels.	96

Figure 5.8. Z-score behavior of key genera and genes for each evaluated ammonia concentration alongside the predicted CH ₄ yield according to the Hill model.	98
Figure 5.9. The RDA illustrating the response in absolute abundance of (a) genera and (b) genes in relation to AD by-products.....	102
Figure 5.10. The heatmap displays z-score of KO counts related to key metabolic pathways in AD and key genes across the ammonia concentrations.	103
Figure 5.11. The heatmaps shows the disrupted metabolic pathways by ammonia and constructed MAG at family level.	104
Figure 5.12. The heatmap depicts the correlations between the a) key genera and b) key genes and AD by-products.....	105
Figure 6.1. Operation of the AnSBR system divided into four processes based on the semi-continuous addition at certain ammonia concentration.....	113
Figure 6.2. Physicochemical characterization of samples from the AnSBR system grouped by ammonia inhibitory levels.	120
Figure 6.3. Response variables of the AnSBR system per operating cycle (cycles 1-7) during the semi-continuous addition of different ammonia concentrations (0, 0.75, 0.37, and 3.78 g TAN/L), variability of OLR (1 and 2 g VS/L-d), and different feedstock sources (FW1, FW2, and FW3)..	123
Figure 6.4. Microbial diversity across ammonia inhibitory levels defined by processes in selected operating cycles..	125
Figure 6.5. Significant response of MI for ammonia inhibitory levels..	127
Figure 6.6. Profiles of MIs based on standardized abundance in each AnSBR processes across selected operating cycles (cycles 1, 3, and 6) and classified by ammonia inhibitory level..	129
Figure 7.1. Steps for the progressive implementation of MIs within with microbial management concept.....	132
Figure 7.2. Future control systems utilizing MIs, integrating the three key areas of microbial management to address, for instance, ammonia inhibition in FW digesters.....	136



LIST OF TABLES

Table 1.1. Overview of the key taxa and genes responses to different behavior in FW digesters.....	25
Table 3.2. General operational characteristics of OSW digesters selected for the meta-analysis.....	45
Table 3.3. Overview of the main characteristics of potential MI identified in the meta-analysis.....	63
Table 4.1. Factorial levels to be evaluated in 8 combinations of treatments.....	67
Table 5.1. Physicochemical characteristics of food waste and granules.....	78
Table 5.2. List of MI reported in the literature considered for this study.....	83
Table 5.3. Kinetic and derivative parameters from Hill model across different studies.....	90

LIST OF ABBREVIATIONS

Term	Definition		
AD	Anaerobic digestion	n	Empirical coefficient controlling the slope of the curve
AIC	Akaike Information Criterion	NIC	Non-inhibitory concentration
ANOSIM	Analysis of similarities	NMDS	Nonmetric multidimensional scaling
AnSBR	Anaerobic sequencing batch reactor	OFMSW	Organic fraction municipal solid waste
ATP	Adenosine triphosphate	OLR	Organic loading rates
AUC	Area under the curve	OSW	Organic solid waste
CCS	Circular consensus sequencing	PCoA	Principal coordinate analysis
CLR	Centered log-ratio	Pi	Among-module connectivity score
COD	Chemical oxygen demand	qPCR	Real-time polymerase chain reaction
EWI	Early warning indicator	RDA	Redundancy analysis
FC	Fold change	ROC	Receiver operating characteristic
FISH	Fluorescence in situ hybridization	Rs	Spearman's correlation coefficients
FW	Food waste	SAOB	Syntrophic acetate-oxidizing bacteria
GAMLS	Generalized additive model for location, scale, and shape	sCOD	Soluble chemical oxygen demand
GC	Gas chromatography	sOTUs	Sub-operational taxonomic units
GCS	Glycine cleavage pathways	SPOB	Syntrophic propionate-oxidizing bacteria
GLM	Generalized linear models	SRA	Sequence read archive
H ₂ S	Hydrogen sulfide	SRB	Sulfate-reducing bacteria
HRT	Hydraulic retention times	TAN	Total ammonia nitrogen
		TRL	Technology Readiness Levels
IC ₅₀	50% inhibitory concentration	TS	Total solids
IQR	Interquartile range	VFA	Volatile fatty acids
KO	KEGG orthology	VFA _t	Total volatile fatty acids
LCFA	Long-chain fatty acids	VMPR	Volumetric methane production rate
MAG	Metagenome-assembled genomes	VS	Volatile solids
MENA	Molecular Ecology Network Analysis	VSS	Volatile suspended solids
MI	Microbial indicators	W-L	Wood-Ljungdahl
MIC	Minimum inhibitory concentration	Zi	Within-module connectivity score

SUMMARY

Bioprocess development is a promising solution for converting organic wastes into valuable bioproducts to improve human well-being. Anaerobic digestion (AD) is among the most mature bioprocesses (TRL 9) and is widely used to treat organic solid waste (OSW), such as the organic fraction of municipal solid waste (OFMSW) and food waste (FW). This process has reached industrial-scale implementation and is of global interest. Conventional FW digesters, which process biodegradable components, such as carbohydrates, proteins, and lipids, efficiently convert waste into bioproducts. Under controlled operational conditions, anaerobic microbial interactions transform organic matter into biogas with a methane content exceeding 60%, and a biodigestate rich in phosphorus and ammoniacal nitrogen. These elements establish FW digesters as crucial processes in waste management, agricultural applications, and sustainable energy production.

The optimization of the AD of FW remains challenging owing to persistent ammonia accumulation despite well-established operational conditions. Ammonia accumulation continues to be a critical issue, even with clear parameters for biogas production, such as the C/N ratio, S_0/X_0 ratio, organic loading rate, hydraulic retention time, pH, temperature, and alkalinity. Further, the impact of ammonia depends on variables such as temperature, pH, and inoculum acclimatization, leading to a wide inhibition range (2.51–26.23 g TAN/L). Consequently, it is challenging to accurately determine when inhibition occurs.

Traditional monitoring systems are generally based on physicochemical indicators, which rarely allow for deciphering the effects of ammonia on the microbial community—changes that could later impact physicochemical variables associated with performance, such as CH_4 production or yield. The problem is often detected only after the accumulation of acetate and propionate, indicating that ammonia has already negatively affected acetoclastic methanogenesis and the syntrophic oxidation of volatile fatty acids (VFAs). At this stage, irreversible changes may occur within the microbial community, as ammonia tends to displace sensitive microorganisms, selecting for those that are resistant. This underscores that microbial indicators can effectively identify ammonia inhibition even before it is observable through physicochemical response variables.

Microbial management is an innovative approach aimed at modernizing anaerobic digesters by analyzing relevant biological information. In essence, it involves the regulation of microbial

dynamics through operational adjustments to achieve process stability. This strategy requires the use of microbial indicators (MIs) such as diversity indices, taxa, or genes that reflect the state of the microbiome. However, a reliable and suitable MI must encompass multiple attributes in order to extend its applicability. Below is a list of key attributes, followed by a brief description.

- **Universality:** This indicator must respond consistently and reproducibly under similar substrate and temperature conditions, making it suitable for application in comparable digesters.
- **Significant changes:** The ability to distinguish categories or groups of interest related to AD performance, such as high or low CH₄ yield, through statistically significant differences.
- **Keystone:** Key ecological components that can trigger disproportionate effects on microbial networks.
- **Early warning signals:** The capacity to predict future issues such as inhibition or disturbances before decrease CH₄ production.
- **Key metabolic role:** Providing critical insights into the metabolic changes leading to AD inhibition.

Each attribute offers a unique perspective, deepening the evaluation of AD performance. Thus, numerous studies have proposed MIs for FW-fed anaerobic digesters, including those capable of detecting ammonia inhibition. However, these indicators often lack reproducibility and reliability owing to their origin in isolated studies, which limits their real-world application. Therefore, to identify reliable MIs, it is crucial to develop a statistical framework that encompasses the widest range of attributes and is applied across multiple digesters fed with FW.

This thesis proposed MIs for monitoring anaerobic processes fed with OSW, such as FW/OFMSW, by integrating the research criteria of neutrality, reliability, and response validation to ensure effectiveness. Indeed, the study employed a meta-analysis, reconstruction of the statistical framework to identify key attributes of the MIs, comparison of potential MIs across multiple scenarios such as batch and semi-continuous digester reactors and utilized a multi-omics approach. This study was structured into three distinct stages.

- **Stage I. Discovery Phase:** A meta-analysis was conducted to identify reliable MIs from 16S rRNA gene region sequencing data (Chapter 3).
- **Stage II. Application Phase 1:** A batch digester fed with FW was operated to determine suitable MIs for ammonia inhibition detection using metagenomics (Chapters 4 and 5).
- **Stage III. Application Phase 2:** A short-term monitoring was performed in a semi-continuous digester system with FW to identify effective MIs for ammonia inhibition detection using full-length 16S rRNA gene sequencing (Chapter 6).

The subsequent sections detail the main results and conclusions of each stage of this doctoral thesis.

Stage I involved the proposal of reliable MIs through a meta-analysis of microbial communities based on 16S rRNA sequencing from AD systems. The identified MIs included *Aminobacterium*, *Clostridium*, HA73, T78, *Corynebacterium*, *Lactobacillus*, and *Prevotella spp.* These indicators were sensitive to changes in abundance associated with the methane yield, albeit with some differences. *Aminobacterium*, *Clostridium*, HA73, and T78 were part of the core microbiome, with an 80% likelihood of their presence in OSW digesters. *Corynebacterium*, *Lactobacillus*, and *Prevotella* displayed a stronger response, distinguishing between low and high CH₄ yields. Additionally, these MIs effectively predicted the CH₄ yield and were suggested as early warning indicators. They were also correlated with inhibitory compounds, such as total ammonia nitrogen (TAN), long-chain fatty acids (LCFA), and VFA, highlighting their potential in addressing the key challenges of FW digesters. A more specific evaluation of these reliable MIs was conducted to assess their impact on AD functionality in relation to specific key challenges.

In Stage II, suitable MIs were proposed to identify the conventional problem of ammonia inhibition in FW digesters. Further, ammonia was identified as the primary inhibitory compound, surpassing other inhibitors, such as LCFA and sulfates. By categorizing ammonia inhibitory levels using derivative parameters from inhibition models and applying a statistical framework, specific microbial indicators such as *Anaerolinea*, *Sphaerochaeta*, *Syntrophobacter*, *Methanomassiliicoccus*, *Methanosarcina*, *fhs*, and *acs* were proposed. These indicators showed significant changes, potential early warnings and also described conventional shifts in microbial metabolism due to ammonia. The MIs enabled identification of the shift from acetoclastic to hydrogenotrophic methanogenesis and increased fermentative activities as the ammonia

concentration increased. Given that these MIs are associated with genera and genes frequently reported in FW digesters, they offer reproducible responses to elucidate metabolic microbial changes in the effects of ammonia in similar processes. Therefore, evaluating these MIs is recommended to address this key challenge within a semi-continuous process, as well as to assess other factors influencing their response, such as operational duration and variations in FW composition.

In stage III, previously identified reliable and suitable MIs were evaluated by considering the challenging factors that could impact their accuracy, such as variations in feedstock composition and microbial community acclimation. The MIs were assessed to define ammonia inhibition through short-term monitoring (35 days) in an AnSBR system that experienced feedstock batch changes, organic loading rate variations, and microbial community changes over time. Despite these disturbances, most MIs provide valuable insights into metabolic shifts related to ammonia inhibition levels. *Anaerolineaceae* (relative to T78) and the *acs* gene detected changes in syntrophic relationships under low ammonia inhibition. In comparison, *Aminobacterium*, *Clostridium* (subgenera sensu stricto 1, 15, 7, and 8), *Sphaerochaeta*, *Syntrophobacter*, *Methanosarcina*, and *Methanomassiliicoccus*, and the *fhs* gene reflected the vulnerability of syntrophic oxidation of acetate and propionate and the dependence on maintaining H₂-dependent methanogenesis under high inhibition levels. This is considered to be a risk factor for VFA accumulation. Therefore, these MI were proposed for future integration into new AI-driven models to predict ammonia inhibition and advance biosystem monitoring development.

Conclusions

This research aimed to identify MI for monitoring AD processes fed with organic solid waste, particularly FW and the OFMSW. The study employed a multi-statistical, multi-omic, and multi-experimental approach, which validated the reliability of the proposed MIs. These indicators demonstrated their potential to provide accurate insights into AD performance, highlighting their applicability in detecting system disturbances and optimizing process stability. By integrating microbial data, this work contributes to advancing monitoring systems, offering a robust framework for improving the efficiency and sustainability of AD operation.

MIs significantly contribute to optimizing biogas digesters by enabling the early detection of microbial changes before observable inhibition effects occur. Conventional monitoring systems

primarily rely on physicochemical variables such as pH, volatile fatty acids, ammonia, and biogas production to confirm inhibition. However, these parameters often fail to identify inhibition until performance metrics, such as CH₄ yield, are affected. This limitation highlights the importance of integrating MIs into existing monitoring systems. Their inclusion can provide a more precise understanding of random and adverse events, enhancing the ability to prevent process instability and improve system resilience. By incorporating a small set of biological variables, MIs offer a reliable and proactive approach to monitoring and managing biogas digester performance.

MIs represent an essential tool for developing experiments that consolidate microbial management in AD systems. Future research should focus on evaluating recovery strategies based on the responses of these indicators to restore system stability. Additionally, identifying new MIs is essential to address other critical challenges in FW digesters and related bioprocesses. Further studies are necessary to optimize quantification methods for long-term monitoring and integrate MIs into existing control system algorithms. These advancements will enhance process efficiency, improve resilience to disturbances, and expand the applicability of MIs to a broader range of biotechnological systems.

RESUMEN

Los bioprocesos son una solución biológica para el tratamiento y valorización de los residuos orgánicos para ser convertidos en bioproductos de valor agregado, contribuyendo a mejorar el bienestar humano. Destaca la digestión anaerobia considerando que es uno de los bioprocesos más avanzados en cuestión de desarrollo tecnológico (TRL 9). Gracias a ello, actualmente la digestión anaerobia es utilizada en la gestión de los residuos sólidos orgánicos como la fracción orgánica de los residuos sólidos urbanos, principalmente por el contenido de residuos de alimentos.

De hecho, es un proceso que ha alcanzado una implementación a escala industrial, y sigue mostrando un interés global, debido que puede contribuir en el cambio de paradigma actual del uso de combustibles fósiles hacia el empleo de biocombustibles siendo más amigable con el ambiente. Particularmente, los digestores de residuos de alimentos son bioprocesos convencionales, capaces de procesar componentes biodegradables como carbohidratos, proteínas y lípidos, convirtiendo eficientemente residuos orgánicos en bioproductos.

En la digestión anaerobia son establecidas condiciones operativas controladas que estructuran una comunidad microbiana anaerobia, siendo el núcleo del proceso para transformar la materia orgánica en un biogás con un contenido de 60% de CH_4 y un biodigestato rico en fósforo y nitrógeno amoniacal. Tales productos hacen que los digestores de residuos de alimentos sean procesos cruciales para establecer las buenas prácticas de manejo de los residuos, aplicaciones agrícolas y lograr la producción de energía renovable.

Aun así, la optimización de la digestión anaerobia sigue siendo todavía un desafío que permita consolidarse como tecnología pionera para la valorización de los residuos de alimentos. Uno de los principales desafíos es la inhibición por amoníaco, dado que es presentado incluso cuando el proceso está operando bajo parámetros operacionales bien conocidos para la producción de biogás, como la relación C/N, la relación S_0/X_0 , la tasa de carga orgánica, el tiempo de retención hidráulica, el pH, la temperatura y la alcalinidad. La inhibición por amoníaco es causada por el aumento en la carga de proteínas dada a la heterogeneidad de los residuos de comida. Una vez las proteínas son degradadas es liberado NH_3 , un compuesto que fácilmente puede permear la biomasa celular e inhibe actividades enzimáticas importantes y necesarias para alcanzar altas eficiencias.

Una detección temprana de la inhibición por amoníaco y su rápido combatimiento, podría evitar el desencadenar otros problemas operativos que suelen ser ocasionados por acumulación de amoníaco, como la generación de espuma y la acumulación de ácidos grasos volátiles. Además, la influencia de parámetros como la temperatura, pH y la aclimatación del inóculo sobre la concentración de amoníaco, amplía el margen de inhibición (2.51–26.23 g nitrógeno amoniacal total/L) siendo difícil de detectar.

Regularmente los sistemas de monitoreo actuales están basados en indicadores fisicoquímicos, por lo que difícilmente permiten descifrar los efectos que el amoníaco ejerce sobre la comunidad microbiana, cambios que posteriormente podrán afectar a variables fisicoquímicas asociadas al desempeño como la producción o rendimiento de CH₄. Con frecuencia el problema es detectado cuando ha sido acumulado tanto el acetato como el propionato, un reflejo que el amoníaco ya ha afectado negativamente la metanogénesis acetoclástica y la oxidación sintrófica de los ácidos grasos volátiles. En este punto, parece haber cambios irreversibles en la comunidad microbiana, ya que el amoníaco tiende a desplazar a los microorganismos sensibles y selecciona aquellos que son resistentes. Esto resalta que los indicadores microbianos podrán efectivamente identificar una inhibición por amoníaco, incluso antes que sea observado por las variables de respuestas fisicoquímicas.

La modernización de los bioprocesos requiere un enfoque en la gestión microbiana, una estrategia innovadora orientada a regular la dinámica de las comunidades microbianas mediante ajustes operativos, como el aumento de la carga orgánica o la bioaumentación. La gestión microbiana busca, en primer lugar, alcanzar la estabilidad del proceso anaerobio y, a futuro, regular la comunidad microbiana para optimizar la generación de bioproductos de interés. Esta estrategia implica el uso de indicadores microbianos, como índices de diversidad, taxones, o genes asociados a categorías específicas. En nuestro estudio, estos indicadores permitieron identificar respuestas biológicas relacionadas con el rendimiento del proceso, tanto en condiciones de alto o bajo desempeño como en escenarios con o sin inhibición por amoníaco.

Para proponer indicadores microbianos adecuados y confiables, debe contener múltiples atributos que permitan extender su aplicabilidad. A continuación, se presenta un listado de cada uno, acompañado de una breve descripción:

- **Universalidad:** Otorgar una respuesta consistente y reproducible sobre el desempeño de procesos que operan bajo mismas condiciones de materia prima y régimen de temperatura.
- **Cambios significativos:** Capacidad para distinguir categorías o grupos de interés relacionadas con el desempeño de la digestión anaerobia, como una abundancia diferencial y significativa hacia bajos o altos rendimientos de CH₄ o hacia distintos niveles inhibitorios de amoníaco.
- **Keystone:** Considerarse como partes ecológicas claves dado que pueden desencadenar diversos efectos desproporcionados en las redes microbianas.
- **Señales de alerta temprana:** Proporcionar una respuesta predictiva sobre un evento futuro que decrezca el rendimiento de metano.
- **Rol metabólico clave:** Ofrecer información clave sobre los cambios metabólicos que ocasionan la inhibición durante la digestión anaerobia.

Cada atributo puede considerarse como un pilar que define el estado del microbioma y facilita una evaluación más precisa del desempeño en la digestión anaerobia. Diversos estudios han propuesto indicadores microbianos para digestores anaerobios que tratan residuos alimentarios, incluyendo algunos para la detección de inhibición por amoníaco. No obstante, al derivarse de estudios aislados, estos indicadores carecen de reproducibilidad y confiabilidad, lo que limita su aplicabilidad en contextos operativos reales. Por ello, para identificar indicadores microbianos confiables y reproducibles fue estructurado y aplicado un marco estadístico que permitiese asociar el mayor número posible de atributos de indicadores microbianos a géneros y genes claves. También fue considerado abarcar múltiples procesos anaerobios que emplearon diversos inóculos, varias materias primas similares y la operación bajo condiciones de temperatura mesofílica, proporcionando así mayor confiabilidad en la respuesta que pueden otorgar los indicadores microbianos.

La presente tesis propone un marco estadístico para encontrar indicadores microbianos para el monitoreo de procesos anaerobios alimentados con residuos sólidos orgánicos, como residuos de alimentos y fracción orgánica de residuos sólidos municipales. La investigación contempló criterios de neutralidad, fiabilidad y validación de respuesta para asegurar la efectividad de los indicadores. De esta manera, fueron contemplados un metaanálisis, la integración de múltiples análisis estadísticos asociadas a los atributos de los indicadores microbianos, la evaluación de

indicadores microbianos sugeridos para detectar un desafío clave en escenarios variados como digestores en lotes y semicontinuos, y el uso de un enfoque multi-ómico.

La investigación involucró tres etapas:

- **Etapla I. Fase de Descubrimiento:** Se realizó un metaanálisis para identificar indicadores microbianos confiables a partir de datos de secuenciación de regiones del gen 16S ARNr (Capítulo 3).
- **Etapla II. Fase de Aplicación 1:** Se operó un digestor por lotes alimentado con residuos de alimentos para determinar indicadores microbianos adecuados para la detección de inhibición por amoníaco usando metagenómica (Capítulos 4 y 5).
- **Etapla III. Fase de Aplicación 2:** Se llevó a cabo un monitoreo a corto plazo en un sistema de digestor semicontinuo con residuos de alimentos para identificar indicadores microbianos efectivos para la detección de inhibición por amoníaco usando la secuenciación completa del gen 16S ARNr (Capítulo 6).

En los siguientes párrafos se detallan cada etapa que constituyeron la tesis doctoral.

Etapla I: Se seleccionaron indicadores microbianos confiables combinando un metaanálisis y el marco estadístico, permitiendo la evaluación sistemática de comunidades microbianas de digestores alimentados residuos orgánicos caracterizadas de las diferentes regiones del gen 16S ARNr.

Como resultado fueron identificados *Aminobacterium*, *Clostridium*, HA73, T78, *Corynebacterium*, *Lactobacillus* y *Prevotella*. Cada uno de ellos mostraron sensibilidad respecto a cambios en su abundancia de acuerdo con categorías creadas a partir de clases de distribución de la variable rendimiento de metano. También mostraron diferencias en los atributos evaluado, lo que les otorgó características únicas. En el caso de *Aminobacterium*, *Clostridium*, HA73 y T78 formaron parte del microbioma central, teniendo una probabilidad de al menos un 80% para encontrar a esos microorganismos lo que da confiabilidad al momento de su detección. En cambio, *Corynebacterium*, *Lactobacillus* y *Prevotella* resaltaron por proporcionar una respuesta más pronunciada para diferenciar bajos y altos rendimientos de CH₄ aunque difícilmente puedan encontrarse en procesos similares.

Entre otros atributos, el conjunto de indicadores microbianos predijo eficazmente el rendimiento de CH₄, sugiriendo características de alertas tempranas. También mostraron correlaciones con compuestos inhibitorios, como el amoníaco, ácidos grasos de cadena larga y ácidos grasos volátiles, evidenciando que podrían ser útiles para detectar los desafíos clave de la digestión anaerobia con residuos de alimentos. Una evaluación más específica de estos indicadores microbianos confiables para valorar la funcionalidad de la digestión anaerobia con respecto a un desafío clave fue sugerido.

Etapa II: Se propusieron indicadores microbianos adecuados para identificar un problema convencional de inhibición por amoníaco en digestores por lotes empleando residuos de alimentos analizando la comunidad microbiana mediante metagenómica. Además, en esta etapa fue determinado que el amoníaco es el principal compuesto inhibidor, incluso por encima de interacciones con otros inhibidores como ácidos grasos de cadena larga y sulfatos.

Aplicando un modelo de inhibición fueron definidos niveles inhibitorios de amoníaco que junto al marco estadístico fueron sugeridos como indicadores microbianos *Anaerolinea*, *Sphaerochaeta*, *Syntrophobacter*, *Methanomassiliicoccus*, *Methanosarcina*, *fhs* y *acs*. En conjunto, esos indicadores mostraron cambios significativos y posibles advertencias tempranas para indicar cuando la concentración de amoníaco tiene un efecto inhibitorio.

Además, permitieron describir los cambios habituales en el metabolismo microbiano causados por el amoníaco. Un claro ejemplo fue la reducción del gen *acs* que participa en la metanogénesis acetoclástica, junto a la posible bacteria oxidadora de acetato *Sphaerochaeta*. Ambos coincidieron con el decremento en la degradación de acetato a medida que aumentaba la concentración de amoníaco. Considerando la perspectiva microscópica, esas respuestas podrían ocurrir antes que respuestas macroscópicas como la acumulación de acetato sea observable. Así, integrar indicadores microbianos en un sistema de monitoreo convencional mejoraría la sensibilidad para detectar a tiempo una inhibición, antes que el proceso colapse causada por la acumulación de ácidos grasos volátiles.

También, los indicadores microbianos al asociarse con géneros y genes claves reportados en el metaanálisis y usualmente reportados en digestores de residuos de alimentos, se intuyó que podrían proporcionar respuestas reproducibles si son evaluados en procesos similares. No obstante, aún quedaba la inquietud por considerar otros factores inusualmente controlables que podrían alterar

su respuesta, como la variación en la composición de los residuos de comida y, cambios en la comunidad microbiana debido al uso continuo del mismo inóculo inicial. Por tal motivo, los indicadores microbianos fueron evaluados en un sistema semicontinuo para responder a tales incertidumbres.

Etapa III: Se realizó una evaluación de los indicadores microbianos previamente identificados en la Etapa I y Etapa II, para detectar una inhibición por amoníaco usando como técnica de análisis de la comunidad microbiana la secuenciación completa del gen 16S ARNr. Para lograrlo un monitoreo a corto plazo (35 días) de indicadores microbianos en un sistema que conjuntó doce reactores anaerobios por lotes secuenciales fue realizado. El experimento consistió en evaluar la capacidad de los indicadores microbianos para identificar niveles de inhibitorios de amoníaco, independiente de factores como cambios en el lote de materia prima, variaciones en la tasa de carga orgánica y cambios en la comunidad microbiana debido a la capacidad selectiva del amoníaco.

A pesar de estas perturbaciones, la mayoría de los indicadores microbianos evaluados proporcionaron información valiosa sobre cambios metabólicos clave que surgieron en cada nivel de inhibición. *Anaerolineaceae* (en relación con T78) y el gen *acs* reconocieron el decremento de las relaciones sintróficas cuando el nivel inhibitorio de amoníaco fue bajo. Mientras *Aminobacterium*, *Clostridium* (subgéneros sensu stricto 1, 15, 7 y 8), *Sphaerochaeta*, *Syntrophobacter*, *Methanosarcina*, *Methanomassiliicoccus* y el gen *fhs* reflejaron la vulnerabilidad en la oxidación sintrófica de acetato y propionato, junto con la necesidad de mantener una metanogénesis dependiente de H₂, lo que indica un riesgo de acumulación de ácidos grasos volátiles en niveles inhibitorios altos de amoníaco.

Claramente los indicadores microbianos ofrecieron respuestas efectivas para describir con mayor detalle y precisión el efecto inhibitorio por amoníaco, llegando a una profundidad sobre el comportamiento del metabolismo microbiano. Considerando este punto, una pronta integración hacia nuevos modelos impulsados por inteligencia artificial es propuesto con un paso para continuar con el desarrollo de la gestión microbiana. Esos modelos permitirían predecir una inhibición por amoníaco empleando un número reducido de variables de entrada, dando un paso hacia el desarrollo de nuevos sistemas de monitoreo basadas en información biológica

simplificada. Esta integración reduciría la brecha para lograr la modernización de los sistemas de control en los actuales digestores anaerobios.

Conclusiones

La presente investigación tuvo como objetivo identificar indicadores microbianos para monitorear procesos de digestión anaerobia que son alimentados con residuos sólidos orgánicos, particularmente la fracción orgánica de los residuos sólidos urbanos y residuos de alimentos. La propuesta contempló un enfoque multi-estadístico, multi-ómico y multi-experimental, que respaldaron la fiabilidad de los indicadores microbianos propuestos.

En general, el uso de indicadores microbianos tiene un gran aporte para alcanzar la optimización de los biodigestores, considerando que, con pocas variables biológicas, es posible detectar cambios microbianos relevantes antes que se desencadene los efectos de una inhibición observable. Esto es importante porque una inhibición usualmente es corroborada midiendo y observando indicadores fisicoquímicos como el pH, ácidos grasos volátiles, amoníaco y producción de biogás que son incluido en sistemas de monitoreo convencionales. Usando únicamente variables fisicoquímicas, difícilmente se pueda detectar una inhibición antes que sea observado en variables de desempeño como el rendimiento de CH₄, mostrando la clara necesidad de integrar los indicadores microbianos a los sistemas de monitoreo actuales para clarificar esos eventos desafortunados y aleatorios.

Como paso inicial, los indicadores microbianos podrían utilizarse para desarrollar una variedad de experimentos que consoliden la gestión microbiana en digestión anaerobia. Futuras investigaciones deberían centrarse en evaluar estrategias de recuperación de estabilidad centrado en la respuesta de los indicadores. También se propone identificar nuevos indicadores microbianos para enfrentar otros desafíos clave en digestores alimentados con residuos de alimentos, así como en otros bioprocesos. Además, se requiere una investigación adicional para seleccionar los métodos de cuantificación adecuados para el monitoreo a largo plazo e integrar los indicadores en algoritmos que son usados actualmente en los sistemas de control.

CHAPTER 1. Theoretical Framework

1.1. Anaerobic digestion process of organic solid waste

The conversion of approximately 105 billion tons of annual organic solid waste (OSW), comprising crop residues, livestock waste, sewage sludge, and food waste (FW), into value-added products using renewable technologies holds promise for mitigating climate change (World Biogas Association, 2021). Anaerobic digestion (AD) is emerging globally as a viable technology for converting OSW into biogas, owing to its maturity (technology readiness level = 9) (World Biogas Association, 2021). This technology can leverage the organic fraction of municipal solid waste (OFMSW) generated in Mexico given an annual availability of 55.7 million tons (SEMARNAT, 2020). Among OFMSW, FW is a suitable feedstock for AD because of its high biodegradability, resulting in a high methane (CH_4) yield potential ranging from 0.3 to 1100 mL $\text{CH}_4/\text{gVS}_{\text{added}}$ (SEMARNAT 2020; Xu et al. 2018). This presents an opportunity to utilize up to 33% of OFMSW and mitigate the environmental issues associated with landfill disposal (Sánchez-Arias, Riojas-Rodríguez, 2019; SEMARNAT, 2020).

AD is characterized by the breakdown of approximately 85% of organic matter through a microbial community that encompasses mainly hydrolytic, acidogenic, acetogenic, and methanogenic activities (Banks et al., 2018). These microbial interactions can produce biogas with 60-70% CH_4 and 30-40% CO_2 , and a nitrogen-rich biodigestate (Li et al. 2018; Xu et al. 2018). Most FW digesters operate under mesophilic conditions, with organic loading rates (OLR) ranging from 1 to 4 g/L-d of volatile solids (VS) and hydraulic retention times (HRT) of up to 80 days (Banks et al., 2018; Li et al., 2018). These conditions assemble the microbial community, making AD a deterministic process (Zhang et al., 2022). The heterogeneous composition of FW (carbohydrates, proteins, and lipids) creates a niche that shapes a unique microbiome, where specific microorganisms, metabolic pathways, and metabolites interact (Fig. 1.1). However, the complex chemical composition of FW can release metabolites that gradually disrupt the native CH_4 -producing microbiome, leading to operational challenges and diminished performance (Theuerl et al., 2018; Wei et al., 2020). These issues diminish reliability and hinder the application of this process in full-scale systems (Peng et al., 2018; Zhang et al., 2022). Typical challenges in FW digesters include over-acidification, ammonia inhibition, foaming, and H_2S production (Xu et al., 2018).

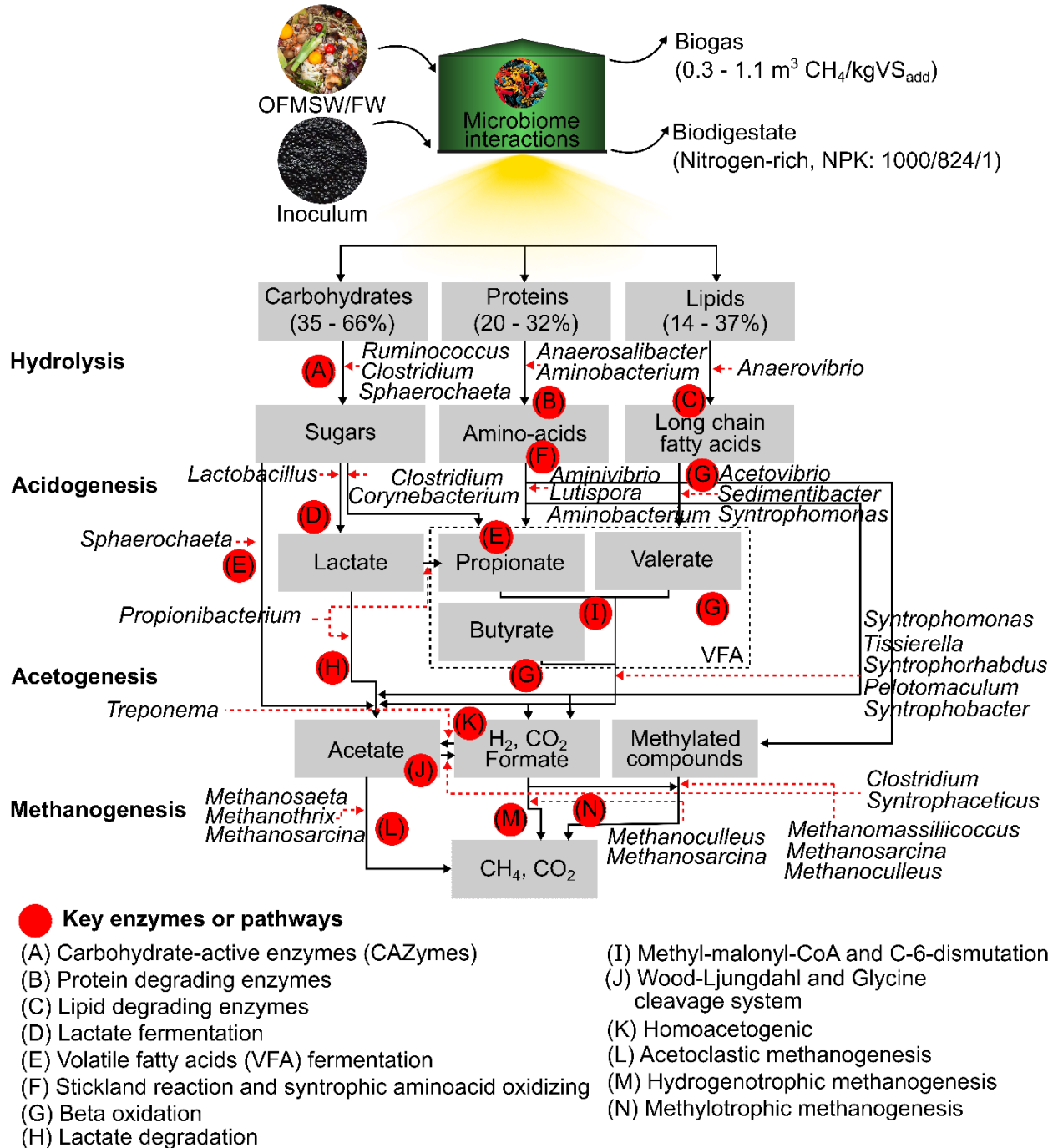


Figure 1.1. Main microorganisms and metabolic activities during AD of OFMSW and FW. This diagram explains how the input of OFMSW/FW into an anaerobic digester can be converted into biogas and digestate through various microbial interactions. The red circles with letters indicate the key enzymes or pathways involved in the conversion of compounds, and the red arrows indicate microorganisms that might be involved. Modified from Wang et al., (2018).

1.2. Key challenges during OFMSW and FW digestion

The effectiveness of FW digesters is constrained by operational challenges, leading to reduced biogas production (Peng et al., 2018; Zhang et al., 2022). Unfortunately, these challenges are often interconnected, where one issue exacerbates another, complicating process stability (Fig. 1.2). During ammonia inhibition, a resistant microbial community typically emerges, primarily performing AD via hydrogenotrophic methanogenesis (Banks et al., 2018; Peng et al., 2018; Zhang et al., 2022). As acetoclastic methanogenesis declines, acetate degradation requires syntrophic relationships ($\Delta G^0 = +175.1$ kJ/mol) (Wu et al., 2024). Under these thermodynamic constraints, AD is prone to instability, frequently resulting in excessive volatile fatty acid (VFA) accumulation, which leads to over-acidification (Alavi-Borazjani et al., 2020). Prolonged operation under such stress conditions often causes the accumulation of additional metabolites, including long-chain fatty acids (LCFAs), which promote foam generation owing to their surfactant properties (He et al., 2017; Xu et al., 2018). In this stressed environment, propionate and butyrate may accumulate, and protein degradation can release sulfate compounds that promote hydrogen sulfide (H_2S) production, negatively affecting biogas quality (Li et al., 2015; Tian et al., 2020). These interconnections highlight shifts in microbial metabolic functionality, leading to the assembly of unique microbiomes that can address specific challenges. Thus, the emergence of key microbial taxa and genes related to these challenges are discussed in the following sections.

1.2.1. Ammonia inhibition

The proteins and other nitrogenous compounds present in FW digesters lead to the release of total ammonia nitrogen (TAN) in both NH_4^+ and NH_3 forms, which vary depending on the temperature and pH (pKa at 35°C, 8.95) (Banks et al., 2018; Jiang et al., 2019; Jo et al., 2018; Tian et al., 2018). The importance of ammonia concentration lies in its dual effect on AD. Low ammonia concentrations (50 – 200 mg/L) promote microbial growth and buffer capacity (Agyeman et al. 2021). Conversely, ammonia concentrations between 1500 and 7000 mg/L are inhibitory (Rajagopal et al. 2013). The wide variability in ammonia inhibition levels can be attributed to intrinsic microbiome factors, including the presence of ammonia-assimilating enzymes, cell morphology, and microbial acclimation (Jiang et al., 2019). Although AD can proceed under ammonia-stress conditions, it reduces CH_4 production by 30% (Li et al., 2018).

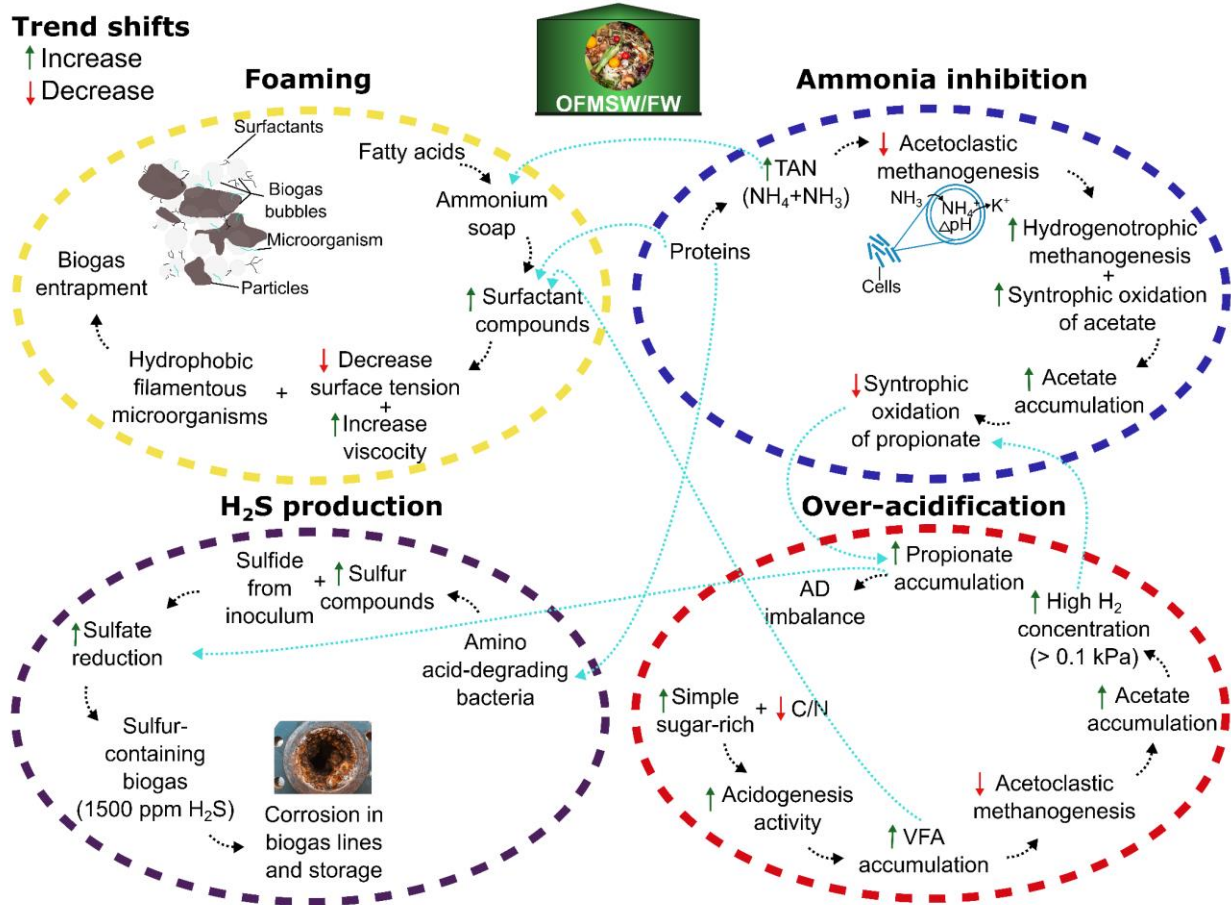


Figure 1.2. Key challenges in FW digesters influenced by feedstock composition, microbiome changes, and metabolites concentration. Each circle with semi-continuous lines is color-coded to highlight the key challenges and the associated changes. Positive trends are indicated by green arrows (increase) and negative trends are indicated by red arrows (decrease). The sequence of changes is shown by black arrows, whereas interactions between key challenges are represented by sky-blue arrows. Modified from Basak et al., (2021); He et al., (2017); Jiang et al., (2019); Tian et al., (2020).

The ammonia inhibition mechanism involves NH₃ diffusion through thin filament acetoclastic methanogens (e.g., *Methanosaeta/Methanothrix*), causing intracellular pH changes and K⁺ leakage, increasing energy needs, and reducing acetate consumption (Jiang et al., 2019; Yu et al., 2020). The syntrophic acetate-oxidizing bacteria (SAOB, e.g., *Syntrophaceticus* and *Clostridium*) restore acetate consumption and produce CO₂ and H₂ via the Wood-Ljungdahl (W-L) and glycine cleavage pathways (GCS) (Li et al., 2022; Yan et al., 2020). These bacteria collaborate with ammonia-tolerant hydrogenotrophic methanogens (e.g., *Methanoculleus*), whose presence of energy-regulating complexes (e.g., energy-converting hydrogenase, Na⁺/H⁺ antiporter, and V/A-type ATP synthase) can modulate energy under varying thermodynamic conditions and maintain low hydrogen pressure (< 0.1 kPa) for favorable VFA oxidation (Hardy et al., 2021; Jiang et al.,

2019; Yan et al., 2020; Zhao et al., 2021). Although AD can occur under these conditions, the shift away from acetoclastic methanogenesis, which typically generates 60–70% of CH₄ production, leads to poor performance (Li et al., 2018; Wu et al., 2021).

Under conditions of ammonia stress, hydrogenotrophic methanogenesis alone leads to a thermodynamic imbalance if disturbances occur (Jiang et al., 2019). Hydrogenotrophic methanogens require at least 0.01 kPa of H₂ and 10 μM formate to sustain their metabolism; however, these concentrations can inhibit SAOB (Xu et al., 2024). In addition, operating under such conditions promotes ammonia accumulation in the medium term (100 – 150 d), deactivating succinyl-CoA synthetase and reducing the activity of syntrophic propionate-oxidizing bacteria (SPOB, e.g., *Pelotomaculum* or *Syntrophobacter*) (Zhang et al., 2022). These microorganisms have low functional redundancy and slow growth (0.06 d⁻¹) compared to SAOB (0.3 d⁻¹), prolonged adaptation time, and promote propionate accumulation (Wu et al., 2022). Therefore, propionate inhibits hydrogenotrophic methanogen activity, causing thermodynamic imbalance, over-acidification, and AD failure (Wu et al., 2022; Zhao et al., 2021). This suggests that ammonia is the initial disturbance that leads to various microbial changes before potential process instability occurs.

1.2.2. Over-acidification

When FW is rich in simple sugars and with a low C/N ratio (14-37) breaks down quickly, excessive VFAs can result, leading to over-acidification (Chatterjee & Mazumder, 2019; Pavi et al., 2017), which may deplete the buffering capacity (mainly HCO₃⁻), weakening the ability to maintain neutral pH levels (6.5-7.6) and increasing un-ionized VFA (pKa 4.75) (Alavi-Borazjani et al., 2020; Basak et al., 2021; Labatut & Pronto, 2018). In some microorganisms, over-acidification can acidify the cell cytoplasm, which consumes adenosine triphosphate (ATP) and releases H⁺ to maintain the cytoplasmic pH balance (Xu et al., 2024). Concentrations between 1200-14000 mg VFA/L usually indicate over-acidification (Gao et al., 2015; Shi et al., 2017). Additionally, factors such as single-stage systems, thermophilic operation, high substrate/inoculum (S₀/X₀) ratios, lack of trace elements, ammonia accumulation, and the buildup of long-chain fatty acids (LCFA) also contribute to over-acidification in FW digesters (Labatut & Pronto, 2018; Patil et al., 2021; Wang et al., 2018; Xu et al., 2018). Nevertheless, this issue often stems from an imbalance between

hydrolytic/acidogenic bacteria and syntrophic acetogens/methanogens, which lead to microbiome shifts (Basak et al., 2021; Wu et al., 2024).

Over-acidification initiates with the repression of acetoclastic methanogens (e.g., *Methanosaeta*), resulting in increased acetate concentration and elevated hydrogen pressure, leading to reduced CH₄ content (Kleyböcker et al., 2012; Li et al., 2017). High hydrogen pressure (> 0.0012 kPa) and acetate accumulation inhibit SPOB activity for thermodynamic barriers, promoting propionate accumulation and inhibiting syntrophic fatty acid oxidizers (e.g., *Syntrophomonas*, *Sedimentibacter*, and *Syntrophorhabdus*) (Amha et al., 2017; Basak et al., 2021; Kleyböcker et al., 2012; Xu et al., 2024). Over time, the proportion of un-ionized VFAs increased, whereas the pH decreased and inhibited hydrogenotrophic methanogens (e.g., *Methanosarcina* and *Methanoculleus*) (Li et al., 2017). These microbial changes intensify the proliferation of hydrolytic bacteria (e.g., *Lactobacillus* and *Clostridium*) and acidogens (e.g., *Aminobacterium*), resulting in the excessive production of VFAs (Amha et al., 2017; Basak et al., 2021; Wang et al., 2018). This issue intuitively reduces microbial richness and diversity, rendering the microbial community sensitive to the instability caused by irreversible acidification (Basak et al., 2021; Wang et al., 2018). Alterations in specific microorganisms coupled with physicochemical parameters can provide insights into this issue.

Apart from ammonia (explained in Section 1.2.1), LCFA are metabolites that contribute to over-acidification in FW digesters (Patil et al., 2021). These compounds arise from the breakdown of lipids catalyzed by lipase enzymes released by hydrolytic bacteria (e.g. *Anaerovibrio*) (Basak et al., 2021; He et al., 2018). The degradation of LCFA involves flagellated microorganisms capable of syntrophic β -oxidation (e.g., *Syntrophomonas*) along with hydrogenotrophic methanogenesis (e.g., *Methanosarcina*), making their degradation complex (Amha et al., 2017; Basak et al., 2021; Kougias et al., 2016). In addition, an increase in lipid content may easily accumulate LCFA to inhibitory levels (> 5 gCOD/gVSS), disrupting the successive cleavage of 2-carbon units into acetyl-CoA, thus promoting propionate generation (Kougias et al., 2016). Furthermore, LCFA can be absorbed or bound to microbial cells, hindering the growth of acetoclastic methanogens (e.g. *Methanosaeta*), leading to increased acetate levels or blocking mass transfer (Kougias et al., 2016; Patil et al., 2021). This suggests that LCFAs could be responsible for the over-acidification caused by their effect on microorganisms and genes associated with VFA metabolism.

Other factors that contribute to over-acidification in FW digesters are those associated with operational parameters or those dismissed as metabolites. Single-stage systems undergo rapid acidification due to the facile inhibition of methanogens in response to various disturbances (Xu et al., 2018). Operating at high temperatures (55 - 60°C) poses challenges that lead to AD disruption, such as low microbial diversity, high NH₃ levels, and increased metabolic flux owing to substrate solubility (Chatterjee & Mazumder, 2019; Lee et al., 2017). An inadequate S₀/X₀ ratio (suggested as 0.5 in FW digesters) can lead to a sudden release of VFAs due to an imbalance between methanogenic and acidogenic bacteria (Zhang et al., 2019). Lastly, the absence of trace elements such as Fe, Co, Mo, and Ni may diminish coenzyme synthesis essential for methanogenesis, impacting tolerant hydrogenotrophic methanogens (e.g., *Methanosarcina*, *Methanoculleus*). This diminishes methanogenic diversity, elevates hydrogen partial pressure, and increases acetate consumption, thereby fostering propionate accumulation (Zhang et al., 2019). Therefore, over-acidification does not primarily cause AD failure; rather, it emerges because of various converging factors that culminate in this operational issue.

1.2.3. Foaming

Foam generation in FW digesters is primarily associated with the reduction of liquid medium surface tension by surfactant compounds, either from the feedstock or released during AD. These compounds, such as detergents, proteins, glycolipids, glycoproteins, glycolipopeptides, and NH₄⁺/LCFA, might increase the viscosity of the digestate (> 782 mPa·s), enhancing foam stability. (Ao et al., 2020; He et al., 2017; Xu et al., 2018). Additionally, filamentous bacteria, variations in temperature and agitation speed, fatty acids, and sudden CO₂ release due to a decrease in pH (pK_a HCO₃⁻, 6.35) exacerbate foam formation (He et al., 2017; Xu et al., 2018). Consequently, the foam may expand the mixed liquor, increase the working volume, obstruct the tank ports, and promote spills in the reactor (Kong et al., 2019).

Some microorganisms benefit from foam conditions and can prolong the foam formation. Hydrolytic-acidogenic bacteria (e.g., *Anaerovibrio*, *Aminobacterium*, and *Lactobacillus*) can produce metabolites, such as VFA, NH₄⁺, and LCFA, or biosurfactants, such as proteins, glycolipidic, glycoproteins, or glycolipopeptides, which decrease surface tension (He et al., 2017, He et al., 2018). Filamentous hydrophobic bacteria (e.g., *Actinomyces*) promote sludge flotation,

which may trap biogas bubbles and prevent the release of biogas (Ganidi et al., 2009; He et al., 2017). Therefore, specific microorganisms have the potential to generate foam.

1.2.4. H₂S generation

Sulfur compounds are inevitable in FW digesters because of the sulfate content (3% of S-total), sulfide (14% of S total), and proteins (69% of S-total) in the feedstock, along with the high sulfide content contributed by anaerobic biomass (2.5% of the cell) (Amani et al., 2010; Tian et al., 2020). However, the reducing conditions in AD (-214 to -305 V) make sulfide the primary chemical form of sulfur, which is easily converted to hydrogen sulfide (H₂S) (Tian et al., 2020). This phenomenon could lead to unpleasant odors in the digestate and elevated H₂S levels in biogas, potentially reaching up to 1500 ppm, thereby corroding biogas lines and storage tanks (Moreno-Andrade et al. 2020; Tian et al. 2020). This implies that biogas may require desulfurization techniques (< 500 ppm of H₂S), which are necessary for energy generation via heat and power engines/turbines (Moreno-Andrade et al., 2020). Additionally, an inhibitory effect on the microbial community may occur, either by sulfides precipitating essential metals or by H₂S permeating the cell membrane, causing protein denaturation (Amani et al., 2010).

The conversion of inorganic sulfur compounds (e.g., sulfite, and thiosulfate) to sulfide/H₂S may involve various microorganisms (Tian et al., 2020). Amino acid-degrading bacteria (e.g., *Aminobacterium*) facilitate the disposition of sulfur compounds in FW digesters (He et al., 2017; Tian et al., 2020). In the presence of sulfate, this compound can be utilized by sulfur-reducing bacteria (SRB) to produce sulfide (Tian et al., 2020). However, some SRB can utilize H₂ and acetate as electron donors, thereby competing with methanogenic archaea (Amani et al., 2010). Additionally, some SPOB (e.g., *Pelotomaculum*) may be capable of utilizing sulfate as an electron acceptor during propionate degradation to acetate (Qiao et al., 2016). This versatility in the effects of sulfur compounds seems intricately tied to the metabolic activity of specific microbial populations. Therefore, understanding the functionality of the microbiome is crucial to understanding the role of sulfur compounds in AD.

1.3. Microbial indicators

Given that FW digester challenges tend to disrupt the process, employing state indicators is suggested as these variables can elucidate the status of AD (Wu et al., 2021). These indicators are

associated with stability and exhibit sensitive responses to disturbances that disrupt AD (Wu et al., 2021). An indicator that can predict instability faster than the change in CH₄ content is defined as an early warning indicator (EWI) (Wu et al., 2021). Currently, a wide range of indicators is linked to physicochemical characteristics, such as biogas production, pH, alkalinity, acetate, propionate, VFA/Ca, and CH₄/CO₂, (Wu et al., 2019). However, factors such as operational conditions, mass transfer, and self-optimized microbiomes lead to drawbacks in the response of these indicators, such as low reproducibility, low accuracy, and a lack of universality (Wu et al., 2019, Wu et al., 2021).

The FW digesters operate via deterministic processes; thus, the use of microbial indicators (MIs) is accessible (Li et al., 2018; Zhang et al., 2022). Because in a deterministic process the microbiome is selected by the operational conditions and serves as a reference for specific AD state. Using MIs, biological or ecological responses that reveal microbiome status, allows detecting microbiome changes affecting process performance through significant responses earlier than physicochemical observations. (Carballa et al. 2015; De Vrieze 2020; Wei et al., 2020). However, incorporating physicochemical indicators along with MIs would facilitate the identification of key challenges, which would help in implementing adequate countermeasures to prevent collapse (Wei et al., 2020; Wijaya et al., 2023). In AD systems, MIs can be categorized into two levels: ecological parameters tied to diversity indices, and indicators microbes associated with key taxa, genes, or transcripts (De Vrieze, 2020; Li et al., 2018).

1.3.1. Diversity indices

Microbial diversity in AD is commonly assessed using alpha and beta diversity indices, enabling the comparison of microbiome structures and treatments (Fig. 1.3) (Pasalari et al., 2021; Peng et al., 2018). Alpha diversity indices, such as the Chao1, Shannon, Pielou, and Faith indices, can be used to estimate the richness, entropy, evenness, and phylogenetic distances within samples (Fig. 1.3a) (Hill et al., 2003; Pielou, 1966; Shade, 2017). High values of these indices may indicate a broad range of microorganisms that provide functional redundancy against disturbances, thereby ensuring stability (Calusinska et al., 2018; Li et al., 2018). However, this response may also suggest a greater likelihood of implementing biological mechanisms to control microbial growth, thereby increasing the susceptibility to deterioration (Calusinska et al., 2018). Conversely, low alpha diversity values may imply adaptive and selective capability of the microbial community,

resulting in high CH₄ yields (Jo et al., 2018). Nonetheless, these responses may also potentially displace the key microorganisms involved in AD, such as methanogenic archaea, thereby revealing a vulnerable microbial community (Nguyen et al., 2019; Zhang et al., 2019). Such contradictory responses may be attributed to the operational conditions, nonlinear responses, sampling methodology, and transient microorganisms (Calusinska et al., 2018; Cordier et al., 2020). Nonetheless, evaluating diversity within a specific study or related studies within the same research framework may yield consistent results (Shade, 2017).

The dynamics of the microbial community composition between the study groups have been assessed using beta diversity measures (Fig. 1.3b). Bray-Curtis, Jaccard, and Unifrac are dissimilarity metrics commonly used to evaluate the abundance, presence, and phylogenetic distances of microbiomes, respectively (Buttigieg & Ramette, 2014). These indices appear to produce more consistent results than alpha diversity indices (De Vrieze et al., 2021). Analyzing microbial community dissimilarities at various points in the process may identify key challenges, such as ammonia inhibition, over-acidification, and foaming (Fig. 1.3b) (Basak et al., 2021; He et al., 2017; Peng et al., 2018). However, it is noteworthy that the response of these indices could be influenced by feedstock type (Bovio-Winkler et al. 2021). This highlights the importance of accounting for factors that alter the microbial community to ensure consistent MI responses in FW digesters.

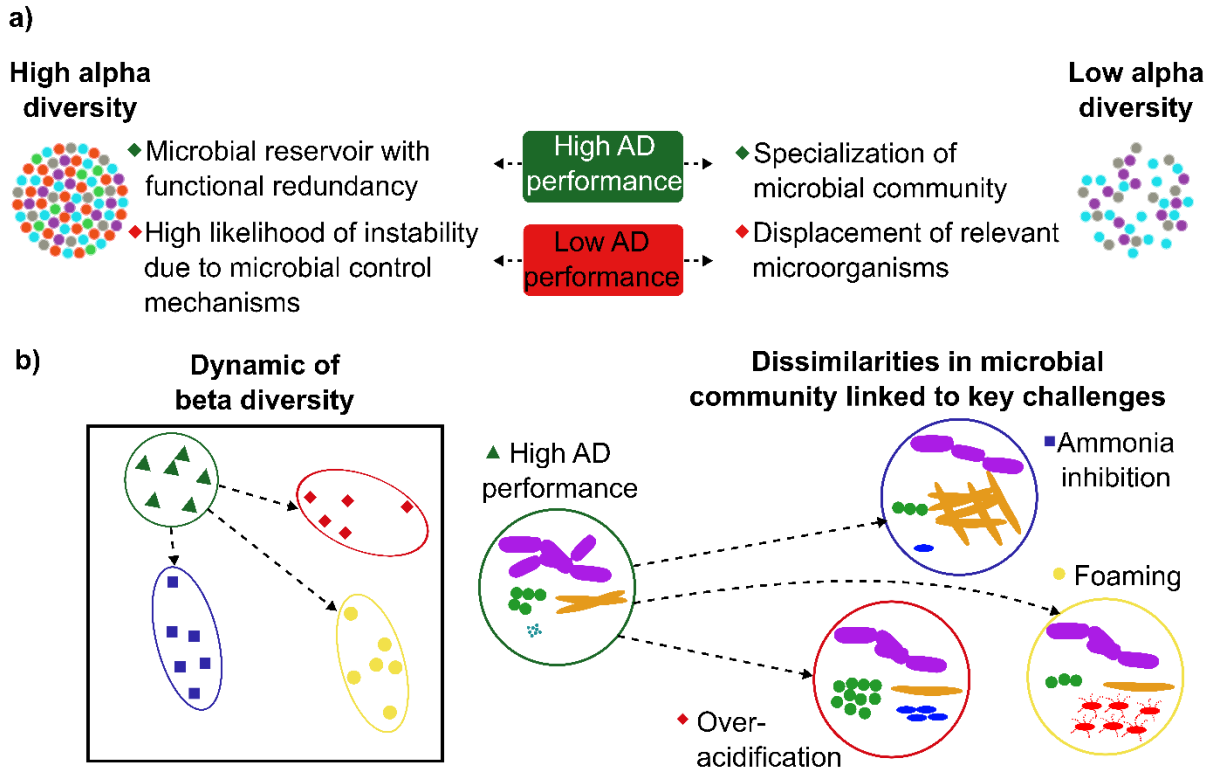


Figure 1.3. Responses of alpha and beta diversity indices in FW digesters. a) Alpha diversity may show conflicting responses, potentially defining process performance. Its evaluation in the FW digestion context is intriguing, revealing its feasible application as a MI. b) Beta diversity may display notable shifts in the microbial community, which is linked to the emergence of significant challenges. This suggests that potential taxa and genes could describe these dissimilarities. Based on Basak et al., (2021; Calusinska et al., (2018); He et al., (2017); Jo et al., (2018); Peng et al., (2018) observations.

1.3.2. Key taxa and genes

Some taxa and genes have been considered potential MIs because they have shown significant changes in their abundance under specific conditions that influence the performance of FW digesters (Table 1.1). By merely considering the abundance of trends, this part of the microbiome can highlight the state of the anaerobic process. For instance, a positive trend in *Methanosaeta*, linked to “good” AD performance, have been used to assess bioaugmentation success in process recovery and proper process operation (Basak et al., 2021; Patil et al., 2021; Zhang et al., 2022). Furthermore, key challenges may be clarified by a combination of trends through key taxa. A positive trend in *Ruminococcus*, *Corynebacterium*, and *Aminobacterium* suggests increased production of surfactant compounds, such as VFA and ammonia. These responses coupled with a negative trend in *Methanosaeta* indicate a stressful environment that can potentially lead to foam formation (Ganidi et al., 2009; He et al., 2017). This finding is relevant because trends provide a

more prudent method for assessing the state of AD than absolute threshold values (Wu et al., 2021). Therefore, since trends originate from biological components such as key taxa and genes, they are closely linked to identifying specific challenges. Consequently, selecting MIs is essential for recognizing operational states based on user requirements.

Functional redundancy is a drawback of key taxa that can be compensated for by combining them with key genes (De Vrieze, 2020). A notable example is the combination of genes associated with acetoclastic methanogenesis, along with strict acetoclastic archaea such as *Methanosaeta/Methanotherix*, and the versatile methanogen *Methanosarcina*. In specific contexts, instability due to ammonia stress can be inferred when genes for acetate degradation are maintained by resilient *Methanosarcina*, whereas the sensitivity of *Methanosaeta* leads to its displacement (Zhang et al., 2022). Therefore, selecting sets of key taxa and genes could specify metabolic changes of interest in the microbiome, highlighting the ability to provide specificity in different environments that perturb AD.

Table 1.1. Overview of key taxa and gene responses to different behaviors in FW digesters.

Key taxa or gene	Metabolic contribution in anaerobic digestion	Response trend	Associative condition	Anaerobic digestion performance
Taxa				
<i>Ruminococcus</i>	Hydrolysis of carbohydrates and acetate production ^[1]	Positive ^[1]	Foaming ^[1]	Poor ^[1]
<i>Anaerovibrio</i>	Hydrolysis of lipids ^[13]	Positive ^[13]	Organic overloading ^[13]	Poor ^[13]
<i>Clostridium</i>	Hydrolysis of carbohydrates and protein ^[3,4] and H ₂ production ^[5]	Positive ^[3]	Ammonia inhibition ^[3]	Poor ^[3]
<i>Sphaerochaeta</i>	Hydrolysis of carbohydrates and acetate production ^[6]	Positive ^[6,7]	Ammonia inhibition ^[6] Food waste addition ^[7]	Good ^[7] Poor ^[6]
<i>Aminobacterium</i>	Hydrolysis of protein and amino acid degradation ^[1]	Positive ^[1,9]	Foaming ^[1] Organic overloading ^[9]	Poor ^[1,9]
<i>Corynebacterium</i>	Phospholipids production ^[1] and carbohydrates fermentation ^[12]	Positive ^[1] Negative ^[12]	Foaming ^[1] Ammonia inhibition ^[12]	Poor ^[1,12]
<i>Treponema</i>	Homoacetogenesis ^[16]	Positive ^[16]	Two-stage system ^[16] Food waste addition ^[7]	Good ^[7,16]
<i>Aminivibrio</i>	Syntrophic oxidation of acetate ^[10] and amino acid degradation ^[11]	Positive ^[9] Negative ^[11]	Low organic loading ^[9] Ammonia inhibition ^[11]	Good ^[9] Poor ^[11]
<i>Sedimentibacter</i>	Syntrophic oxidation of VFA ^[14]	Negative ^[14,15]	Organic overloading ^[14] Ammonia inhibition ^[15]	Poor ^[14,15]
<i>Syntrophomonas</i>	Syntrophic oxidation of VFA ^[14]	Positive ^[17,14]	Formate addition ^[17] Bioaugmentation ^[14]	Good ^[17,14] Poor ^[14]
<i>Syntrophobacter</i>	Syntrophic oxidation of propionate ^[17]	Negative ^[14] Positive ^[17]	Organic overloading ^[14] Formate addition ^[17]	Poor ^[14] Good ^[17]
<i>Pelotomaculum</i>	Syntrophic oxidation of propionate ^[11]	Negative ^[11]	Ammonia inhibition ^[11]	Poor ^[11]
<i>Methanosaeta</i>	Acetoclastic methanogenesis ^[11]	Positive ^[14] Negative ^[1,9,11]	Bioaugmentation ^[14] Foaming ^[1]	Good ^[14] Poor ^[1,9,11]
<i>Methanoculleus</i>	Hydrogenotrophic methanogenesis ^[14]	Positive ^[11,14]	Ammonia inhibition ^[11] Bioaugmentation ^[14]	Good ^[14] Poor ^[11]
<i>Methanomassiliicoccus</i>	Methylotrophic methanogenesis ^[15]	Positive ^[15]	Ammonia inhibition ^[15]	Poor ^[15]
<i>Methanosarcina</i>	Versatile methanogenesis ^[14]	Positive ^[1,11] Negative ^[14]	Foaming ^[1] Ammonia inhibition recovery ^[11] Bioaugmentation ^[14]	Poor ^[1] Good ^[11,14]

continued

Enzymes (genes)				
Protease	Hydrolysis of proteins ^[18]	Positive ^[18]	Process acclimatization to cow manure addition ^[18]	Good ^[18]
Glycine hydroxymethyltransferase (<i>glyA</i>)	Acetate degradation through glycine cleavage pathways ^[8]	Positive ^[8]	Ammonia inhibition ^[8]	Poor ^[8]
Acyl-CoA dehydrogenase (<i>ACADM</i>)	Butyrate degradation through β -oxidation ^[8]	Negative ^[8]	Process acclimatization to cow landfill leachate addition ^[8]	Good ^[8]
Acetyl-CoA C-acetyltransferase (<i>acat</i>)	Butyrate degradation through β -oxidation ^[8]	Negative ^[8]	Process acclimatization to landfill leachate addition ^[8]	Good ^[8]
Phosphate butyryltransferase (<i>ptb</i>)	Butyrate degradation through β -oxidation ^[2]	Positive ^[2]	Biogas slurry reflux application ^[2]	Good ^[2]
Succinyl-CoA (<i>sucC/D</i>)	Propionate degradation ^[11]	Negative ^[11]	Ammonia inhibition ^[11]	Good ^[11]
Malate dehydrogenase (<i>mdhod</i>)	Propionate degradation ^[2]	Positive ^[2] Negative ^[2]	Biogas slurry reflux application ^[2] Organic overloading ^[2]	Good ^[2] Poor ^[2]
Hydrogenase subunit alpha (<i>hydA</i>)	Hydrogen production ^[9]	Negative ^[9]	Low organic loading ^[9]	Good ^[9]
Acetate kinase (<i>ack</i>)	Acetoclastic methanogenesis ^[11]	Positive ^[11]	Ammonia inhibition recovery ^[11] Biogas slurry reflux application ^[2]	Good ^[11,2]
Phosphate acetyltransferase (<i>pta</i>)	Acetoclastic methanogenesis ^[11]	Positive ^[11]	Ammonia inhibition ^[11]	Good ^[11]
Acetyl-CoA decarbonylase (<i>ACDS</i>)	Acetoclastic methanogenesis ^[11]	Positive ^[11]	Ammonia inhibition ^[11]	Good ^[11]
Coenzyme F420 hydrogenase (<i>frh</i>)	Hydrogenotrophic methanogenesis ^[2]	Positive ^[2] Negative ^[2]	Biogas slurry reflux application ^[2] Organic overloading ^[2]	Good ^[2] Poor ^[2]
Methyl coenzyme-M reductase (<i>mcrA</i>)	Methane production ^[9]	Positive ^[9]	Low organic loading ^[9]	Good ^[9]

References: [1] (He et al., 2017) ; [2] (Li et al., 2024); [3] (Poirier et al., 2020); [4] (Ma et al., 2020); [5] (Mugnai et al., 2021); [6] (Xu et al., 2024); [7] (Zhang et al., 2018); [8] (Peng et al., 2022); [9]; (Patil et al., 2021); [10] (Li et al., 2022); [11] (Zhang et al., 2022); [12] (Wang et al., 2020); [13] (He et al., 2018); [14] (Basak et al., 2021); [15] (Hardy et al., 2021); [16] (Amha et al., 2019); [17] (Lv et al., 2020); [18] (Xing et al., 2020) .

1.4. Attributes of microbial indicators

Although several diversity indices, taxa, and genes have been suggested as microbial indicators (MIs), their reliability often suffers due to the lack of multiple attribute assignments surrounding a suitable MI (Fig. 1.4) (Huerta et al., 2024; Li et al., 2018). These attributes include: (1) reproducible responses across diverse processes, implying universality; (2) differential responses proportional to changes in the microbial community/AD, (3) keystones with significant ecological roles within the microbial community; (4) early warning responses; and (5) key microbial metabolism in AD (Huerta et al., 2024; Li et al., 2018; Xu et al., 2018). Each attribute can be defined through an adequate statistical framework to identify step-by-step features of MIs relevant to a specific case study, such as determining suitability for specific key challenges (Li et al., 2018; Navarro-Díaz et al., 2020; Poirier et al., 2020). Therefore, a suitable MI is reliable because it might maintain reproducible responses (attribute 1) across similar processes (e.g., FW digesters) and differentiate multiple microbiome statuses (attribute 2). Additionally, suitable MIs would be essential for maintaining microbiome network structure or functionality under specific conditions (attribute 3), predicting potential operational issues (attribute 4), and describing microbial metabolism (attribute 5). Diversity indices likely satisfy criteria (1), (2), and (4), whereas taxa and genes may fulfill all criteria. Further details of each MI attribute are provided in the following section.

General characteristics of the microbiome in food waste digesters

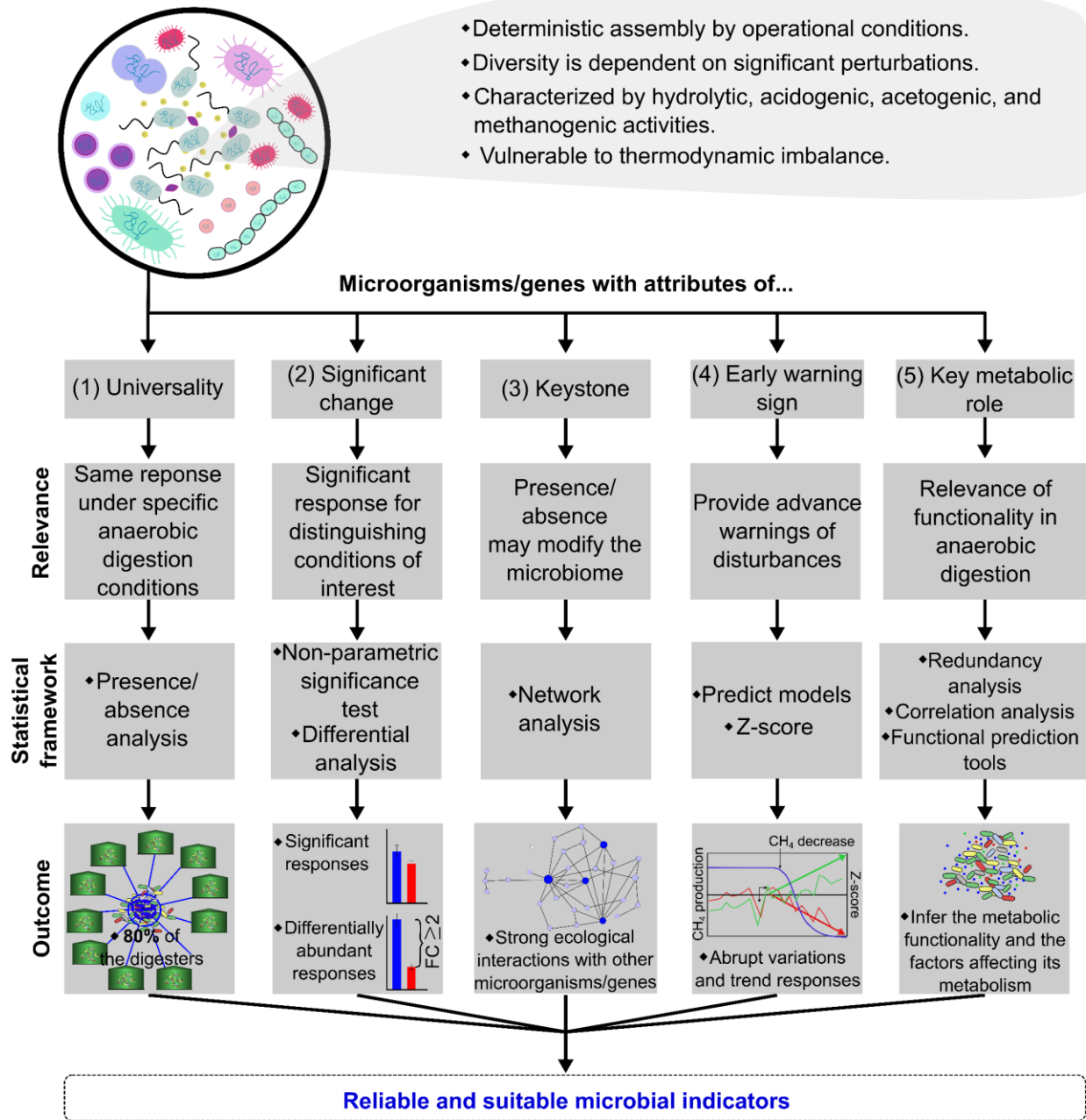


Figure 1.4. Attributes for determining key taxa and genes as suitable MI. Each characteristic encompasses multiple approaches that contribute to the establishment of suitable MI for FW digesters. A comprehensive MI incorporating all attributes would be a reproducible and relevant indicator for maintaining microbiome structure or functionality. Furthermore, it could significantly discern various states of the process, likely owing to its importance in AD metabolism.

1.4.1. Universality

An MI with a universal attribute should exhibit consistent responses under specific AD conditions (Li et al., 2018). This goal may be achieved by considering systems with similar feedstock types and temperatures and recognizing trend responses to significant perturbations that alter the process (Calusinska et al., 2018; Rui et al., 2015; Theuerl et al., 2018; Wu et al., 2021). In this context, the core microbiome may fulfill this attribute. The core microbiome comprises resilient and co-occurrence biological components (e.g., taxa or genes) in ecological niches that are potentially linked to specific microbiome states or environmental conditions (Berg et al., 2020; Theuerl et al., 2018). In AD, this portion of the microbiome is crucial for process functionality and contributes to hydrolysis, VFA oxidation, and methanogenesis (Ma et al., 2021).

The core microbiome of AD is defined by the prevalence of microorganisms across a range of similar processes, particularly under consistent feedstock and temperature conditions. Rui et al. (2015) determined a core microbiome in household biogas digesters, considering a 90% prevalence of OTUs across 43 processes at mesophilic temperatures (18 – 35°C). Similarly, Calusinska et al. (2018) identified two core microbiomes in different mesophilic (33 – 44°C) AD systems: one for biowaste (agriculture and municipal solid waste), and another for sewage-activated sludge. In this study, the core microbiome was defined by OTUs present in over 80% of 250 samples across 20 processes. Both studies observed that certain core microbiome members exhibited correlative responses to inhibitory compounds. Therefore, defining and evaluating the core microbiome under various perturbations affecting FW digesters in the same temperature regime may lead to the identification of universal attribute.

1.4.2. Significant changes

MI should effectively infer the differences of AD conditions, such as stability, key challenges, or recovery states (Wu et al., 2021). For this purpose, significant changes in microbial communities are typically determined using non-parametric tests given that microbiome data, such as OTU or gene counts, often follow a non-normal distribution (Pan et al., 2021). These tests help identify trends associated with AD performance categories, including comparisons between low and high performance or non-inhibited and ammonia-inhibited conditions. Significant changes in microbial abundance are generally classified into two categories: significant and differentially abundant responses. The distinction between these categories largely depends on how the raw data are

transformed, the types of data distributions used in the analysis, and bias correction methods (Pan et al., 2021).

Standard tests, such as the Kruskal-Wallis and Wilcoxon rank-sum tests, have been used to evaluate alpha diversity, taxa, and microbiome functionality across different groups. For example, alpha diversity in sludge, agro-industrial waste, FW, and municipal solid waste digesters have been statistically evaluated (De Vrieze et al., 2021). These analyses have also been used to identify taxa with significant abundance across different feedstocks (Calusinska et al., 2018). Additionally, they have been used to determine which defined functional profiles, based on SEED subsystems and KEGG functions, underline the CH₄ composition (Rahman et al., 2021). Therefore, these statistical analyses provide clear insights into the behavior of key components of the AD microbiome and are recommended for evaluating the core microbiome.

Differential analysis methods (e.g. ALDEx2, DESeq2, edgeR, and LEfSe) encompass the entire microbiome and employ probability distribution models or count ratio transformations to enhance group comparison (Nearing et al., 2022). These analyses reduce false positives among differentially abundant features and provide robust biological interpretation when comparing multiple differential abundance methods (Nearing et al., 2022). Consequently, these biological components are characterized by their discriminative capacity to respond to perturbations that significantly affect AD. Within this framework, differential gene expressions have been observed in response to H₂ addition (Zhu et al., 2020) and key taxa that distinguish feeding regimes have been identified (Svensson et al., 2018). These analyses offer more precise and sensitive insights into critical changes in the entire microbial community than standard tests.

1.4.3. Keystones

Reconstructing ecological networks from microbiomes can reveal positive (cooperative) and negative (antagonistic) interactions, based on their topological properties under specific conditions or challenges, thereby defining their ecological roles (Muller et al., 2018). These analyses identified keystones, either taxa or genes, which are crucial in the ecological interactions of the microbiome and impact ecosystem dynamics (Berg et al., 2020). The removal of keystone elements would mean the elimination of microorganisms or genes that can affect microbiome assembly, alter richness, and potentially disrupt ecosystem functionality (Berry & Widder, 2014). This analysis can be performed using Molecular Ecology Network Analysis (MENA), which

employs random matrix theory with standard parameters to calculate network topological features (e.g. modularity, clustering coefficient, average path length, graph density, and average degree). Network modularity allows keystones to be categorized based on within-module connectivity (Z_i) and among-module connectivity (P_i) scores. Keystones are classified as generalists (highly connected with others: $Z_i > 2.5$, $P_i > 0.62$; or $Z_i < 2.5$, $P_i > 0.62$) or specialists (less connected with others: $Z_i < 2.5$, $P_i < 0.62$) (Pan et al., 2021).

Keystone species in AD have been identified as indicators of process regulation (Xu et al., 2018). For instance, *Tepidimicrobium* and *Clostridium* are the keystones of a microbiome that is subject to variations in the C/N ratio. These genera are crucial for maintaining high biogas production at low abundances, considering their negative relationship with C/N (Fernandez-Bayo et al., 2020). Additionally, keystones defining ecological roles based on temperature regimes have been identified, such as *Streptococcus* and *Methanospirillaceae* in mesophiles and *Ruminofilibacter*, *Paludibacter*, *Fibrobacter*, *Lachnospira*, and *Anaerobaculaceae* in thermophiles (Guo et al., 2022). These findings suggest that keystones can serve as indicators of specific conditions, although their responses to key challenges remain unclear (Berg et al., 2020). Therefore, incorporating the keystone characteristic into an MI is essential to reveal the stability of the conditions to be evaluated.

1.4.4. Early warning signs

The importance of proposing EWI lies in its ability to predict process instability, thus enabling the development of strategies to maintain AD stability (Wu et al., 2021). Given that changes in the microbiome precede macroscopic changes, the predictive capacity of MI can be inferred (Li et al., 2018; Wu et al., 2021). This capability can be attributed to abrupt changes in the microbiome (taxa or genes) that anticipate AD before disturbances occur (Cordier et al., 2020; Wu et al., 2021). These irregular changes include increased variance, signifying an abrupt response (e.g., z score $> |1|$), along with a correlation indicating the direction (positive or negative slope) from one state to another (Faust et al., 2015; Mirza et al., 2020). Predictive models can also provide trends that indicate possible perturbations (Faust et al., 2015). In AD, linear regression showed a sudden reduction in the *mcr* gene (methyl-coenzyme M reductase), which serves as an indicator of decreased methanogenic activity, offering an early warning of reduced CH_4 production (Yu et al.,

2020). These trends could set a benchmark for warning alerts regarding the conditions that significantly disrupt AD.

Evidence indicates that microorganisms respond days before an operational issue occurs in AD. Within a range of 8 to 11 d before over-acidification occurred, *Methanomassiliicoccus* and *Syntrophobacter* exhibited declining abundance (Goux et al., 2015; He et al., 2018). *Anaerolinea* and *Methanosarcina* showed negative abundance trends at approximately 2 and 14 d, respectively, before CH₄ production ceased (He et al., 2018; Tonanzi et al., 2020). The relative fluorescence intensity of coenzyme F420 linked to the *frh* gene decreased approximately 20 d before over-acidification (Shamurad et al., 2020). The *hdr* gene exhibited a positive trend approximately 20 d before instability (Li et al., 2024). The increase in the *acs* gene seems to signal at least 23 days before ammonia inhibition occurs (Yu et al., 2020). These results support the idea that changes in functionality precede variations in taxonomic composition, thereby offering an advantage to MI based on genes (Cordier et al., 2020). Additionally, an MI with early warning attributes provides crucial timeframes for planning system recovery strategies.

1.4.5. Key metabolic roles

Understanding the metabolic pathways involved in different AD states is crucial for advancing bioprocess engineering to achieve high-efficiency and productive stability (Xu et al., 2018). A suitable MI should represent specific metabolic pathways that are modified and can indicate a state change in AD (Huerta et al., 2024; Li et al., 2018). First, this attribute can be suggested through correlational (e.g., Spearman's correlation) and multivariate (e.g., redundancy analysis) analyses using monotonic and linear relationships. This approach employs taxonomic and functional information, in addition to physicochemical parameters (Liu et al., 2021; Ramette, 2007). These results may provide insights into microbial functionality or reveal the factors influencing the variability of taxa and genes (Buttigieg & Ramette, 2014; Carballa et al., 2015). This is clearly supported by information from literature.

In general, correlational and multivariate analyses are essential for identifying key taxa and genes that influence AD processes and performance. For instance, redundancy analysis (RDA) indicated that propionate and acetate accumulation were precursors to ammonia inhibition, which decreased CH₄ yield. These conditions created an environment favoring acid-producing, acid-resistant, or

ammonia-resistant microbes, such as *Proteiniphilum*, *Ruminococcaceae*, and *Methanobacterium*, but negatively affected syntrophic VFA-oxidizing bacteria, such as *Sedimentibacter* (Peng et al., 2018). Spearman's correlation has also been used to identify important metabolic activities in AD, such as *Methanosarcina*, owing to its positive correlation with CH₄ concentration (Rahman et al., 2021). Although RDA indicates which key taxa or genes may be beneficial or detrimental, based on physicochemical variables, correlational analyses specify which metabolites are directly linked to each taxon.

On the other hand, functional prediction tools enable deeper insights into genes associated with metabolic pathways affected under various conditions. For instance, PICRUSt2 has highlighted the relevance of the F-type ATPase functional gene, which is present in some microorganisms and helps them persist during ammonia inhibition. This is because it encodes a protein complex that releases H⁺ by consuming ATP when NH₃ permeates the cell, an action triggered by high ammonia concentrations (Yu et al., 2021). Prokka, used for metagenomics, has provided an associative insight between genera and genes through metagenome-assembled genomes (MAG), allowing functional characterization of key microorganisms in key challenges. For instance, it has been confirmed that the bacterium *Eubacterium callanderi* TJU0021 is a significant SAOB in ammonia-inhibited processes because it possesses marker genes *acsB*, *acsC*, *acsD*, and *fhfs* related to the W-L pathway (Xu et al., 2024). These tools enhance our understanding of microbiome functionality under various challenges, enabling the identification of critical associations between taxa and genes, thereby providing more specific insights into the status of the microbial community.

1.5. Hypotheses and objectives

1.5.1. Hypotheses

- The application of a statistical framework to explore microbial indicator attributes using taxonomic and functional information from various food waste digesters will validate the discovery of reliable and suitable microbial indicators for monitoring anaerobic processes fed with organic solid waste.

1.5.2. General objective

- To validate the application of a statistical framework for identifying suitable and reliable microbial indicators for monitoring anaerobic processes fed with organic solid waste.

1.5.3. Specific objectives

- To identify reliable microbial indicators to detect key challenges in anaerobic digestion of the organic fraction of municipal solid waste and food waste, specifically related to CH₄ yield, through a meta-analysis.
- To determine suitable microbial indicators to detect a key challenge (ammonia inhibition) in anaerobic digestion processes using food waste.
- To evaluate the response of reliable and suitable microbial indicators for detecting ammonia inhibition by monitoring an anaerobic sequencing batch reactor system under perturbations.

CHAPTER 2. Research design

The identification of reliable and suitable MIs involved a research design focused on a systematic methodology considering research criteria, such as neutrality, reliability, and validity, as outlined by Johnson and Waterfield (2004) (Fig. 2.1). This thesis comprises of three stages. First, the discovery phase involved a meta-analysis to identify reliable MIs. Subsequently, two application phases were conducted to pinpoint key challenges in FW digesters and monitoring indicators in a semi-continuous process. This study utilized a multi-omics approach to ensure consistent MI responses, regardless of the sequencing technology used. General details of each experimental stage are provided below, with specific methodologies detailed in the corresponding chapters.

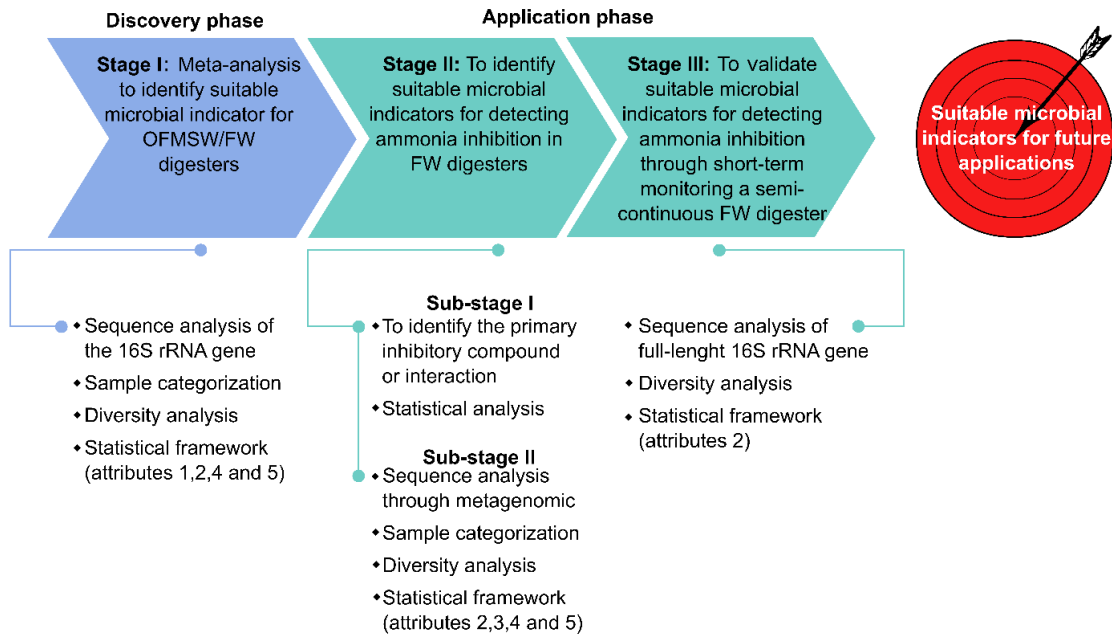


Figure 2.1. Research design for identifying suitable microbial indicators for FW digesters. The numbering shown in the statistical framework indicates the MI attributes analyzed at each stage: (1) universality, (2) significant change, (3) keystone, (4) early warning sign, and (5) key metabolic roles.

The first stage involved a meta-analysis of samples with taxonomic information related to 16S rRNA gene sequences from various anaerobic processes fed with OFMSW/FW (Chapter 3 of this thesis). This section focuses on the reliability and neutrality research criteria. The aim was to ensure that suitable MIs provided reproducible responses regardless of the process configuration, primer region, and sampling techniques within a context encompassing multiple anaerobic systems. Samples were initially identified through a literature search on microbial community evaluation in similar processes. Samples were chosen based on a selection criterion, and physicochemical characteristics (e.g., VFA, ammonia, LCFA, and CH₄ yield) were determined. The samples were categorized based on the CH₄ yield, and the microbial communities were analyzed. A statistical framework was then applied considering the attributes of (1) universality, (2) significant change, (4) early warning signs, and (5) key metabolic roles. The outcome was the identification of suitable MIs capable of indicating the performance of the OSW digesters.

The second stage involved testing the response of suitable MIs to detect a specific challenge in FW digesters. Because of the interactions between inhibitory metabolites released in FW digesters, an experimental design with two substages was necessary. In sub-stage I, an experimental assay identified the primary compound or interaction with the most significant inhibitory effect on CH₄ yield in an AD batch system fed with FW (Chapter 4 of this thesis). Statistical analyses confirmed that ammonia was the inhibitory compound of interest, which is a recurrent challenge in FW digesters. Consequently, in sub-stage II, the response of the potential MI reported in the literature was evaluated for its capacity to describe ammonia inhibition (Chapter 5 of this thesis). An ammonia concentration gradient was designed to cover three levels: non-inhibitory, inhibitory, and minimum inhibitory. Metagenomics provided taxonomic and functional information about the microbiome at each inhibitory level. A statistical framework was then applied, incorporating the attributes of (2) significant change, (3) keystone, (4) early warning signs, and (5) key metabolic roles. The results identified a suitable MI for efficiently detecting ammonia inhibition issues in FW digesters.

In the third stage, reliable and suitable MIs were evaluated to detect ammonia inhibition in samples from an anaerobic sequencing batch reactor (AnSBR) under perturbations (Chapter 6). The experiment was divided into four processes, each distinguished by the concentration of ammonia added at the start of the operating cycle. All processes involved an AnSBR system subjected to

variations in the feedstock composition. The microbial community was monitored in key cycles characterized by the peak CH₄ productivity, lowest CH₄ production, and process recovery. Community structure was assessed by full-length 16S rRNA gene sequencing. To confirm the effectiveness of the MIs in detecting ammonia inhibition, only attribute (2) significant change was evaluated using center log ratio (CLR) transformation for data standardization. The combination of genera and genes revealed metabolic profiles linked to syntrophic activities affected by ammonia that were undetectable through physicochemical parameters. These MIs were deemed reliable for identifying ammonia inhibition in an FW digester system, regardless of feedstock variations.

CHAPTER 3. Identifying reliable microbial indicators in anaerobic digestion of organic solid waste: Insights from a meta-analysis

3.1. Abstract

The identification of microbial indicators holds great potential for detecting key challenges in anaerobic digestion, driving microbial management. However, reliable microbial indicators must possess attributes such as universality, significant abundance changes under stress, and the ability to predict CH₄ yield. A meta-analysis of 178 publicly available 16S rRNA gene sequences from 12 studies on the digestion of organic solid waste was conducted to evaluate microbial indicators' performance. Alpha diversity analysis revealed that a specialized genus-level microbial community, with a high number of sOTUs, was essential for achieving high CH₄ yield. Key taxa such as *Aminobacterium*, *Clostridium*, HA73, T78, *Corynebacterium*, *Lactobacillus*, and *Prevotella* exhibited the greatest number of microbial indicator attributes, including significant changes, predictive capability for CH₄ yield, and association with inhibitory compounds. Based on these unique characteristics, various detection applications were suggested. *Corynebacterium*, *Lactobacillus*, and *Prevotella* were recommended for their robust fold-change attribute, indicating a high likelihood of successful categorization. *Aminobacterium*, *Clostridium*, HA73, and T78, as core microbiome members, were linked to universality, suggesting their easy detection across various anaerobic digestion processes. Understanding the strengths and limitations of these indicators will support the selection of appropriate detection techniques. These microbial indicators could help address key challenges, improve conventional monitoring systems, and be implemented in models for the development of new control systems

Reference to the published work

Jonathan Cortez-Cervantes, Iván Moreno-Andrade, Ana E. Escalante, Daniel de los Cobos-Vasconcelos, Julián Carrillo-Reyes. *Identifying reliable microbial indicators in anaerobic digestion of organic solid waste: Insights from a meta-analysis* **Journal of Environmental Chemical Engineering**, 12 (5), 2024 <https://doi.org/10.1016/j.jece.2024.113392>

3.2. Introduction

AD is an industrial process for valorizing organic solid wastes, like the OFMSW and FW, into CH₄, producing typically 400-500, or up to 700 L of CH₄ per kg of added volatile solids (VS_{added}), a yield which strongly depends on the biodegradability of the feedstock (Mao et al., 2015; Wang et al., 2018). Despite the steady growth in AD utilization, several operational challenges persist, impacting CH₄ production and yield. These challenges include the accumulation of metabolic compounds, foaming, among others, which can also induce alterations in the microbiome (Wu et al., 2021). To ensure the stability of CH₄ production, indicators sensitive to disturbances and linked to process stability must be monitored (Wu et al., 2019). If an indicator responds faster to disturbances than to changes in CH₄ production, it can be used as an EWI of process instability. Currently, the indicators used are typically based on physicochemical parameters such as biogas content and yield, pH, total and individual VFA, alkalinity ratios, and ammonia (Wu et al., 2021). However, physicochemical indicators have limitations in identifying the underlying causes of key challenges, offering only a broad process overview and having only a limited number of parameters suitable for EWI (Sun et al., 2019; Wu et al., 2021; Wu et al., 2019). Therefore, there is a pressing need to discover supplementary indicators that fill those gaps in conjunction with physicochemical indicators.

Microbial communities play a crucial role in the AD process by driving the conversion of organic waste into valuable products through complex metabolic interactions. As a result, the concept of microbial management has emerged, encompassing the application of techniques to modulate microbial communities to enhance the efficiency of AD (Carballa et al., 2015; Li et al. 2018). The implementation of microbial management relies on microbial indicators (MI), which are biological responses at different biological organization levels that provide valuable insights into the conditions of the microbial community involved in the AD process (Carballa et al. 2015; Huerta et al., 2024). In this sense, MI might be conceived from two approaches: i) focusing on the whole community perspective by diversity indices, or ii) on specific microorganisms by key taxa (Carballa et al., 2015; De Vrieze, 2020).

The alpha and beta diversity metrics can profile patterns in the entire microbial community structure depending on process performance (De Vrieze, 2020). For instance, the Shannon diversity index and OTU count revealed a reduction in their values as CH₄ yield decreased, which

CHAPTER 3. Identifying reliable microbial indicators in anaerobic digestion of organic solid waste: Insights from a meta-analysis

was attributed to elevated substrate concentrations (Basak et al., 2021). Beta diversity analysis enabled visualization of distinct microbial community clusters corresponding to different state phases of AD, mirroring the variations in physicochemical indicators such as total VFA (VFAt), ammonia, and CH₄ yield (Peng et al., 2018). While diversity indices capture microbial community alterations, it is essential to acknowledge their specificity to individual studies, potentially lacking equivalent responses across different processes (Li et al., 2018).

Key taxa have been proposed as an explanation for perturbations in AD. For example, deficiencies in ammonia, nutrients, and trace elements can hinder the activity of acetoclastic methanogens, leading to the accumulation of acetate and affecting CH₄ production (Li et al., 2017). Shifts in the archaea community were linked to the inhibitory power of ammonia, observed a transition from acetoclastic methanogen *Methanosaeta* to versatile methanogen *Methanosarcina*, followed by the emergence of hydrogenotrophic methanogen *Methanoculleus* (Hardy et al., 2021). This transition of the methanogenic pathway may result in a decrease in CH₄ production by up to 30% (Li et al., 2018). Understanding the relationship between key taxa dynamics and their responses to physicochemical parameters are promising for diagnosing and addressing key challenges in AD systems.

In a scenario with similar feedstocks, such as the OFMSW and FW, and identical temperature regimes, it becomes easier to identify common microorganisms forming a representative core microbiome (Xu et al. 2018). This will enable the discovery of reproducible microbial communities. The core microbiome refers to a ubiquitous and consistent set of microorganisms that are commonly found in microbial communities within similar habitats (Berg et al., 2020). Detecting the presence of the core microbiome is feasible and has been suggested that its abundance and presence is crucial for AD performance and stability (Xu et al., 2018). Therefore, evaluating the core microbiomes of different AD systems with common feedstocks and temperature is a viable strategy for identifying universal MI. Previous studies highlight MI attributes such as universality, differential abundance between categories of interest (fold change), binary response (e.g., presence or absence), predicted response as potential early warning signals, and have a relevant role in AD (Carballa et al., 2015; Huerta et al., 2024; Li et al., 2018). The incorporation of multiple characteristics is indicative of suitable MI (Huerta et al., 2024). Although MI has been suggested to have some of these attributes for specific AD processes, proving its

CHAPTER 3. Identifying reliable microbial indicators in anaerobic digestion of organic solid waste: Insights from a meta-analysis

viability remains challenging (Li et al., 2018; De Vrieze 2020; Wu et al., 2021). In this sense, integrative studies analyzing several processes with standard operational attributes, such as a meta-analysis with a proper analytical framework, have been suggested to identify reliable MI, minimizing bias related to process specificity (Navarro-Díaz et al., 2020; Poirier et al., 2020).

This study aimed to find a reliable MI to detect key challenges in AD of OFMSW and FW associated with CH₄ yield through a meta-analysis. It introduces a statistical framework using publicly available 16S rRNA gene sequences for the analysis of diversity indices, core microbiome, and the whole microbial community. This approach integrates various MI attributes, including significant abundance variations across groups (such as methane yield categories), their occurrence within specific AD systems (core microbiomes), their predictive capability for CH₄ yield, and their response in association with AD metabolites. Defining reliable MI is a promising strategy for implementing microbial management to control the performance of AD systems.

3.3. Material and methods

3.3.1. Data collection

This meta-analysis targeted similar feedstocks such as OFMSW and FW to pinpoint reliable MIs, considering the impact of feedstock composition on microbial community structure (Li et al., 2018; Xu et al., 2018). The 16S rRNA sequences were selected from a comprehensive search in the Scopus database employing the following terms within article titles, abstracts, and keywords: “OFMSW” OR “food waste” AND “anaerobic digestion” OR “methanogenesis” AND “microbial community” OR “16S rRNA” OR “16S” OR “metagenomic”. The following selection criteria were applied to the studies included in the meta-analysis: SRA database, demultiplexed paired-end sequences with publicly available anaerobic digesters producing CH₄, and the sample names matching between metadata submission and article information. After the selection process, 12 studies with 178 samples consisting of 1% full-scale, 24% pilot-scale, and 75% lab-scale processes, were included (Table 3.1). Information about operative and physiochemical parameters from the studies was used to create a metadata set, including types of feedstocks, reactors and scales-up, inoculum source, general operational parameters, TAN, free ammonia, LCFA, VFA, and CH₄ yield.

3.3.2. 16S rRNA sequencing datasets processing

The raw reads (.fastq) sequenced from microbial samples in the OSW digester were retrieved using run accession through SRA toolkit software. Sequences quality was analyzed using the FastQC tool (Wingett & Andrews, 2018) ensuring an efficient and accurate retrieval of the desired sequencing data, facilitating subsequent analysis and interpretation. The files and metadata were introduced into Qiime2 (v. 2021.4) (Bolyen et al., 2019) as artifacts and analyzed using a modified protocol proposed in (Estaki et al., 2020). The samples were sorted by 16S rRNA region groups, namely the V3-V4 and V4 regions for the bacteria-archaea set (n = 158) and the V3-V5 region for the archaea set (n = 20). This grouping was carried out to minimize bias during sequence processing because the Deblur algorithm has limitations regarding the diversity of the amplicon sequences (Amir et al., 2017).

The quality filter method was used to filter the raw sequences using default settings (Phred quality score = 4). Deblur was then employed to denoise the filtered sequences using default settings, with the trim length varying depending on the group analyzed: 220 bp for the bacteria-archaea set and

200 bp for the archaea set. The result of the analysis was the creation of sub-operational taxonomic units (sOTUs) that utilize error profiles to achieve a level of single-nucleotide resolution, which helps deduce the most likely true sequences present in each sample (Amir et al., 2017). The fragment-insertion method was used to enhance the accuracy of phylogenetic diversity analyses, which involved aligning the sOTUs against a reference tree using the Silva 128 SEPP reference database. This process also helped to remove erroneous sequences from the dataset (Estaki et al., 2020; Janssen et al., 2018; Quast et al., 2013). Additionally, the classify-sklearn algorithm was used to assign annotations to each sOTUs by mapping them against the Silva 138 99% OTUs full-length sequence (Bokulich et al., 2018). The sOTUs tables obtained were combined, and only five samples that did not identify both bacteria and archaea populations were excluded, resulting in 153 samples. Random subsampling without replacement was conducted using the first quartile frequency (11542 sOTUs) to rarefy sequencing depth across all. This approach guaranteed that richness estimates remained unaffected by variations in sequencing depth. As a result, 39 samples were excluded ($n = 114$). The analysis was conducted using the "rarefy_even_depth" function from the "phyloseq" package (McMurdie & Holmes, 2013). The nature of the meta-analysis introduces variability in the 16S rRNA gene, leading to differences in the classification of sOTUs among the studies. Therefore, the statistical analyses used to highlight MI attributes were conducted at the genus level to help minimize these difference (Martínez-Porchas et al., 2016).

3.3.3. Categorization of samples according to CH₄ yield.

CH₄ yield (measured in mL CH₄/gVS_{added}) is commonly used as a process indicator; thus, it was selected as both a categorical and quantitative variable for classifying AD performance (Wu et al., 2021). This classification, known as the methane yield category, was derived from the classes of a beta distribution histogram following the Freedman-Diaconis rule (Han et al., 2012). The establishment of frequency and intervals for each class in the distribution histogram was determined using the Freedman-Diaconis rule (Eq. 3.1). This rule enables the creation of histograms from continuous and unimodal probability distributions and minimizes the difference between empirical and theoretical probability distributions (Freedman & Diaconis, 1981).

$$\text{Class width} = 2 \frac{\text{IQR}}{\sqrt[3]{n}} \quad \text{Eq. 3.1}$$

where IQR is the interquartile range of the data, and n is the number of observations.

Methane yield data were determined to follow a beta distribution using the "descdist" function from the "fitdistrplus" package (Delignette-Muller & Dutang, 2015). To define methane yield categories, the "nclass.FD" function from the "grDevices" package was applied to establish class ranges. These categories were evaluated using the Kruskal-Wallis test (p-value < 0.05) via the "kruskal.test" and "p.adjust" functions from the "stats" package. Pairwise comparisons within methane yield categories were performed using the Wilcoxon rank sum test with Benjamini-Hochberg correction (p-value < 0.05), utilizing the "pairwise.wilcox.test" function from the "stats" package. Data visualization was conducted through boxplot analysis using the "ggplot2" package (Wickham, 2016).

3.3.4. Diversity analysis

Diversity analyses were performed and compared using a rarefied count table at sOTU level and genus level. Comparing different biological classifications would yield distinct results for each level, helping to formulate a more consistent hypothesis (Martínez-Porchas et al., 2016). Alpha diversity was grouped from methane yield categories and assessed using multiple indices, including Chao1, Pielou's evenness, Shannon, and Hill numbers (q0, q1, and q2). Beta diversity was measured using the Bray-Curtis distance. Alpha diversity indices were calculated using the "phyloseq" and "hilldiv" packages. The beta diversity index and its corresponding statistical tests were calculated using Qiime2 software.

3.3.5. Selecting the core microbiome

The sOTU table at the genus level was used to identify the core microbiome. This process involved creating a presence-absence matrix, where "1" and "0" values represent the presence or absence of genera, respectively. Considering the influence of temperature on microbial community structure (Rahman et al., 2021; Xu et al., 2018), the core microbiome was defined as the genera present in at least 80% of mesophilic AD process samples. This approach increases the number of microorganisms of interest within 84% of the total collected samples. The presence-absence matrix was visualized using the "pheatmap" package (Kolde, 2012).

Table 3.1. General operational characteristics of OSW digesters selected for the meta-analysis

Article	Run accession	Feedstock	Reactor type	Temperature (°C)	Feeding regime	Inoculum source	16S rRNA gene region	Reference	DOI	
F27	SRR5410170, SRR5410182, SRR5410186, SRR5410188, SRR5410196, SRR5410199, SRR5410205, SRR5410209, SRR5410212	SRR5410171, SRR5410183, SRR5410187, SRR5410190, SRR5410198, SRR5410200, SRR5410207, SRR5410212	Food waste and fats oil grease	CSTR	55	Batch	Anaerobic digester fed wastewater	V4	Amha et al., 2017	https://doi.org/10.1016/j.watres.2017.06.065
F2	SRR13078098, SRR13083415, SRR13083583, SRR13083619	SRR13083404, SRR13083422, SRR13083608,	Food waste leachate	CSTR	37	Batch	Anaerobic digester	V3-V4	Basak et al., 2021	https://doi.org/10.1016/j.scitotenv.2020.144219
F21	SRR6488989, SRR6488993, SRR6488997	SRR6488991, SRR6488995,	Food waste recycling wastewater	AnCMBR	36	Semi continuous	Domestic wastewater	V3-V4	Cho et al., 2018	https://doi.org/10.1016/j.biortech.2018.02.015
F24	SRR6067591, SRR6067593, SRR6067614, SRR6067618	SRR6067592, SRR6067607, SRR6067616,	Acidogenic effluent from food waste fermenter	CSTR	37	Semi continuous	Anaerobic digester fed food waste	V3-V4	Gaby et al., 2017	https://doi.org/10.1186/s13068-017-0989-4
F25	SRR4434290, SRR4434487, SRR4434489, SRR4434528, SRR4434577, SRR4436424, SRR4436427, SRR4436429, SRR4436431, SRR4436433, SRR4436435, SRR4436436	SRR4434482, SRR4434488, SRR4434490, SRR4434576, SRR4434578, SRR4436426, SRR4436428, SRR4436430, SRR4436432, SRR4436434,	Food waste	SBR	37	Semi continuous	Anaerobic digester fed household waste	V3-V4 V3-V5	He et al., 2017	https://doi.org/10.1038/s41598-017-14258-3
F17	SRR5650604, SRR5650606, SRR5650608, SRR5650609	SRR5650605, SRR5650607,	Food waste and fats oil grease	CSTR	35	Semi continuous	Anaerobic digester fed food waste	V3-V4	He et al., 2018	https://doi.org/10.1186/s13568-018-0623-2

CHAPTER 3. Identifying reliable microbial indicators in anaerobic digestion of organic solid waste: Insights from a meta-analysis

F4	SRR12007279, SRR12007282, SRR12007284, SRR12007286, SRR12007288, SRR12007290,	SRR12007281, SRR12007283, SRR12007285, SRR12007287, SRR12007289, SRR12007291	Food waste	SBR	55	Semi continuous	Anaerobic digester fed food waste sewage sludge	V3-V4	Lim et al., 2020	https://doi.org/10.1016/j.biortech.2020.123751
F17	SRR13976544, SRR13976546	SRR13976545,	Food waste	Batch	37	Batch	Anaerobic digester aerobic- system	V3-V4	Patil et al., 2021	https://doi.org/10.1016/j.biortech.2021.125123
F19	SRR3629052, SRR3629058, SRR3629149, SRR3629151, SRR3629153, SRR3629253, SRR3629264, SRR3629273, SRR3629279, SRR3629300,	SRR3629054, SRR3629059, SRR3629150, SRR3629152, SRR3629154, SRR3629255, SRR3629270, SRR3629277, SRR3629280, SRR3629328	Food waste	CSTR	36	Semi continuous	Anaerobic digester fed food waste	V3-V4 V3-V5	Peng et al., 2018	https://doi.org/10.1016/j.biortech.2018.04.076
F16	SRR6484246, SRR6484248, SRR6484250, SRR6484252, SRR6484254, SRR6484256, SRR6484258, SRR6484260, SRR6484265, SRR6484267, SRR6484269, SRR6484271, SRR6484273, SRR6484275, SRR6484277, SRR6484279, SRR6484281	SRR6484247, SRR6484249, SRR6484251, SRR6484253, SRR6484255, SRR6484257, SRR6484259, SRR6484263, SRR6484266, SRR6484268, SRR6484270, SRR6484272, SRR6484274, SRR6484276, SRR6484278, SRR6484280,	Food waste	semi CSTR	37	Semi continuous	Anaerobic digester fed food waste	V3-V4	Svensson et al., 2018	https://doi.org/10.1016/j.biortech.2018.08.096

continued

3.3.6. Statistical analysis

A comprehensive statistical approach was applied to identify reliable MIs by incorporating univariate and differential, and correlation analyses alongside a generalized additive model for location, scale, and shape (GAMLSS). All statistical analyses were performed using R version 4.2.1. The statistical approach evaluates the entire microbial community through key diversity indices and identifies key taxa based on the presence of the following MI attributes: i) an approximation of the characteristic of universality was associated with significant changes in the core microbiome (Li et al., 2018; Xu et al., 2018); ii) the robust fold-change attribute was associated with relatively significant changes in the abundance of members of the whole microbial community (Nearing et al., 2022; Xu et al., 2018); iii) the ability of key alpha diversity and key taxa to predict CH₄ yield was evaluated (Carballa et al., 2015); and iv) the relevant role of key taxa under stress conditions in AD was correlated with metabolites commonly associated with inhibition phenomena, including TAN, LCFA, and VFA (Huerta et al., 2024; Li et al., 2018). The following sections detail the statistical analysis applied to identify MI attributes.

3.3.6.1. Key diversity indexes

The methane yield categories were employed to compare the responses of alpha and beta indices through boxplots and principal coordinate analysis (PCoA), respectively. The results were used to identify key diversity indices within and among the methane yield categories. Alpha diversity was categorized and evaluated based on methane yield categories. The interaction among these categories and alpha diversity was evaluated using Kruskal-Wallis and Wilcoxon rank sum tests with Benjamini-Hochberg correction as detailed in section 3.3.3. The beta diversity analysis was conducted by categorizing data based on methane yield and case study. The relationship between groups and beta diversity was visualized using a vega editor (<https://vega.github.io/>) and assessed using analysis of similarities (ANOSIM) with 999 permutations ($p < 0.05$).

3.3.6.2. Universality

The core microbiome was determined based on its high occurrence properties ($\geq 80\%$ occurrence of samples from mesophilic anaerobic processes). The Hellinger transformation was applied to reduce the possibility of low counts and numerous zero values in the relative abundance of core microbiome (Buttigieg & Ramette, 2014). The core microbiome was analyzed using Kruskal-Wallis test for differences between categories and Wilcoxon rank sum test with Benjamini-Hochberg correction within categories.

3.3.6.3. Robust fold change

Differential analyses assessed the abundance of the entire microbial community across methane yield categories. Multiple differential analyses, recommended for identifying robust fold changes in genera were applied due to the varying data distributions inherent to metanalyses (Nearing et al., 2022). These analyses models read count data across a range of distributions and apply diverse data transformations and hypothesis tests. Genera considered robust fold change attribute appeared in at least two differential analyses (Nearing et al., 2022). Typically, differential analyses identify genera with significant fold changes between two relevant study groups (Zhang et al., 2021). Considering theoretical CH₄ yield (~ 400 mL CH₄/gVS_{added}) and the methane yield categories then were defined as two groups: low CH₄ yields (methane yield categories C1, C2, and C3, encompassing intervals < 400 mL CH₄/gVS_{added}) and high CH₄ yields (methane yield categories C4, C5, and C6, intervals > 400 mL CH₄/gVS_{added}) (Li et al., 2018).

Different analytical methods require either rarefied or non-rarefied genus abundance data. The non-rarefied genus count table (n = 158) was used in ALDEx2, DESeq2, and edgeR to minimize potential false positives. In contrast, the rarefied genus abundance table (n = 114) was applied in LEfSe to account for read depth variations (Nearing et al., 2022). ALDEx2 employed a Monte Carlo simulation within a Dirichlet distribution to estimate genus counts, followed by a centered log-ratio (CLR) transformation. Welch's t-test, adjusted with Benjamini-Hochberg p-values, tested median CLR differences (Fernandes et al., 2013). DESeq2 modeled the variance-mean relationship of genus counts using a negative binomial distribution and tested log₂ fold changes with the Wald test (Love et al., 2014). EdgeR also used negative binomial distribution, applying an empirical Bayes procedure to address overdispersion, with Fisher's exact test to assess log₂ fold changes (Robinson et al., 2009). LEfSe detected significant genera using the Kruskal-Wallis and Wilcoxon rank-sum tests, estimating effect sizes with linear discriminant analysis (Segata et al., 2011). A Venn diagram showing overlapping taxa across these differential methods. The ALDEx2, DESeq2, edgeR and LEfSe analysis were performed according to the conventional workflow described in their documentation of "ALDEx2", "DESeq2", "edgeR" and "lefsr" packages respectively. The Venn diagram was created using the "ggvenn" package.

3.3.6.4. Predictive capability

The capability of key alpha diversity indices and key taxa with universality or robust fold changes attributes to predict the CH₄ yield were evaluated applying GAMLSS (Rigby et al., 2005). Additionally, to test whether the model performance could be improved, reported physicochemical indicators, such as TAN and acetic acid, were added. Two models were considered: the first model utilized only potential MI as an explanatory variable (Eq 3.2), whereas the second model used both microbial and physicochemical indicators (Eq. 3.3) to predict CH₄ yield:

$$E[M_i|MI_i] = \beta_0 + f_i(MI_i) + \epsilon_i \quad \text{Eq. 3.2}$$

$$E[M_i|MI_i, PI_i] = \beta_0 + f_i(MI_i) + f_i(PI_i) + \epsilon_i \quad \text{Eq. 3.3}$$

Where M_i is the response variable given by the CH₄ yield (mL CH₄/gVS_{added}), MI_i is the value of the microbial indicator (rarefied relative abundance or index value), PI_i is the value of the physicochemical indicator (mg/L), f_i is a penalized B-spline function (non-parametric smooth function) to fit the estimator coefficients to a nonlinear response variable and ϵ_i is the residual error of the model. In some cases, the first term was removed from the equation because some indicators had a better fit to a linear regression.

The generalized R-squared (R^2) values were used to determine the proportion of variance explained by each model, while the Akaike Information Criterion (AIC) was employed to evaluate the importance of the indicators in predicting the CH₄ yield. Models with higher R^2 values, preferably close to 1, and lower AIC values selected microbial indicators that were the most effective in predicting CH₄ yield. The Wald test was used as a statistical test to assess whether the estimated coefficients for a predictor variable used in the GAMLSS significantly differed from zero based on the estimated standard error of the coefficient and assuming a normal distribution. GAMLSS and its statistical significance were obtained using the "gamlss" package (Rigby et al., 2005).

3.3.6.5. Relevant roles in inhibition

Correlation analysis was used to determine the potential role of key taxa with metabolites associated with inhibition. The results provide insights into how the abundance of key taxa may be related to the concentration of these metabolites and their possible metabolic roles. Complete

CHAPTER 3. Identifying reliable microbial indicators in anaerobic digestion of organic solid waste: Insights from a meta-analysis

matrices were constructed resulting in a TAN matrix (n = 46), LCFA matrix (n = 26), and VFA matrix (n = 23). Each matrix was assembled to include the largest number of samples that assessed these metabolites along with their respective microbial community characterization, with a focus on key taxa. Other common metabolites between the studies were incorporated to confirm the reproducible responses of the MI.

Variables in the matrices may not meet statistical assumptions, such as normal distribution, or may be incompatible due to differing units (Buttigieg & Ramette, 2014). Hellinger transformation was applied to the microbial community (see section 3.3.6.2.), and logarithmic transformation was used to reduce skewness and achieve linearity in concentrations of AD by-products and CH₄ yield. (Buttigieg & Ramette, 2014). The correlation matrix was constructed using Spearman's correlation coefficients (R_s) with the "cor" function from the "stats" package. The "cor.mtest" function from the "corrplot" package was used to determine the p-values (p-value < 0.05) of correlation matrix (Wei & Simko, 2021).

3.4. Results and discussion

3.4.1. Sample selection, processing, and categorization

From the initially chosen AD manuscripts focused on OFMSW and FW carrying out microbial characterization, the number of manuscripts decreased as the selection criteria were applied in sequence. The criteria included Scopus systematic search, public database sequences, demultiplexed paired-end data from MiSeq sequencing, and CH₄-producing process data matching with sample names in the data repository. These resulted in a total of 358, 53, 30, and 12 studies respectively, after applying each criterion. In total, 178 samples were collected from these 12 selected studies recovering 11,267,664 raw sequences from the bacteria-archaea set and 1,202,736 raw sequences from the archaea set. Following a quality filter and denoising algorithm, 3,256,743 sequences were retained for the bacteria-archaea set and 697,922 for the archaea set. Upon merging both sets, an average of 440 ± 250 sOTUs per sample were recovered. Despite the limited number of studies analyzed, the repeated responses and similar observations in literature support the reliability of the proposed MIs within these processes. The following sections explain and explore these findings.

The CH₄ yield data, ranging from 0 to 685 mL CH₄/gVS_{added}, were collected from 98 samples, establishing six methane yield categories (C1 to C6) based on the corresponding bin widths determined by the Freedman-Diaconis rule. Each category comprised an interval of 114 mL CH₄/gVS_{added} and exhibited significant differences in relevant physicochemical parameters (Fig 3.1). Compared with C2 and C5 - C6, the accumulation of isobutyric acid, acetic acid, TAN, and VFA_t negatively impacted CH₄ yield. Interestingly, these compounds have been identified as inhibitory in AD and suggested as physicochemical indicators (He et al., 2017; Wu et al., 2021). The proposed categorization elucidated the dynamic performance of anaerobic processes by discarding factors like feedstock composition and operational conditions that could distort the classificatory method. Therefore, the exploration of significant relationships between the microbial community structure and abundance concerning methane yield categories were assessed.

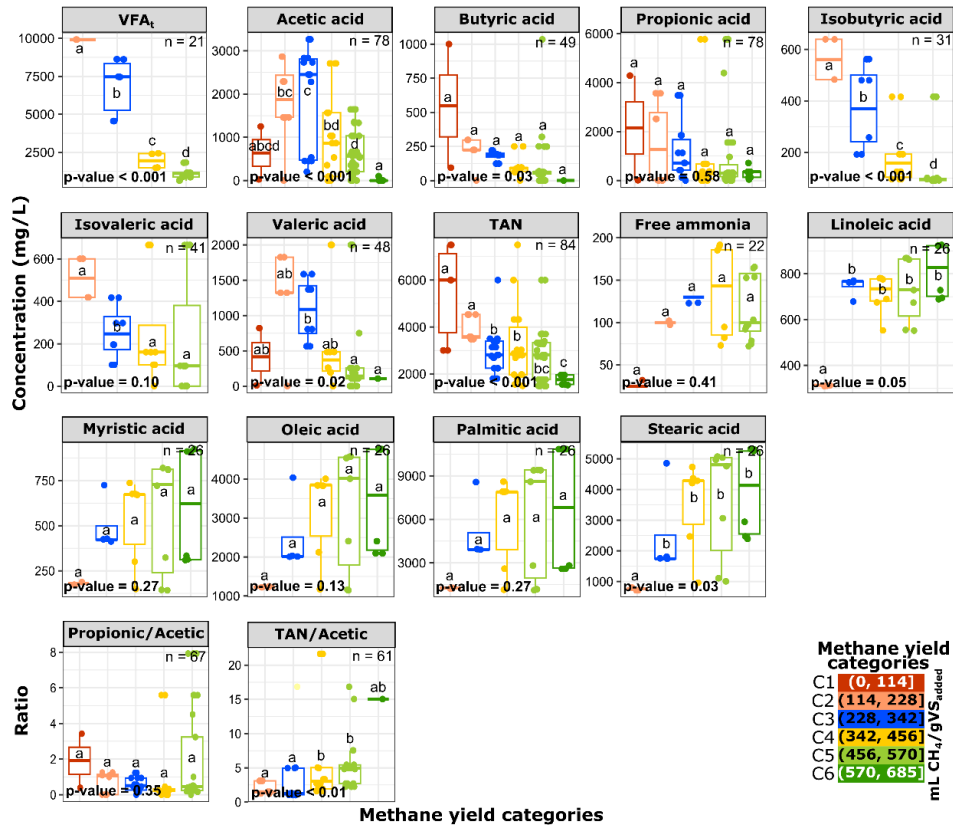


Figure 3.1. Distribution of physicochemical parameters across methane yield categories. Boxplots depicted median, quartiles, and extreme values, with sample size (n) and Kruskal-Wallis h test-derived p-values ($p < 0.05$). Pairwise comparisons utilized Wilcoxon rank sum tests ($p < 0.05$). Lowercase letters inside boxplots stand for groups with statistically significant differences.

3.4.2. Microbial community diversity in response to the methane yield categories

The richness and diversity indices showed significant variations among methane yield categories, depending on the sOTU and genus levels, respectively (Fig. 3.2). An increase in sOTU richness was observed with higher CH_4 yield. Chao1 and q0 indices revealed a significant positive trend when comparing C1 and C2 with C6 (Fig. 3.2a). This suggests that a higher number of microorganisms were required to maintain a high CH_4 yield (Hill et al., 2003; Rahman et al., 2021). However, variations in the regions of the 16S rRNA gene utilized for sequencing may result in the classification of individual sOTUs, leading to inconsistencies in diversity assessment (Hill et al., 2003; Martínez-Porchas et al., 2016). Thus, diversity analyses that also take abundance and evenness into account may offer other responses at higher taxonomic levels, allowing for the integration of these specific sOTUs (Martínez-Porchas et al., 2016).

CHAPTER 3. Identifying reliable microbial indicators in anaerobic digestion of organic solid waste: Insights from a meta-analysis

A reduction in genus diversity indicated an increase in CH₄ yield. Pielou's evenness, Shannon, and q1 indices showed a significant decreasing trend from C1 to C4 (Fig. 3.2b). This negative response in diversity may be due to a reduction in the specialization of the microbial community at the genus level, which enhanced CH₄ yield. (Nguyen et al., 2019). Furthermore, these alpha diversity metrics have been previously associated with process performance parameters, including operational temperature (Guo et al., 2022), CH₄ concentration (Rahman et al., 2021) and feeding frequency (Svensson et al., 2018). Although a less diverse community indicated better AD performance, it also presents a potential limitation as it becomes more susceptible to instability, a common operational issue in processes utilizing these feedstocks (Li et al., 2018; Nguyen et al., 2019). In contrast, richness-based metrics were inconsistent in their association with or predicting methane yield categories. This implies that the genera count was homogenized across categories, making it necessary to introduce abundance metrics to determine a significant diversity assessment (Hill et al., 2003).

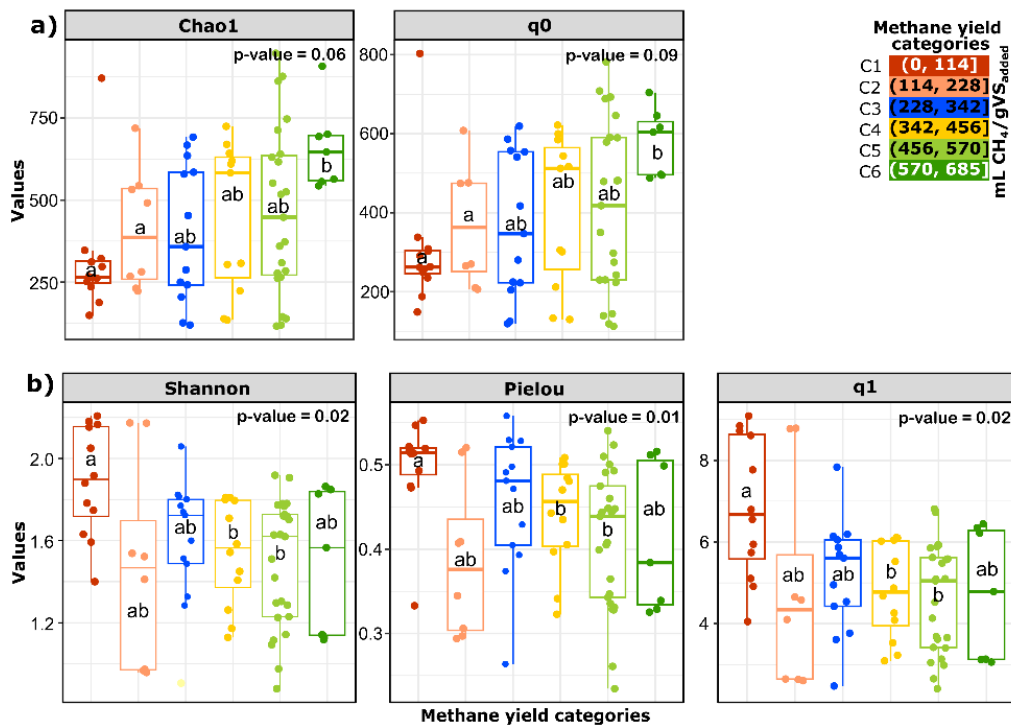


Figure 3.2. Distribution of significant alpha diversity indices grouped by methane yield categories identified by different colors (C1-C6) at both the a) sOTUs and b) genus levels. The boxplots represent the median, quartiles, and outliers of the data, with significance determined using the Kruskal-Wallis h test ($p < 0.10$). Pairwise comparisons were performed using Wilcoxon rank sum tests ($p < 0.10$). Lowercase letters inside boxplots stand for groups with statistically significant differences.

CHAPTER 3. Identifying reliable microbial indicators in anaerobic digestion of organic solid waste: Insights from a meta-analysis

The microbial community structure, whether at the sOTU or genus level, cannot be solely explained by the CH₄ yield, as demonstrated by beta diversity analysis using the Bray-Curtis distance (Fig. 3.3). In both PCoA analyses, the two main coordinates explained 12 - 38% of the variance significantly (ANOSIM, $p < 0.01$), albeit with low R-values (0.12 - 0.17). Beta diversity analysis showed that it depended heavily on the specific operational conditions of each system (Fig. 3.4). This analysis provides valuable insights into the changes in microbial communities associated with AD performance, as demonstrated by studies of individual processes (Basak et al., 2021; Peng et al., 2018; Svensson et al., 2018). Hence, it is not advisable to employ beta diversity indices to compare AD performance based solely on CH₄ yield between different processes, even when feedstocks are similar.

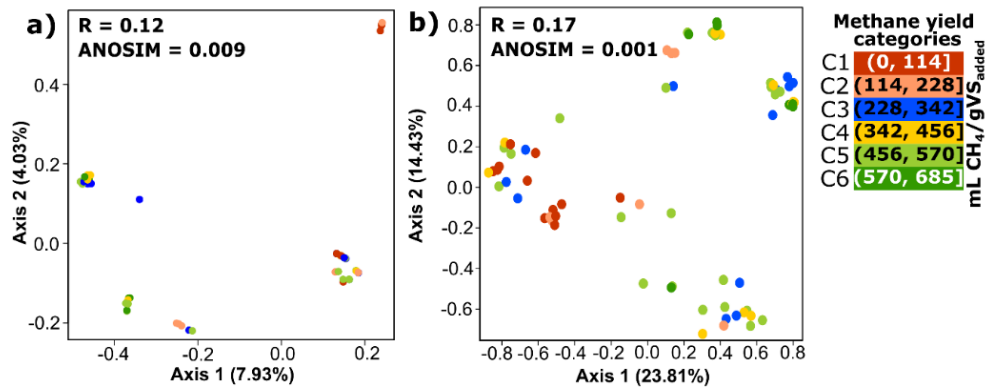


Figure 3.3. Principal coordinate analysis (PCoA) depicts microbial community dynamics through methane yield categories (C1-C6) at both the a) sOTUs and b) genus levels. The ANOSIM test ($p < 0.05$) and the R value based on Bray-Curtis were used to test the dissimilarities between clusters. The percentage of total variation explained by each PCoA axis is shown in parentheses. The points in different colors indicate each methane yield category.

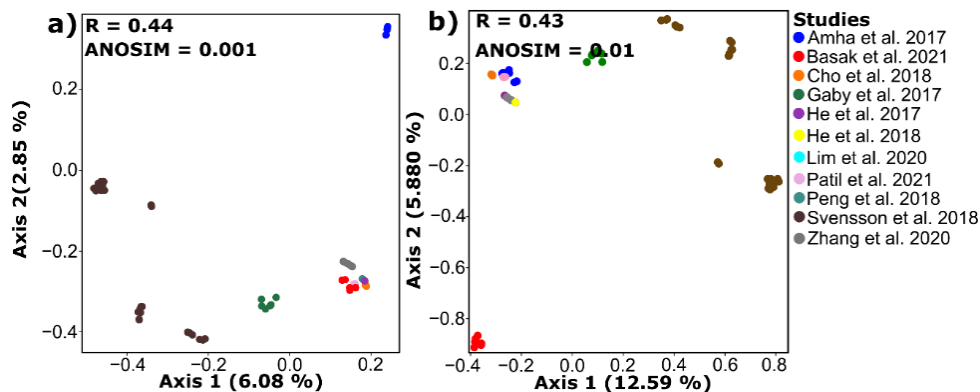


Figure 3.4. Principal coordinate analysis (PCoA) depicts microbial community dynamics through a case study at both the a) sOTUs and b) genus levels. The ANOSIM test ($p < 0.05$) and R value based on Bray-Curtis were used to test the dissimilarities between clusters. The percentage of the total variation explained by each PCoA axis is shown in parenthesis. The points in different colors represent the individual studies examined.

3.4.3. The Core Microbiome: Key Players in AD

The core microbiome obtained comprised of nine genera: *Aminobacterium*, *Clostridium*, HA73, *Methanoculleus*, *Methanosarcina*, *Pelotomaculum*, *Syntrophomonas*, T78, and *Treponema*. Although some of these genera have been proposed as MIs in isolated studies (Li et al., 2016; Poirier et al., 2016), this study suggests its potential universality given their high frequency and significant responses in the performance of the analyzed processes for mesophilic OFMSW and FW digesters. For instance, *Methanoculleus* and *Methanosarcina* have been proposed as EWIs in response to phenol inhibition (Poirier et al., 2016). Additionally, *Syntrophomonas* and *Treponema* have been suggested as EWIs to detect the excessive accumulation of VFA caused by high OLR (Li et al., 2016). Additionally, such core microbiome taxa might play essential roles in AD, including hydrolyzing polysaccharides and proteins, fermenting carbohydrates, oxidizing VFA through syntrophic interactions (especially acetate, propionate, and butyrate), homoacetogenesis, and the production of CH₄ through both hydrogenotrophic and acetoclastic pathways (Basak et al., 2021; Giordani et al., 2021; He et al., 2017; Kim et al., 2019; Ruiz-Sánchez et al., 2018; Sieber et al., 2012; Wang et al., 2018; Zamanzadeh et al., 2016). This suggests that the core microbiome is related to the maintenance of AD system stability, adaptability, and functionality (Berg et al. 2020; Xu et al. 2018).

Several genera from the core microbiome displayed significant variation among the methane yield categories (Fig. 3.5). *Aminobacterium*, *Clostridium*, HA73, and T78 were predominantly found in C1 (< 114 mL CH₄/gVS_{added}) and displayed a negative response as the AD performance improved. In contrast, *Methanosarcina* showed a higher abundance in C2-C6 (>114 CH₄/gVS_{added}), with no significant differences between these categories. These taxa have been suggested to be potential MI for detecting operational problems in AD processes (Guo et al., 2022; He et al., 2017; Poirier et al., 2016, Poirier et al., 2020; Rahman et al., 2021; Zhang et al., 2020). Still, this study corroborates a reproducible significant response based on CH₄ yield, highlighting the potential universal response of core microbiome members, specifically in mesophilic anaerobic processes fed with OFMSW and FW. For example, *Aminobacterium* has been proposed as an indicator of foam formation because of its notable up to 25-fold increase in abundance (He et al., 2017). Two *Clostridium* species, *C. sensu stricto 15* and *C. butyricum*, have been recommended as indicators of ammonia inhibition and non-inhibitory conditions, respectively (Poirier et al., 2020). *Methanosarcina* has served as an indicator for detecting ammonia and phenol inhibition, and CH₄

concentration in anaerobic processes (Poirier et al. 2016, Poirier et al., 2020; Rahman et al. 2021). Interestingly, this meta-analysis corroborated the relevance of unclassified genera in potential MI. T78, with its high normalized betweenness and interactions with other microorganisms, has been proposed as a process indicator for systems supplied with FW and blackwater (Guo et al., 2022). Regarding HA73, its abundance notably increased when activated carbon was introduced into AD, enhancing system performance (Zhang et al., 2020). In summary, some of these key taxa, *Methanosarcina* and HA73, showed a significant response only to opposite ends of the methane yield categories, revealing their potential to indicate extreme operational problems. *Aminobacterium*, *Clostridium* and T78, led to a gradual significant response as the CH₄ yield increased, revealing a valuable response to differentiate between two or more methane yield categories.

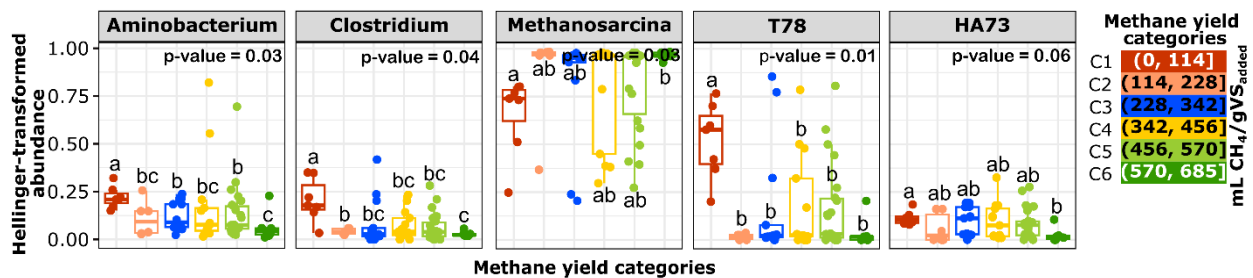


Figure 3.5. The boxplots display the median, quartiles, and extreme values of data, with significance determined using the Kruskal-Wallis h test ($p < 0.10$). Pairwise comparisons were performed using Wilcoxon rank sum tests ($p < 0.10$). Lowercase letters inside boxplots stand for groups with statistically significant differences.

3.4.4. Association between differentially abundant taxa and methane yield categories

Six genera displayed robust significant abundance changes between low (< 342 mL CH₄/gVS_{added}) and high CH₄ yield groups (> 342 mL CH₄/gVS_{added}) (Fig. 3.6), which were found in at least two different statistical analyses (Fig. 3.7). Notably, *Prevotella*, *Corynebacterium*, and *Lactobacillus* demonstrated a presence/absence response depending on the methane yield category, which is a desirable binary feature for MI. The significant fold change in these taxa has been linked to negative or positive responses to AD performance associated with inhibitory phenomena (He et al., 2017; Khafipour et al., 2020; Mugnai et al., 2021; Poirier et al., 2020; Wang et al., 2020). Key taxa with a negative response have been associated with VFA generation and linked to W5 and *Lactobacillus* (He et al., 2017; Mugnai et al., 2021). Meanwhile, key taxa with a positive response were related to *Sedimentibacter* for propionate and *Prevotella*, *Sphaerochaeta*, and

Corynebacterium for ammonia (Khafipour et al., 2020; Poirier et al., 2020; Ruiz-Sánchez et al., 2018; Wang et al., 2020). These findings confirm the existence of key and robust taxa that serve as direct representatives in the low or high-performing AD processes evaluated in this study.

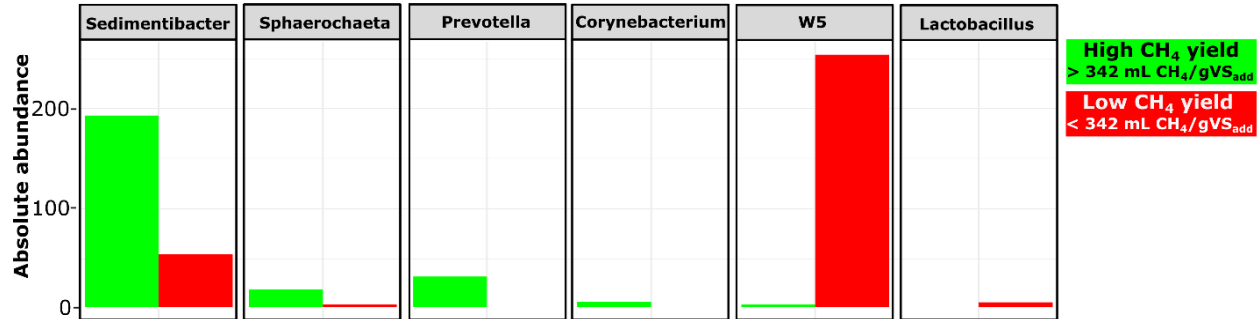


Figure 3.6. The average absolute abundances of key taxa selected from differential abundances within the entire microbial community are depicted. In the chart, the red bars represent the mean abundance observed in the low ch₄ yield group (c1, c2, and c3 methane yield categories), while the green bars represent the mean abundance in the high ch₄ yield group (c4, c5, and c6 methane yield categories).

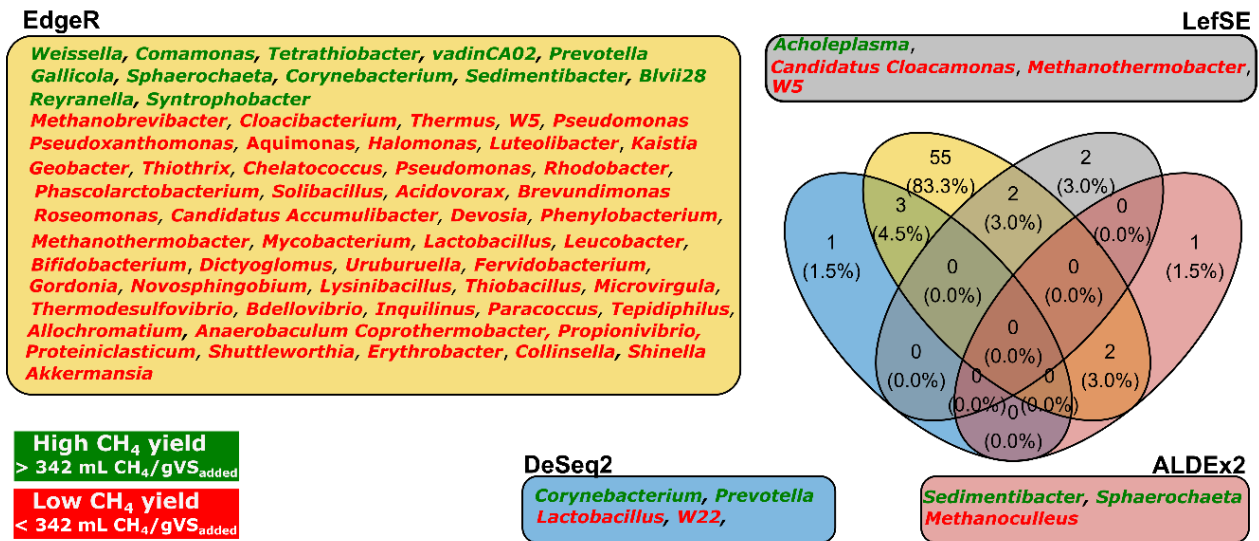


Figure 3.7. A Venn diagram illustrates the number of genera obtained and shared between differential analysis methods (EdgeR, LefSe, DESeq2, and ALDEx2). Genera that predominantly appeared at high CH₄ yields (categories C4, C5, and C6) are marked with green labels, while those predominant at low CH₄ yields (categories C1, C2, and C3) are labeled in red. The key taxa with significant abundance were grouped into different rectangles and color-coded according to the differential analysis method used. The yellow rectangle represents EdgeR (n = 62), the gray rectangle represents LefSe (n = 4), light red rectangle represents ALDEx2 (n = 3), and blue rectangle represents DESeq2 (n = 4).

3.4.5. Key alpha indices and key taxa can predict the CH₄ yield

The predictive capability of the potential MIs was confirmed through GAMLSS modelling, particularly concerning key diversity indices, key taxa identified from the core microbiome, and robust fold change analysis. *Corynebacterium*, HA73, *Lactobacillus*, *Prevotella*, *Sphaerochaeta*, T78, and W5 and key alpha diversity indices (Chao1 and q0 for sOTUs level, and Pielou, q1, and Shannon indices for genera level) were significant predictors of CH₄ yield (R^2 : 0.09 – 0.81 and $p < 0.05$). Other taxa, *Aminobacterium* and *Clostridium*, exhibited predictive capacity only by adding TAN and acetic acid to the model (R^2 : 0.50 – 0.75 and $p < 0.05$; supplementary material Table S5). Collectively, these potential MIs possess attributes to being considered EWIs, signaling potential issues that may affect AD performance. These capabilities were aligned with previous research citing *Aminobacterium*, *Corynebacterium*, *Lactobacillus*, and *Sphaerochaeta* in anaerobic systems (He et al., 2017; Li et al., 2016; Poirier et al., 2020), and genes such as *hydA* associated with *Clostridium* are linked to H₂ production (Cabrol et al., 2017). Additionally, the Shannon index demonstrated a positive trend during propionate inhibition (Khafipour et al., 2020). In contrast, the Pielou evenness index has been dismissed as a warning indicator, as it did not show significant trends when a process was perturbed by increases in the OLR (Goux et al., 2015). Despite the promising application as possible EWIs suggested by this meta-analysis, such indicators need to be validated in continuous AD systems over operation time and different inhibition and stable CH₄ production scenarios.

3.4.6. Correlations between key taxa and AD by-products

The key taxa demonstrated a proportional association, primarily with either low or high CH₄ yields, indicating that a response to varied environments affects AD performance. Given that TAN, LCFA, and VFA are the principal AD by-products influencing their performance (Wu et al., 2019), a correlation analysis with key taxa was conducted. The results provided insight into the specific conditions associated with their responses and suggested their potential metabolic roles that may promote such conditions.

3.4.6.1. Key taxa from the core microbiome

The behavior of key taxa from the core microbiome was significantly correlated with the AD by-product concentrations (Fig. 3.8). *Aminobacterium* displayed a positive correlation with butyric acid, propionic acid, acetic acid, and TAN, suggesting a link between protein hydrolysis and amino

acid degradation, indicating signs of low performance when organic overloading exists (He et al., 2017; Jo et al., 2018; Wang et al., 2018). A positive correlation between *Clostridium* abundance and LCFA was observed, attributed to its role in LCFA degradation, which may exemplify inhibitory conditions by organic overloading (Basak et al., 2021). The positive correlations between HA73 and acetic acid, propionic acid, and TAN are possibly related to its ability to break down amino acids (Giordani et al., 2021), evident from its increased abundance with increasing NH_3 content and the concurrent decrease in CH_4 production (Gaby et al., 2017). T78 displayed positive correlations with CH_4 yield and some LCFA, such as linoleic, myristic, and palmitic acids. This genus is presumably a syntrophic bacterium that promotes a high CH_4 yield when exposed to feedstocks potentially containing a high content of LCFA (Bovio-Winkler et al., 2021; Giordani et al., 2021). Positive correlations were observed between *Methanosarcina* and acetic acid and TAN, whereas negative correlations were noted with LCFA. This genus utilizes a mixotrophic pathway for CH_4 production, demonstrating higher resilience than acetoclastic archaea under specific stress conditions, although it may be susceptible to elevated LCFA (Amha et al., 2017; Basak et al., 2021; Hardy et al., 2021).

3.4.6.2 Key taxa from the whole microbial community

Most of the key taxa within the entire microbial community, such as *Lactobacillus*, *Corynebacterium*, *Sphaerochaeta*, and *Sedimentibacter*, exhibited significant correlations with AD by-products (Fig. 3.8). *Lactobacillus* was negatively correlated with CH_4 yield and positively associated with acetic acid, propionic acid, TAN, and valeric acid. This trend can be related to *Lactobacillus* carbohydrate fermentation activities, production of lactic and acetic acids, and VFA accumulation (Amha et al., 2017; Luo & Wong, 2019). *Corynebacterium* displayed a positive correlation with CH_4 yield and TAN and a negative correlation with propionic acid. This fermentative bacterium has demonstrated the ability to assimilate NH_4^+ , ensuring its survival even at non-inhibitory concentrations of ammonia, thereby sustaining CH_4 production (Tesch et al., 1998; Wang et al., 2020). Positive and negative correlations with LCFA and acetic acid, respectively, were observed in *Sphaerochaeta*, indicating its capacity for acetate production and tolerance to high LCFA concentrations (Zhang et al., 2022) Positive correlations between *Sedimentibacter* and CH_4 yield, along with stearic acid, were observed, along with negative correlations with propionic acid, acetic acid, and TAN. This genus can perform syntrophic

degradation of LCFA and proteins aiding in maintaining AD, and any disturbance in its activity may signify propionic acid inhibition (Basak et al., 2021; Khafipour et al., 2020; Peng et al., 2018).

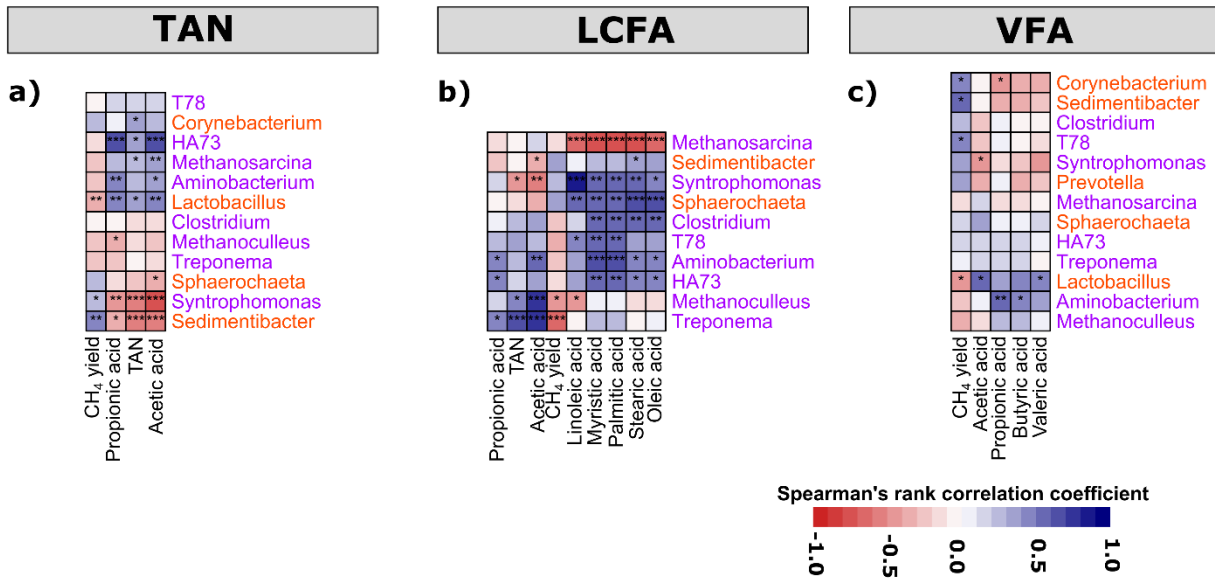


Figure 3.8. The heatmap illustrates the correlations between the key taxa and AD by-products. a) TAN, b) LCFA, and c) VFA matrices. Significant correlations based on Spearman's correlation coefficient (R_s) are indicated with *, **, and *** to denote p-values <0.05, <0.01, and <0.001, respectively. Purple labels indicate that key taxa belong to the core microbiome. Orange labels indicate the key taxa from the entire microbial community.

3.4.7. Applications of reliable MI: Detecting key challenges

Statistical analyses have pinpointed reliable MI with distinct attributes specifically linked to anaerobic processes using OFMSW and FW feedstocks. These MI exhibit inherent differences due to the approach used for microbial community evaluation (Table 3.2). In the case of the core microbiome, *Aminobacterium*, *Clostridium*, HA73, and T78 displayed traits of universality, significant responses to various metabolic byproducts that can disrupt AD and predict CH₄ yield. These potential MI represented up to 24% in relative abundance, enhancing the likelihood of easy detection and offering qualities suitable for future validation to identify early stress conditions with the help of physicochemical parameters. Taxa from entire microbial community such as *Corynebacterium*, *Lactobacillus*, and *Prevotella* exhibited relevant metabolic roles associated with inhibitory compounds, predictive capabilities for CH₄ yield, and presence/absence responses between low and high CH₄ yield samples. These genera may establish effective ranges linked to CH₄ yield categories, reduce noise, and enhance the probability of effective categorization. Moreover, they may provide early warning before stressful conditions challenge AD stability.

However, a drawback is their low relative abundance, which reaches up to 1.8%, emphasizing the need to select adequately sensitive detection techniques for possible identification.

Additionally, previous studies have noted potential applications for the MI identified in this research, its specific role in indicating process performance or inhibition issues has not been evaluated. Given the low abundance of some reliable MIs and their correlation with inhibitory metabolic compounds, validation experiments are recommended. Thus, the experiments should combine high-throughput technologies and physicochemical instrumentation (Li et al., 2018; Wu et al., 2021). Although, fluorescence in situ hybridization (FISH), real-time polymerase chain reaction (qPCR), and biosensors may be utilized for faster detection (e.g., within hours) and cost-effective molecular methods (Li et al., 2018). These findings would generate sufficient data to develop machine learning models based on linear (e.g., logistic regression) and non-linear (e.g., random forest) approaches. Such models would enhance accuracy in predicting specific challenges (e.g., acidification, foaming, or ammonia inhibition), considering only MIs and physicochemical indicators, and selecting appropriate molecular detection methods (Wijaya et al., 2023). This approach would facilitate the development of monitoring systems to guide decision-making in resolving key challenges and maintaining AD stability.

CHAPTER 3. Identifying reliable microbial indicators in anaerobic digestion of organic solid waste: Insights from a meta-analysis

Table 3.2. Overview of the main characteristics of potential MI identified in the meta-analysis

Microbial indicator	Attributes ⁽¹⁾	Range of relative abundance	Association with CH ₄ yield	Contribution in AD ⁽²⁾	Intuitive response ⁽³⁾
Alpha diversity					
Chao1 and q0 (a)	Universal, Predictable	NA	Positive	NA	High number of CH ₄ producing microorganisms (Hill et al., 2003)
Shannon, q1, Pielou (b)	Universal, Predictable	NA	Negative	NA	Specialization of CH ₄ producing microbial community (Jo et al., 2018)
Core microbiome					
<i>Aminobacterium</i>	Universal, Predictable	0 – 12 %	Negative	Hydrolysis of protein and amino-acids degradation (He et al., 2017; Wang et al., 2018).	Accumulation of acetate, butyrate propionate, and ammonia (He et al., 2017; Jo et al., 2018)
<i>Clostridium</i>	Universal, Predictable	0 – 6%	Negative	LCFA degradation (Basak et al., 2021)	Accumulation of LCFA (Basak et al., 2021)
HA73	Universal, Predictable	0 – 4%	Negative	Amino acids degradation (Giordani et al., 2021)	Accumulation of VFA and ammonia (Gaby et al., 2017; Giordani et al., 2021)
<i>Methanosarcina</i>	Universal	0 – 52%	Positive	Mixotrophic methanogenesis (Amha et al., 2017)	High CH ₄ yield (Basak et al., 2021)
T78	Universal, Predictable	0 – 24%	Positive/Negative	Syntrophic activity (Bovio-Winkler et al., 2021)	Degradation of LCFA (Zamanzadeh et al., 2016)
Whole microbial community					
<i>Sedimentibacter</i>	Robust fold change	0 – 8.8%	Positive	Protein degradation and syntrophic LCFA oxidation (Basak et al., 2021; Peng et al., 2018)	High CH ₄ yield (Basak et al., 2021)
<i>Corynebacterium</i>	Robust fold change, Binary, Predictable	0 – 0.3%	Positive	NH ₄ ⁺ assimilation (Tesch et al., 1998)	High CH ₄ yield (Wang et al., 2020)
W5	Robust fold change, Predictable	0 – 0.4%	Negative	Not identified	Accumulation of VFA (Mugnai et al., 2021)
<i>Lactobacillus</i>	Robust fold change, Binary, Predictable	0 – 0.09%	Negative	Acetate and lactate production (Luo & Wong, 2019)	Accumulation of VFA (Amha et al., 2017)
<i>Prevotella</i>	Robust fold change, Binary, Predictable	0 – 1.8%	Positive	Hydrolytic activity (Khafipour et al., 2020)	High CH ₄ yield (Ruiz-Sánchez et al., 2018)
<i>Sphaerochaeta</i>	Robust fold change, Predictable	0 – 0.8%	Positive	Acetate production (Zhang et al. 2022)	High CH ₄ yield (Zhang et al., 2018)

(1) Universal: Members from core microbiome with significant abundance differences between methane yield categories; Robust fold change: Members from entire microbial community selected by at least two differential analyses; Binary: Key taxa with robust fold change attribute but associated with presence or absence abundance at low CH₄ yield group (C1, C2 and C3 methane yield categories) or high CH₄ yield group (C4, C5 and C6 methane yield categories); Predictable: Key alpha diversity and taxa identified as capable of predicting CH₄ yield through GAMLSS models, utilizing index values, relative abundance, or in combination with physicochemical indicators like TAN and acetic acid. (2) The potential metabolism derived from correlation analysis and supported by the literature. (3) Intuitive response derived from the statistical framework and supported by the literature. NA: Not applicable. (a) sOTU level. (b) Genus level.

3.5. Conclusions

Reliable MIs for AD processes fed with the OFMSW and FW were identified through a meta-analysis and statistical framework. Despite the limitations of available public database sequences and useful data, the reliability of the proposed MIs for these systems was supported by consistent statistical responses across various studies and corroborative literature. Within this context, *Aminobacterium*, *Clostridium*, HA73, T78, *Corynebacterium*, *Lactobacillus*, and *Prevotella* emerged as reliable MIs, exhibiting significant responses and predictive capabilities for CH₄ yield, alongside key metabolic roles linked to inhibitory compounds in these processes. Recognizing the potential applicability of these reliable MIs, it is imperative to consider the future implementation of MI surveillance during AD operations fed with OFMSW and FW. Monitoring these MIs holds promise for optimizing anaerobic systems by potentially predicting stress conditions, thereby enhancing overall performance and CH₄ production efficiency. Finally, this methodology represents an initial step towards proposing a statistical analytical framework to identify MIs in other large-scale processes requiring optimization, such as sewage sludge, livestock waste, or energy crops.

CHAPTER 4. Ammonia as a key inhibitory compound in food waste digestion: Challenges of heterogeneous feedstock composition

4.1. Abstract

The heterogeneity of food waste introduces various inhibitory compounds such as sulfates, long-chain fatty acids, and ammonia, which significantly affect CH₄ yield and microbiome functionality. In a batch experiment using a 2³ factorial design, ammonia was confirmed to be the primary inhibitory compound in anaerobic digestion, exerting a stronger effect than interactions with other inhibitory elements. At inhibitory concentrations (7560 mg TAN/L), ammonia caused the greatest reduction in CH₄ yield and accumulation of volatile fatty acids, surpassing the effects of inhibitory levels of long-chain fatty acids (1214 mg oleic acid/L) and the high concentration of sulfates (500 mg Na₂SO₄/L). Ammonia inhibition resulted in the over-acidification of reactor due to accumulation of acetate (1850 – 3034 mg COD_{eq}/L), butyrate (304 – 1018 mg COD_{eq}/L), propionate (393 – 1074 mg COD_{eq}/L) and ceasing CH₄ production. These physicochemical responses indicate a metabolic shift from methanogenesis to fermentation, reflecting the strong inhibitory effect of ammonia. The study underscores the importance of early detection of ammonia inhibition to prevent over-acidification in food waste digesters, which requires further evaluation.

4.2. Introduction

Food waste (FW) is feedstock of industrial anaerobic processes is characterized by significant variations in carbohydrate (0–59%), protein (1.4–38.9%), and lipid (0.8–41.5%) content (Xu et al., 2018). This heterogeneous composition leads to the release of various compounds during the anaerobic conversion of FW to methane (CH₄), some of which can inhibit microbial activity under specific conditions (Li et al., 2018). Although, ammonia is a well-known inhibitor in FW digesters (Banks et al., 2018), interactions with other metabolites, such as sulfates and long-chain fatty acids (LCFAs), may also significantly impact anaerobic digestion (AD). This is because these compounds can impact key microbial groups involved in biogas production. For instance, the sulfur compounds are released during protein degradation, potentially producing H₂S, which requires H₂ as an electron donor via sulfate-reducing bacteria (SRB) (Chatterjee & Mazumder, 2019; Moreno-Andrade et al., 2020). This process can result in competition for H₂ between SRB and hydrogenotrophic microorganisms, such as methanogens, within the AD system, as methanogens rely on H₂ for CH₄ production (Li et al., 2015). Additionally, LCFAs released during fat degradation can bind to cell walls, hindering mass transfer and primarily affecting methanogenic archaea (Patil et al., 2021). Therefore, the primary inhibitory compound in AD remains unidentified, and interactions between metabolites could exacerbate inhibition.

This study aimed to evaluate the interactions between inhibitory compounds—ammonia, LCFAs, and sulfates—at inhibitory concentration levels on CH₄ yield in a batch anaerobic process fed with FW. The experiment was designed to determine whether a single inhibitory compound or the interaction between these metabolites has the most significant impact on the AD of FW.

4.3. Material and Methods

4.3.1. Inoculum and feedstock

Granular sludge from a mesophilic anaerobic digester, treating organic waste from the flour industry, served as inoculum. It was stored in an open container at room temperature for 15 d to reduce organic matter and facilitate degassing. Raw FW was sourced from a central market in Querétaro, Mexico. It was ground to a particle size of less than 0.5 mm using a meat grinder and then stored in 2-liter bags at -20 °C until needed. Both the inoculum and FW were characterized including analyses for VFA, TAN, total carbohydrates, total solids (TS), volatile solids (VS), and chemical oxygen demand (COD) (Fig. 4.1).

4.3.2. Experimental design

A 2³ factorial design encompassing two concentration levels (Table 4.1). A low level (-1) represented the compound concentration found in FW, and a high level (1) represented inhibitory concentrations reported in the literature. Specifically, ammonia was set at 7560 mg TAN/L, LCFA at 1214 mg oleic-acid/L, and the sulfate concentration was set at 500 mg Na₂SO₄/L (which enhances H₂S production) according to studies by Ruiz-Sánchez et al., (2018), Chen et al., (2008) and Qiao et al., (2016) respectively. To simulate inhibitory effects: (i) 20 g NH₄Cl/L was used to replicate ammonia inhibition levels, (ii) 18.51 g pork fat/L represented the inhibitory effects of LCFA, and (iii) Na₂SO₄ was used to replicate sulfate conditions, which have been associated with changes in the microbial community.

Table 4.1. Factorial levels to be evaluated in 8 combinations of treatments.

Conditions	Ammonia	Greases	Sulfates
Condition 1 (positive control)	-1	-1	-1
Condition 2	1	1	-1
Condition 3	1	1	1
Condition 4	1	-1	-1
Condition 5	1	-1	1
Condition 6	-1	1	-1
Condition 7	-1	1	1
Condition 8	-1	-1	1
Condition 9 (endogenous control)	0	0	0

4.3.3. Batch assays

The evaluation of interactions between inhibitory compounds was conducted in a batch anaerobic process fed with FW. Triplicate batch assays were conducted using an AMPTS II automated system (Bioprocess Control, Sweden). The system utilized glass bottles with a volumetric capacity of 600 mL, with a working volume of 360 mL, and each bottle was equipped with a stirring device. Temperature control was achieved using thermostatic water bath equipment. To create anoxic conditions, each bottle was injected with N₂ for a duration of 30 seconds. A CO₂ trap system was employed, consisting of bottles containing 80 mL of 3 M NaOH solution, supplemented with a pH indicator solution (thymolphthalein). The system also featured an online biogas volume measurement system. Throughout the experiments, the following parameters were maintained at constant levels: temperature at 37°C, S₀/X₀ ratio of 0.5 g VS/g-VS, substrate concentration of 10 g VS/L, addition of 4 g NaHCO₃/L, pH 8, and shaking speed set at 144 rpm with intermittent mixing (1 min of mixing per 3 min of incubation) (Angelidaki et al., 2009; Moreno-Andrade et al., 2020; Pavi et al., 2017)

4.3.4. Stastitcal analysis

To analyze the impact of inhibitory compounds on CH₄ yield, a half-normal plot was used, with values near zero considered insignificant and greater distances indicating more significant effects. This analysis employed Shapiro-Wilk test ($p < 0.05$) to determine whether the unique or interactive effects followed a normal distribution. A main effects plot was constructed to identify significant differences between the two levels of inhibitory compounds in relation to the overall average CH₄ yield. Significant differences ($p < 0.05$) in CH₄ yield and VFA across combinations were determined using analysis of variance (ANOVA). The semi-normal and main effects plots were generated using “DanielPlot” and “MEPlot” respectively from "FrF2" package (Groemping, 2019). The ANOVA was performed with the “aov” function from the vegan package (Oksanen et al., 2020).

4.4. Results and discussion

4.4.1. The effects of ammonia, greases and sulfates on CH₄ yield

The investigated compounds displayed distinct effects on CH₄ yield, with ammonia consistently reducing it (ANOVA, $p < 0.001$) (Fig. 4.1). No significant differences were found between the different ammonia conditions (C2, C3, C4) (Tukey, $p < 0.05$). Compared to the control, ammonia conditions (C2, C3, C4, C5) led to increased VFA production (Fig. 4.2), especially acetate (1850–3034 mg COD_{eq}/L), butyrate (304–1018 mg COD_{eq}/L), and propionate (393–1074 mg COD_{eq}/L). These results indicate the functional resilience of fermentative bacteria within the microbial consortium, which increased VFA content under ammonia stress (Nakakubo et al., 2008). This supports the idea that ammonia triggers over-acidification in FW digesters, causing operational disruptions (Peng et al., 2018; Zhang et al., 2022).

A relevant effect related to ammonia was its combination with sulfates (C5), which significantly enhanced CH₄ yield (30 ± 2 mL CH₄/gVS_{added}) and reduced VFA concentration. Acetate (1850 ± 362 mg COD_{eq}/L), propionate (393 ± 85 mg COD_{eq}/L), and butyrate (304 ± 70 mg COD_{eq}/L) concentrations were significantly decreased compared to the sole addition of ammonia. This improvement is likely due to the stimulation of SRB and syntrophic propionate-oxidizing bacteria (SPOB), which oxidize propionate and H₂ through sulfate reduction, supporting VFA degradation (Qiao et al., 2016). Possibly, these activation of oxidation of propionate and H₂ also minimized the accumulation of acetate and butyrate, contributing to a slight increase in CH₄ yield. However, while sulfate addition may offer a recovery method for overcoming ammonia inhibition in FW digesters, it may also elevate hydrogen sulfide (H₂S) concentrations in biogas, necessitating subsequent gas stream purification (Moreno-Andrade et al., 2020).

CHAPTER 4. Ammonia as a key inhibitory compound in food waste digestion: Challenges of heterogeneous feedstock composition

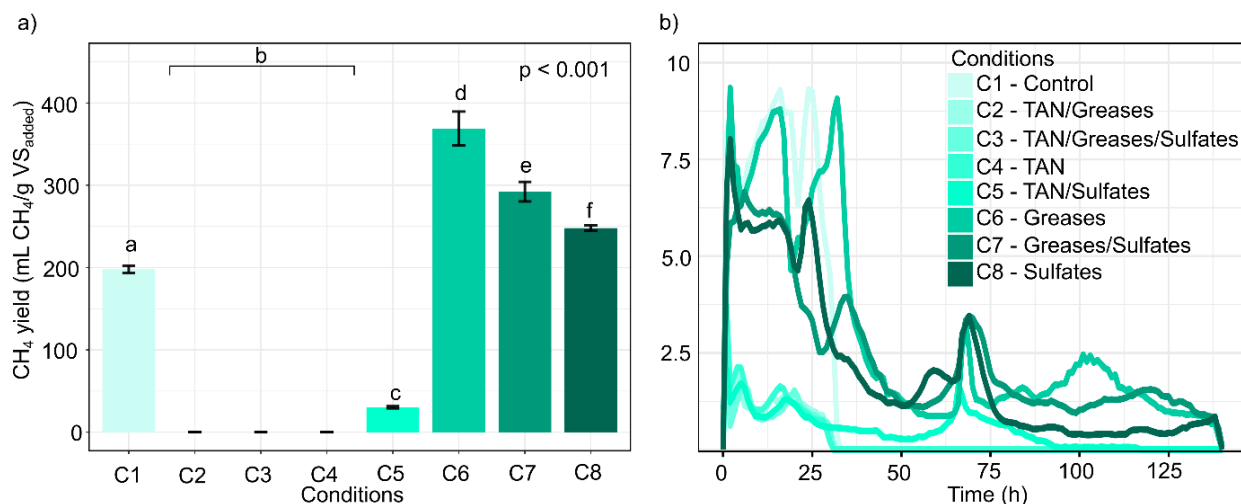


Figure 4.1. The CH₄ yields for each condition evaluated. a) The barplots display the average CH₄ yield for each condition. The analysis revealed significant differences (ANOVA, p -value < 0.001) among the conditions, with only the addition of ammonia (C2, C3, C4, C5) showing a negative impact on CH₄ yield. The significant differences between CH₄ yield categories are indicated by lines connecting the corresponding barplots (Tukey test, p -value < 0.05). The same letters denote conditions where there was not statistical significance (Tukey test, p -value > 0.05). b) The graph illustrates the CH₄ yield over time. The addition of greases and sulfates resulted in a resumption of CH₄ production after approximately 60 h.

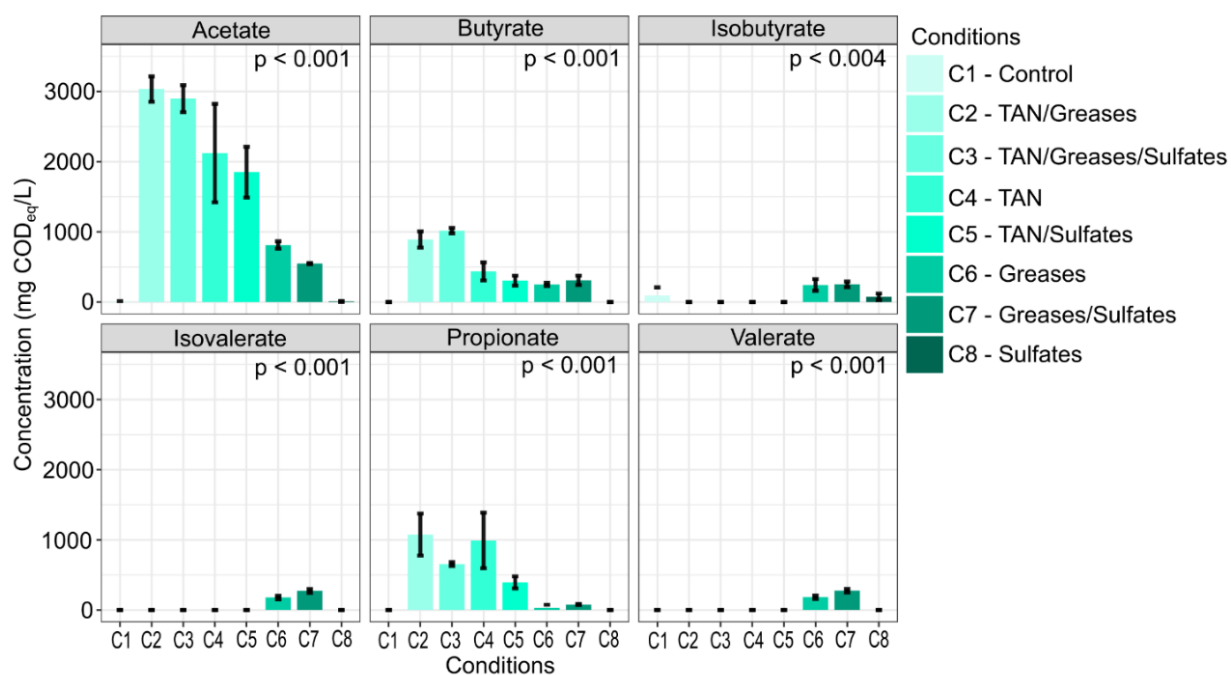


Figure 4.2. The distribution of metabolites in the different conditions evaluated. Significant differences (ANOVA, p -value < 0.05) were observed in the distribution of individual volatile fatty acids (VFAs) among the conditions.

The half-normal plot confirmed that ammonia had a greater effect on CH₄ yield, while greases and sulfates were classified as less influential compounds (Fig. 4.3). The main effects plot further illustrates these findings, showing ammonia with a negative effect (-1), fats with a positive effect (1), and sulfates with no significant impact on CH₄ yield. Although some studies have reported inhibitory effects of high concentrations of greases and sulfates, these compounds may also benefit AD under specific conditions (Amha et al., 2017; Qiao et al., 2016). These results align with previous observations made by other researchers, remarkabbling the importance of ammonia to shape on microbiome in FW digesters (Hadj et al., 2009; Peng et al., 2018; Ruiz-Sánchez et al., 2018; Zhang et al., 2020).

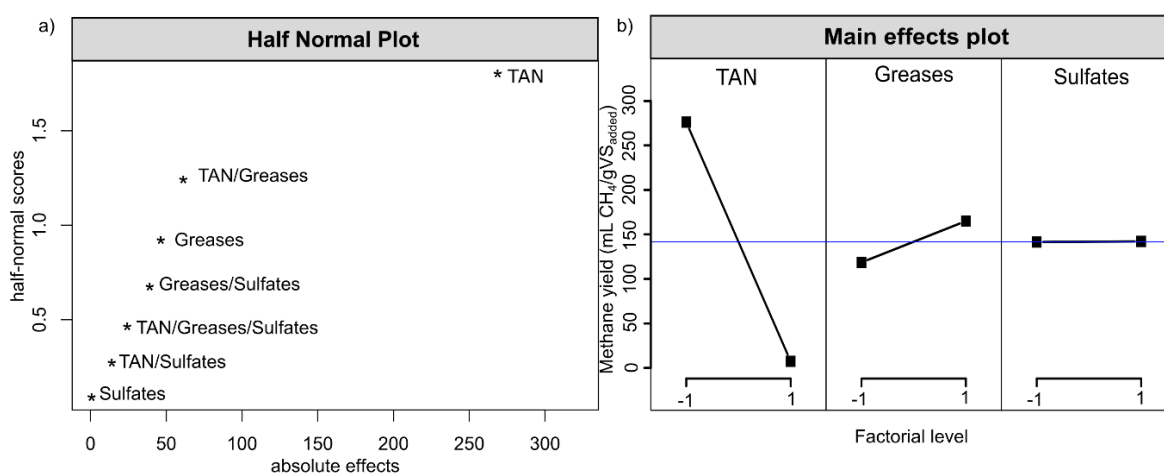


Figure 4.3. Half-normal (a) and main effects (b) plots. In the half-normal plot, factors with scores farthest from 0 and the greatest absolute effect deviating from the slope were considered important effects based on the Shapiro-Wilk test ($p > 0.05$). The main effects plot displays the global average of the response variable indicated by the blue line.

4.5 Conclusions

The variability in FW composition destabilizes AD due to its effects on metabolites such as ammonia, LCFA, and sulfate, which influence the microbial metabolism in AD. This study identified ammonia as the primary inhibitor of CH₄ yield, surpassing the effects of LCFA and sulfate. Ammonia disrupts methanogenesis by shifting microbial metabolism toward VFA production, further limiting CH₄ generation. Additionally, the addition of sulfates may facilitate the rapid recovery of propionate accumulation processes affected by ammonia inhibition; however, this approach is most effective when a system for capturing or removing H₂S from biogas is in place. These findings underscore ammonia as the critical factor inhibiting the methane-producing microbial community, highlighting the urgent need for strategies to mitigate and detect its effects in FW digesters.

CHAPTER 5. Suitable microbial indicators for detecting ammonia inhibition in anaerobic digestion of food wastes

5.1. Abstract

Ammonia inhibition in the anaerobic digestion of food waste poses significant challenges for detection and prevention. This study integrates inhibitory levels, metagenomic analysis, and a statistical framework to identify reliable microbial indicators for ammonia inhibition detection. Observations confirmed that at non-inhibitory concentrations (< 2702 mg TAN/L), acetoclastic methanogenesis transitions to hydrogenotrophic methanogenesis with syntrophic acetate oxidation, demonstrating microbial sensitivity to physicochemical changes. At inhibitory concentrations (2702 – 5805 mg TAN/L), denitrification decreases while nitrification, methylotrophic methanogenesis, and acetogenic activity increase, leading to acetate and propionate accumulation. Above minimum inhibitory concentrations (> 5805 mg TAN/L), hydrolysis and fermentation intensify, indicating that ammonia contributes to over-acidification in food waste digesters. Interestingly, these metabolic changes were linked to suitable microbial indicators identified through the statistical framework, including *Anaerolinea*, *Sphaerochaeta*, *Syntrophobacter*, *Methanomassiliicoccus*, *Methanosarcina*, *fhs*, and *acs*. These indicators also provided consistent responses for inferring inhibitory levels but also offer early warning signs. Their integration into monitoring systems, control algorithms, and countermeasure validation represents a significant advancement for the biofuels sector.

Reference to the submitted work

Jonathan Cortez-Cervantes, Iván Moreno-Andrade, Pabel Cervantes-Avilés, Julián Carrillo-Reyes.
Suitable microbial indicators for ammonia inhibition detection in food wastes anaerobic digestion

Submitted to Chemosphere

5.2. Introduction

During AD of FW and OFMSW, the breakdown of proteins and amino acids releases ammoniacal nitrogen ($\text{NH}_4^+ - \text{NH}_3$), affecting the process efficiency (Agyeman et al., 2021; Hadj et al., 2009; Wang et al., 2018). Ammonia can have a dual effect on AD: beneficial as a nutrient for microbial growth and buffering capacity, but inhibitory at high concentrations ($> 3 \text{ g/L}$) (Agyeman et al., 2021; Jiang et al., 2019). Therefore, identifying variables that indicate ammonia inhibition is essential, as it reduces methane (CH_4) production by 30% and promotes the accumulation of acetate and propionate, disrupting the AD process (Li et al., 2018; Zhang et al., 2022).

The effect of ammonia on AD can be described using the Hill equation, which provides a profile curve describing stimulation, inhibition, and cessation of CH_4 production (Agyeman et al., 2021). This model defines kinetic parameters such as IC_{50} (the 50% inhibitory concentration) and n (an empirical coefficient controlling the slope of the curve), essential for calculating umbral concentrations such as non-inhibitory concentration (NIC) and the minimum inhibitory concentration (MIC) (Lambert & Pearson, 2000). Determination of these concentrations is valuable for standardizing the effect of ammonia. In this way, applying the method proposed by Lambert and Pearson (2000) to AD, NIC represents the concentration at which the inhibiting substance begins to show observable effects. In terms of AD, NIC is the threshold concentration where CH_4 yield starts declining. MIC would indicate the lowest concentration where CH_4 production ceases and the range between NIC and MIC would indicate concentration with an inhibitory effect. However, factors such as pH, temperature, microbial acclimatization, among others, led to variable ranges of inhibitory thresholds (Jiang et al., 2019; Wu et al., 2021). Therefore, other reliable indicators besides ammonia concentration are desirable.

MIIs have emerged as consistent alternative due to MIIs reveal significant microbial dynamics aligned with ammonia effects (Poirier et al., 2020). In addition, MIIs are crucial for implementing microbial management strategies aimed at optimizing and updating biological processes within reactors (Carballa et al., 2015; Cortez-Cervantes et al., 2024). Interestingly, ammonia inhibition causes microbial communities to become more uniform and phylogenetically similar, differentiating them from non-inhibited microbial assemblies, an ideal aspect for identifying MI (Cardona et al., 2022; Li et al., 2018). In addition, operational temperatures and feedstock types

significantly influence microbial communities (Theuerl et al., 2018). Therefore, both factors must be considered to achieve consistent responses from the MIs tests for detecting ammonia inhibition.

Several studies have suggested potential MIs around specific genera or genes that are related to ammonia inhibitory levels in widely used systems like mesophilic FW digesters. Non-ammonia inhibitory concentrations (< 3 g/L) are characterized by acetoclastic methanogenesis, indicated by *Methanosaeta* and acetyl-CoA decarboxylase/synthase activity (Chen et al., 2016; Ruiz-Sánchez et al., 2018; Zhang et al., 2022). Ammonia inhibition (> 3 g/L) promotes the syntrophic acetate oxidation (SAO) pathway, associated with *Clostridium*, *Syntrophomonas*, and formyltetrahydrofolate synthetase activity. Hydrogenotrophic methanogenesis, featuring *Methanosarcina*, *Methanomassiliicoccus*, and *Methanoculleus*, also prevails (Ruiz-Sánchez et al., 2018; Wang et al., 2020; Zhang et al., 2020). Ammonia beyond a certain threshold induces VFA accumulation and AD collapse, disrupting syntrophic propionate oxidation involving *Pelotomaculum*, *Syntrophobacter*, and succinyl-CoA synthase (Zhang et al., 2022). However, unclear thresholds for ammonia inhibitory levels hinder reproducibility and reliability of MIs across anaerobic processes (Poirier et al., 2020).

Additionally, suitable MI must meet essential attributes that impact its response reliability, which can be addressed through a statistical framework (Cortez-Cervantes et al., 2024; Huerta et al., 2024). A key attribute of an indicator is its ability to differentiate between non-inhibitory and inhibited environments, especially when inhibition occurs due to ammonia (Huerta et al., 2024; Zhang et al., 2022). Another important expected attribute is that the MI should be a keystone within a microbial network, meaning that variations in its abundance might impact on the stability and functionality of the microbiome (Pan et al., 2021; Skovmand et al., 2018). Additionally, MIs should provide early warning signals before ammonia inhibition occurs, essential for predictive monitoring and timely corrective actions (Wu et al., 2021). A suitable MI should also be associated with specific taxa or genes linked to affected metabolic pathways, offering relevant insights into taxonomic and functional changes related to AD performance (Yu et al., 2020). Characterizing MIs by these attributes could contribute to developing microbial management strategies for selecting effective monitoring systems or MI quantification methods (Carballa et al., 2015; Cordier et al., 2020).

CHAPTER 5. Suitable microbial indicators for detecting ammonia inhibition in anaerobic digestion of food wastes

This study proposes an integrative analysis to identify suitable MIs for ammonia inhibition in the AD of FW. By combining metagenomic analysis and the Hill model, suitable MIs were identified at different inhibitory ammonia levels: NIC, inhibition, and MIC. Identification of MIs also responded to attributes like (I) keystone, (II), significant abundance changes, (III) potential early warning attributes, and (IV) metabolic roles related to metagenome-assembled genomes (MAGs). These findings can be used to recommend improved monitoring systems for AD operations from a biological perspective.

5.3. Material and methods

5.3.1. Batch assay for identifying ammonia inhibition levels

5.3.1.1. Inoculum and substrate

Granular sludge from a mesophilic anaerobic digester, treating organic waste from the flour industry, served as inoculum. It was stored in an open container at room temperature for 15 d to reduce organic matter and facilitate degassing (Pavi et al., 2017). Raw FW was sourced from a central market in Queretaro city, Mexico. It was ground to a particle size of less than 0.5 mm using a meat grinder and then stored in 2-liter bags at -20 °C until needed. Both the inoculum and FW were characterized including analyses for VFA, NH_4^+ , NH_3 , TAN, total carbohydrates, total solids (TS), volatile solids (VS), and chemical oxygen demand (COD) (Table 5.1).

5.3.1.2. Experimental setup

Biochemical methane potential experiments were conducted to model the effect of ammonia and determine the NIC and MIC. NH_4Cl was used as the ammonia source, creating a concentration gradient of 0, 188, 377, 755, 1890, 3780, and 7560 mg TAN/L. This gradient was chosen based on the highest concentration known to cease CH_4 production in a comparable process, considering similar pH, temperature regimes, and feedstock (Hadj et al., 2009). Triplicate batch assays were conducted using an AMPTS II automated system with online CH_4 volume measurement (Bioprocess Control, Sweden) following a modified protocol from Holliger et al., (2016). Operational conditions included 35 °C, S_0/X_0 ratio of 0.5 gVS/gVS, FW concentration of 10 gVS/L, a working volume of 360 mL (total volume of 600 mL), 4 g NaHCO_3 /L as buffer, pH adjustment to 8 with 5 N NaOH and discontinuous mixing at ~150 rpm (60s ON/120s OFF cycles). Each experiment was conducted over 10 d, enough time to observe a stationary phase in methane production in all evaluated conditions (Moreno-Andrade et al., 2020). At the end of the AD process, samples were collected to determine biogas composition, individual VFAs, TAN, total carbohydrates, total solids (TS), volatile solids (VS), and the microbial community structure. Subsequently, based on the evaluated parameters, various statistical analyses were applied using R software version 4.2.1 to interpret the data, as detailed later.

Table 5.1. Physicochemical characteristics of food waste and granules

Parameters	Food waste	Granules
TS (g/L)	81.9	0.0803 ^(a)
VS (g/L)	67.4	0.0664 ^(b)
VS/TS	0.82	1.21
pH	7.2	6.8
Total carbohydrates (g/L)	5.2	ND
COD total (g/L)	84.4	0.114 ^(c)
COD soluble (g/L)	53.75	ND
COD particulate (g/L)	30.65	ND
NH ₃ (mg/L)	190	ND
NH ₄ ⁺ (mg/L) ^(d)	1662.86	ND
Acetate (mg/L)	1698	ND
Propionate (mg/L)	0	ND
Butyrate (mg/L)	0	ND
Valerate (mg/L)	0	ND

a) gTS/g-granules; b) gVS/g-granules; c) g-COD/g-granules; d) NH₄⁺ was calculated using the equation $NH_3 = NH_4^+ / (1 + 10^{-pH/Ka})$, used by Zhang et al. (2020).

TS: Total solids; VS: Volatile solids; COD: Chemical oxygen demand; FW: food waste; ND: Not determined.

5.3.1.3 Determination ammonia inhibitory levels

Three inhibitory levels based on the Hill model curve grouped the samples according to effects of ammonia on AD. The model used CH₄ yield (mL CH₄/g VS_{added}) as the dependent variable and ammonia concentration (mg TAN/L) as the explanatory variable using the equation 5.1 (Agyeman et al., 2021).

$$\mu = \mu_m + (\mu_0 - \mu_m) \frac{1}{\left(1 + \left(\frac{IC_{50}}{S}\right)^n\right)} \quad \text{Eq. 5.1}$$

Where μ was the CH₄ yield (mL CH₄/gVS_{added}), μ_m was the maximum CH₄ yield (mL CH₄/gVS_{added}), μ_0 was the minimum CH₄ yield (mL CH₄/gVS_{added}), S was the ammonia concentration, IC₅₀ was the ammonia concentration when $\mu_m/2$, and n was an empirical coefficient.

The reliability of model was validated by comparing the coefficient of determination (R²) observed in similar processes. A selection criterion included similar feedstocks (FW/OFMSW), mesophilic temperatures (37 °C), and neutral pH (7-8) (Chen et al., 2016; Hadj et al., 2009; Yu et al., 2020; Zhang et al., 2020). The “nlsML” function from “minpack.lm” package was utilized to estimate the IC₅₀ and n parameters of the Hill model (Elzhov et al., 2016).

The IC₅₀ (50% inhibition of CH₄ yield) and n (empirical coefficient) parameters obtained from Hill model calculated the NIC and the MIC according to equation 5.2 and 5.3 (Lambert & Pearson, 2000).

$$\text{NIC} = 10^{\left(\log_{10} \text{IC}_{50} - \frac{1.718}{n}\right)} \quad \text{Eq. 5.2}$$

$$\text{MIC} = 10^{\left(\log_{10} \text{IC}_{50} + \frac{1}{n}\right)} \quad \text{Eq. 5.3}$$

Ammonia inhibitory levels were classified as NIC for concentrations < NIC, inhibition for NIC–MIC, and MIC for concentrations > MIC. Significant differences in CH₄ yield and VFA across ammonia levels were determined using one-way analysis of variance (ANOVA) and Tukey's test (p < 0.05). These analyses were performed with the "aov" and "TukeyHSD" functions from the vegan package (Oksanen et al., 2020).

5.3.2. DNA collection and metagenomic analysis

Metagenomic analysis was chosen to characterize the microbiome at both the genus and gene levels, for each assessed ammonia concentration by duplicate. The selected samples were 0-A, 0-B, 188-B, 188-C, 377-A, 377-B, 755-A, 755-B, 1890-B, 1890-C, 3780-B, 3780-C, 7560-A, and 7560-B. The numerical values indicate the concentration of ammonia added (mg TAN/L), and the letter corresponds to the selected replicate. A total of fourteen samples were processed for DNA extraction using the DNeasy PowerSoil Pro Kit (Qiagen, Germany). The quality of the purified DNA was assessed with the 260/280 absorbance ratio using NANODrop 2000c (Thermo Scientific, USA). The DNA samples were sequenced using NovaSeq 6000, Illumina (~8 million PE 150+150 bp reads) at the National Genomic Sequencing Laboratory Tec-BASE (Tecnológico de Monterrey, Mexico).

Metagenomic data were obtained from selected samples. The raw metagenomic data underwent quality assessment with FastQC (v0.11.9). Low-quality reads and ambiguous bases were filtered out with Trimmomatic (v0.33) using the parameters: LEADING:3, TRAILING:3, SLIDINGWINDOW:4:15, MINLEN:36 (Bolger et al. 2014). High-quality reads were assembled into contigs using MEGAHIT (v1.2.9) with settings: --k-list 21,33,55,77,99,111,127 -t 8 (Duan et al. 2021; Li et al. 2015). Taxonomic classification of contigs was performed using Kaiju (v1.6.2) with the proGenomes database. Classification was assigned at the genus level to enhance precision and sensitivity (Menzel et al., 2016). Gene prediction and annotation were conducted using Prokka

(v 1.14.6) using parameters: --mincontiglen 500, --kingdom Bacteria, --kingdom Archaea -force (Seemann, 2014). To mitigate sequencing depth variations, count tables were rarefied by random subsampling without replacement, adhering to minimum count thresholds for each dataset (229,393 sequence reads for genera and 143,899 protein-coding sequences for genes). The rarefied count tables for genera and genes were utilized as input for subsequent diversity and statistical analyses aimed at identifying MI attributes. Raw metagenomic sequences were deposited into the NCBI sequence read archive (SRA) database under the project number PRJNA1138064.

5.3.3. Diversity analysis

The taxonomic and functional diversity across ammonia inhibitory levels was assessed using alpha and beta diversity indices. Alpha diversity included Hill numbers (q_0 , q_1 , q_2) and Pielou's evenness indices at both the genus and gene level. These indices were compared between and within inhibitory levels using the Kruskal-Wallis test with Bonferroni correction and Wilcoxon rank-sum test with Benjamini-Hochberg correction (both adjusted $p < 0.05$), respectively. The Hill numbers (q_0 , q_1 , and q_2) were determined using the "hill_div" function from the "hilldiv" package with q values of 0, 1, and 2, respectively (Alberdi & Gilbert, 2019). The Pielou index was calculated with the "estimate_richness" function from the "phyloseq" package (McMurdie & Holmes, 2013). Significance tests were performed using the Kruskal-Wallis test and the Wilcoxon rank-sum test with Benjamini-Hochberg correction, utilizing the "kruskal.test" and "pairwise.wilcox.test" functions from the "stats" package.

For beta diversity, nonmetric multidimensional scaling (NMDS) was utilized to assess inhibitory levels based on Bray-Curtis and Jaccard metrics. The goodness of the NMDS model was assessed by stress value (values < 0.1 indicated a good fit). The analysis of group similarities (ANOSIM) was employed to assess dissimilarities between levels, with an R value near 1.0 indicating significant dissimilarity. Bray-Curtis and Jaccard metrics were calculated using the "vegdist" function. The NMDS solution was obtained via the "metaMDS" function, and the ANOSIM test was performed using the "anosim" function. All beta diversity functions were from the "vegan" package (Oksanen et al., 2020).

5.3.4. Statistical framework to identify MIs attributes

A statistical framework integrated non-parametric rank tests, differential analyses, discriminatory analysis, z-scores, multivariate analysis, and MAGs was applied to identify multiple MI attributes

from processed reads and abundance data of genera and genes. (I) Keystone species were inferred from topological properties of co-occurrence networks within the microbiome belong to NIC level (Pan et al., 2021). (II) Significant abundance changes were identified through significance tests comparing NIC levels to inhibition or MIC levels (Huerta et al., 2024; Zhang et al., 2022). (III) Potential early warning signs were linked to the first significant change in abundance (z -score ≥ 1) before ammonia concentration reached the inhibitory level (Mirza et al., 2020). (IV) Metabolic roles were analyzed through three approaches: correlative analysis inferred metabolic pathways and potential role; z -score analysis indicated metabolic functional changes in microbiome; and MAGs linked changing metabolic pathways and key genes to key genera, highlighting their metabolic relevance.

5.3.4.1. Keystone

Keystones within microbiome at the NIC level in the batch assay were identified using Molecular Ecology Network Analysis (MENA) (<http://ieg4.rccc.ou.edu/mena>), accomplishing the sample size requirement ($n \geq 8$). Network modularity analysis using within-module connectivity (Z_i) and among-module connectivity (P_i) scores classified genera and genes. Highly connected generalists, including module hubs ($Z_i > 2.5$; $P_i < 0.62$), network hubs ($Z_i > 2.5$; $P_i > 0.62$), and connectors ($Z_i < 2.5$; $P_i > 0.62$), were identified as keystones. Peripherals ($Z_i < 2.5$; $P_i < 0.62$) were excluded due to their low interaction with other genera or genes (Pan et al., 2021).

5.3.4.2. Significant abundance changes

Genera and gene abundances were compared between non-inhibitory concentrations (NIC), inhibition, and minimum inhibitory concentrations (MIC) using two significance testing methods. Comparisons were conducted between NIC and inhibition, as well as between inhibition and MIC. The first method evaluated differential responses by focusing on pre-selected MIs and keystone species, both identified for their ecological roles and sensitivity to ammonia effects. Specifically, 25 key genera and 26 genes were considered potential MIs for ammonia inhibition in mesophilic digesters processing FW/OFMSW (Table 5.2). The Kruskal-Wallis test with Bonferroni correction (adjusted p -value < 0.05) was applied to rarefied count data to identify significant differences in genera and gene abundances.

The second approach involved multiple differential analysis methods, including LefSe, DESeq2, EdgeR, Limma voom, and metagenomeSeq, to cover all identified genera and genes. This

minimized inherent variations in taxonomic and functional data distribution, ensuring consistent results. The term robust FC was introduced, defined as results consistent in at least two differential analyses with a $FC \geq |2|$ (Nearing et al., 2022). LEfSe was applied to normalized rarefied data using the Kruskal-Wallis test ($p < 0.05$) and linear discriminant analysis (LDA) with a score > 2 (Segata et al., 2011). DESeq2 analyzed non-rarefied data using negative binomial generalized linear models (GLM) and the Wald test with Benjamini-Hochberg correction (adjusted $p < 0.05$) (Love et al., 2014). EdgeR calculated dispersion parameters in a negative binomial GLM and used the likelihood ratio test ($p < 0.05$) for model comparison (Robinson et al., 2009). Limma-voom applied precision weights to rarefied log₁₀-transformed data and used an empirical Bayes moderated t-test with Benjamini-Hochberg correction (adjusted $p < 0.05$) (Law et al., 2014). MetagenomeSeq used a zero-inflated Gaussian mixture model with an empirical Bayes t-test for rarefied log₁₀ data (Paulson et al., 2013).

The differential analyses were conducted using the “run_lefse,” “run_deseq2,” “run_edger,” “run_limma_voom,” and “run_metagenomeseq” functions from the “microbiomeMarker” package (Cao et al., 2022). Key genera and genes were identified by overlapping outcomes from at least two differential analyses, visualized with a Venn diagram using the “venn” function from the “ggvenn” package.

Table 5.2. List of MI reported in the literature considered for the study

Potential microbial indicator	Biological relevance in AD	Association with ammonia	E.C. number	COG number	Reference
Taxa					
<i>Syntrophomonas</i> ⁽¹⁾	Syntrophic VFA oxidation	Negative	NA	NA	Cortez-Cervantes et al., (2024)
<i>Treponema</i> ⁽¹⁾	Homoacetogenesis	Positive	NA	NA	
<i>Methanosarcina</i> ⁽¹⁾	Methanogenesis	Negative/Positive ⁽²⁾	NA	NA	
<i>Methanoculleus</i> ⁽¹⁾	Methanogenesis	Positive	NA	NA	
HA73 ⁽¹⁾	N.D.	Positive	NA	NA	
<i>Sedimentibacter</i>	Syntrophic LCFA oxidation Protein degradation	Negative	NA	NA	
<i>Corynebacterium</i>	NH ₄ ⁺ assimilation	Positive	NA	NA	
<i>Lactobacillus</i>	Carbohydrate fermentation	Positive	NA	NA	
<i>Methanosaeta/Methanotherix</i>	Methanogenesis	Negative	NA	NA	Chen et al., (2016)
<i>Anaerolinea</i>	Syntrophic acetate oxidation	Positive	NA	NA	Ruiz-Sánchez et al., (2018)
<i>Methanobrevibacter</i>	Methanogenesis	Negative/Positive	NA	NA	
<i>Methanomassiliicoccus</i>	Methanogenesis	Negative/Positive	NA	NA	
<i>Pelotomaculum</i>	Syntrophic propionate oxidation	Negative	NA	NA	Zhang et al., (2022)
<i>Syntrophobacter</i>	Syntrophic propionate oxidation	Negative	NA	NA	
<i>Lutispora</i>	Amino acid degradation	Positive	NA	NA	
<i>Candidatus Syntrophosphaera</i>	Syntrophic propionate oxidation	Negative	NA	NA	
<i>Anaerosalibacter</i>	Protein degradation	Positive	NA	NA	Poirier et al., (2020)
<i>Sphaerochaeta</i>	Carbohydrate degradation	Positive	NA	NA	
<i>Clostridium</i>	Syntrophic acetate oxidation	Positive	NA	NA	
<i>Defluviitalea</i>	Carbohydrate degradation	Positive	NA	NA	
<i>Tepidimicrobium</i>	VFA production	Positive	NA	NA	
<i>Tissierella</i>	Carbohydrate degradation	Positive	NA	NA	
<i>Caldicoprobacter</i>	Carbohydrate degradation	Positive	NA	NA	
<i>Aminobacterium</i>	Hydrolysis of protein and amino acids degradation	Positive	NA	NA	Poirier et al., (2016)

continued

CHAPTER 5. Suitable microbial indicators for detecting ammonia inhibition in anaerobic digestion of food wastes

<i>Ruminococcus</i>	Hydrolysis of carbohydrates	Negative	NA	NA	
Genes					
acetyl-CoA synthetase (<i>acs</i>)	Carbohydrates and propionate metabolism	Positive	EC:6.2.1.1	COG0365	
phosphate acetyltransferase (<i>pta</i>)	Methanogenesis Acetoclastic methanogenesis	Negative	EC 2.3.1.8		
Methyl-coenzyme M reductase I subunit alpha (<i>mcrA</i>)	Methanogenesis	Negative		COG4058	
Methyl-coenzyme M reductase I subunit beta (<i>mcrB</i>)	Methanogenesis	Negative		COG4054	
Methyl-coenzyme M reductase I subunit gamma (<i>mcrG</i>)	Methanogenesis	Negative		COG4057	
Methyl-coenzyme M reductase II subunit alpha (<i>mrtA</i>)	Methanogenesis	Negative		COG4058	
Methyl-coenzyme M reductase II subunit beta (<i>mrtB</i>)	Methanogenesis	Negative	EC:2.8.4.1	COG4054	
Methyl-coenzyme M reductase II subunit gamma (<i>mrtG</i>)	Methanogenesis	Negative		COG4057	
Methyl-coenzyme M reductase subunit alpha (<i>mcrA</i>)	Methanogenesis	Negative		COG4058	Yu et al., (2020)
Methyl-coenzyme M reductase subunit beta (<i>mcrB</i>)	Methanogenesis	Negative		COG4054	
Methyl-coenzyme M reductase subunit gamma (<i>mcrG</i>)	Methanogenesis	Negative		COG4057	
Ferredoxin/F(420)H(2)-dependent CoB-CoM heterodisulfide reductase subunit A (<i>hdrA</i>)	Methanogenesis	Negative		COG1148	
Ferredoxin/F(420)H(2)-dependent CoB-CoM heterodisulfide reductase subunit B (<i>hdrB</i>)	Methanogenesis	Negative		COG2048	
Ferredoxin/F(420)H(2)-dependent CoB-CoM heterodisulfide reductase subunit C (<i>hdrC</i>)	Methanogenesis	Negative	EC:1.8.7.3	COG1150	
Ferredoxin:CoB-CoM heterodisulfide reductase subunit A (<i>hdrA</i>)	Methanogenesis	Negative		COG1148	
Ferredoxin:CoB-CoM heterodisulfide reductase subunit B (<i>hdrB</i>)	Methanogenesis	Negative		COG2048	

continued

CHAPTER 5. Suitable microbial indicators for detecting ammonia inhibition in anaerobic digestion of food wastes

Ferredoxin:CoB-CoM heterodisulfide reductase subunit C (<i>hdrC</i>)	Methanogenesis	Negative		COG1150	
acetate kinase (<i>AK</i>)	Acetate metabolism	Negative/Positive	EC. 2.7.2.1	ND	
Acetyl-CoA decarbonylase/synthase complex subunit alpha (<i>cdhA</i>)	Acetoclastic methanogenesis	Negative/Positive	EC 1.2.7.4	COG1152	
Acetyl-CoA decarbonylase/synthase complex subunit beta (<i>acsB</i>)	Acetoclastic methanogenesis	Negative/Positive	EC 2.3.1.169	COG1614	
Acetyl-CoA decarbonylase/synthase complex subunit delta (<i>acsD</i>)	Acetoclastic methanogenesis	Negative/Positive	ND	COG2069	Zhang et al., (2022)
Acetyl-CoA decarbonylase/synthase complex subunit epsilon (<i>acsE</i>)	Acetoclastic methanogenesis	Negative/Positive	ND	COG1880	
Acetyl-CoA decarbonylase/synthase complex subunit gamma (<i>acsC</i>)	Acetoclastic methanogenesis	Negative/Positive	EC 2.1.1.245	COG1456	
Succinate--CoA ligase [ADP-forming] subunit alpha (<i>sucA</i>)	Propionate metabolism	Negative	EC 6.2.1.5	COG0074	
Formate--tetrahydrofolate ligase (<i>fthfs</i>)	Acetate oxidation	Negative/Positive	EC 6.3.4.3	ND	Ruiz-Sánchez et al., (2018)
glycine cleavage system complex (<i>Gcs</i>)	Acetate oxidation	Negative/Positive	ND	ND	

(1) Listed as members from core microbiome (potential universal microbial indicators) of anaerobic process fed with OFMSW or FW. (2) Samples show a dual response according to an inhibitory threshold. ND: Not determined. NA: Not applicable.

The key genera and genes from two significance testing approaches were compared using the area under the curve (AUC) to evaluate their standardized ability to discriminate against ammonia inhibition levels. A binomial GLM was implemented to adjust the response of key genera and genes, predicting ammonia inhibitory levels. Inhibition and MIC levels were encoded as 0, and the NIC level as 1. Model performance was assessed through AUC values derived from the receiver operating characteristic (ROC) curve. Higher AUC values, approaching 1, indicate a higher likelihood of true positive responses and a greater discriminatory capacity of the evaluated indicators. The binomial GLM was implemented using the "glm" function within the "stats" package, and AUC values were determined through the "prediction" and "performance" functions in the "ROCR" package (Sing et al., 2005).

5.3.4.3. Potential early warnings signs

The potential early warning attribute was identified by the first absolute change of one unit or more in the z-score ($z\text{-score} \geq |1|$) in the abundance of key genera or genes before reaching the inhibition level, excluding control condition values (Mirza et al., 2020). This attribute was analyzed exclusively for key genera and genes exhibiting significant abundance changes.

The z-scores were calculated through equation 5.4:

$$Z\text{-score} = \frac{x - \mu}{\sigma} \quad \text{Eq. 5.4}$$

where x represents the genus or gene abundance for each ammonia concentration, and μ and σ denote the average and standard deviation across all ammonia concentrations, respectively.

5.3.4.4. Metabolic roles

The metabolic role of each key genus and gene was revealed using multiple statistical analyses and the creation of MAGs. Initially, redundancy analysis (RDA) was employed to identify relevant AD byproducts. This analysis explored positive and negative relationships with ammonia concentration gradients, utilizing both genus and gene data as response variables. To enhance the precision and efficiency of RDA models a data transformation strategy was implemented. Hellinger method for rarefied count data and standardized method for AD by-products. Hellinger and normalization transformations were obtained by "decostand" function from the "vegan" package (Oksanen et al., 2020). The effectiveness of the RDA models was assessed through coefficients of determination (R^2) values and ANOVA, employing a regression model with 999

permutations ($p < 0.05$). The assessment of RDA was conducted using the "rda" and "anova.cca" functions from the "vegan" package (Oksanen et al., 2020).

To interpret the functional impact of ammonia and highlight altered or enriched metabolic pathways, a KEGG pathways/modules analysis was conducted. The analysis targeted pathways/modules linked with AD and key genes. Contigs from each sample were annotated using the KEGG Automatic Annotation Server (<https://www.genome.jp/kegg/kaas/>) to generate a KEGG orthology (KO) count table. The abundance of KOs for each KEGG pathway/module was evaluated across the ammonia concentration gradient using z-scores (see Eq. 5.4). Scores closer to -2 indicated a decrease in the annotated gene count, while scores near 2 indicated an increase in annotated gene count. Relevant metabolic pathways and modules related to AD and key genes were selected, and prefix codes were obtained using the "keggGet" function from the "KEGGREST" package. The percentages of biochemical conversion reactions in KEGG pathways were visualized in a heatmap using the "ggballoonplot" function from the "ggpubr" package.

MAGs offered insights into the functionality of key genera by analyzing the relationship between these genera and ammonia-altered metabolic pathways. The MAGs were constructed through the co-assembly of all samples using the MEGAHIT with previous settings (see 5.3.2). The BMAP tool (v. 38.18) mapped individual reads, calculated read recruitment, and established contig coverage. The resulting alignment file underwent sorting and indexing through SAMtools (v. 1.18). Utilizing the jgi_summarize_bam_contig_depths tool allowed for per-contig coverage computation from BAM files. Metagenomic binning was performed on co-assemblies using MetaBAT2 (v. 2.12.1) with options: --minCVSum 0, --saveCls, -d, --minCV 0.1, and -m 2000, yielding potential genome bins. The binning results were integrated using Das Tool (v 1.1.6) with parameters --search_engine blastp and --write_bins, resulting in an optimized and non-redundant bin set. Taxonomic classification of the bins was performed using GTDBTK (v 2.3.2) with default settings. Protein-coding sequences (CDSs) within the MAGs were predicted using Prodigal (v2.6.3) and annotated using KofamScan (v1.3.0) with KOfam profiles as of 2023-04-01. Only pathways containing at least 80% of the biochemical conversion reactions in KEGG pathways were considered (Hao et al., 2020).

Pearson correlation analysis was performed to explore relationships between key genera, genes, and AD by-products, validating their potential metabolic roles observed in the experiment. The

data for correlation analysis was transformed similarly to the RDA process. Linear relationships between potential MIs and AD by-products were assessed using Pearson correlation significance test. Correlation coefficients were computed with the "cor" function from the "stats" package. The significance of these correlations ($p < 0.05$) was evaluated using the "corr.mtest" function from the "corrplot" package (Wei & Simko, 2021).

5.3.5. Analytic methods

The composition of biogas and VFA (AD by-products) were analyzed using gas chromatography (GC) equipped with a thermal conductivity detector, and GC equipped with a flame ionization detector, respectively, as reported previously (Moreno-Andrade et al., 2020). COD, ammonia, TS and VS were determined following Standard Methods (APHA, 2005).

5.4. Results and discussion

5.4.1. Definition of ammonia inhibitory levels

The validated Hill model ($R^2 > 0.87$) accurately defined ammonia inhibitory levels for each anaerobic process evaluated. NIC and MIC values, which indicate ammonia effect thresholds, varied among studies (Fig. 5.1. and Table 5.3). For this study, the Hill model determined TAN concentrations below 2702 mg/L as the NIC level, 2702 – 5805 mg/L as the inhibition level, and above 5805 mg/L as the MIC level. Each inhibitory level significantly impacted key AD by-products ($p < 0.05$), with acetate and propionate showing notable accumulation increases at inhibition and MIC levels (Fig. 5.2). NIC level obtained the highest CH_4 yield ($308.8 \pm 41.4 \text{ mL CH}_4/\text{gVS}_{\text{added}}$), followed by inhibition ($247.8 \pm 24.7 \text{ mL CH}_4/\text{gVS}_{\text{added}}$) and MIC levels ($0 \text{ mL CH}_4/\text{gVS}_{\text{added}}$). These findings highlight the difficulty of standardizing inhibitory concentrations in FW digesters. However, the ammonia inhibitory levels could be standardized based on Lambert and Pearson (2000) concept, reflecting a consistent response in AD by-products, as suggested by previous research (Hardy et al., 2021; Zhang et al., 2022).

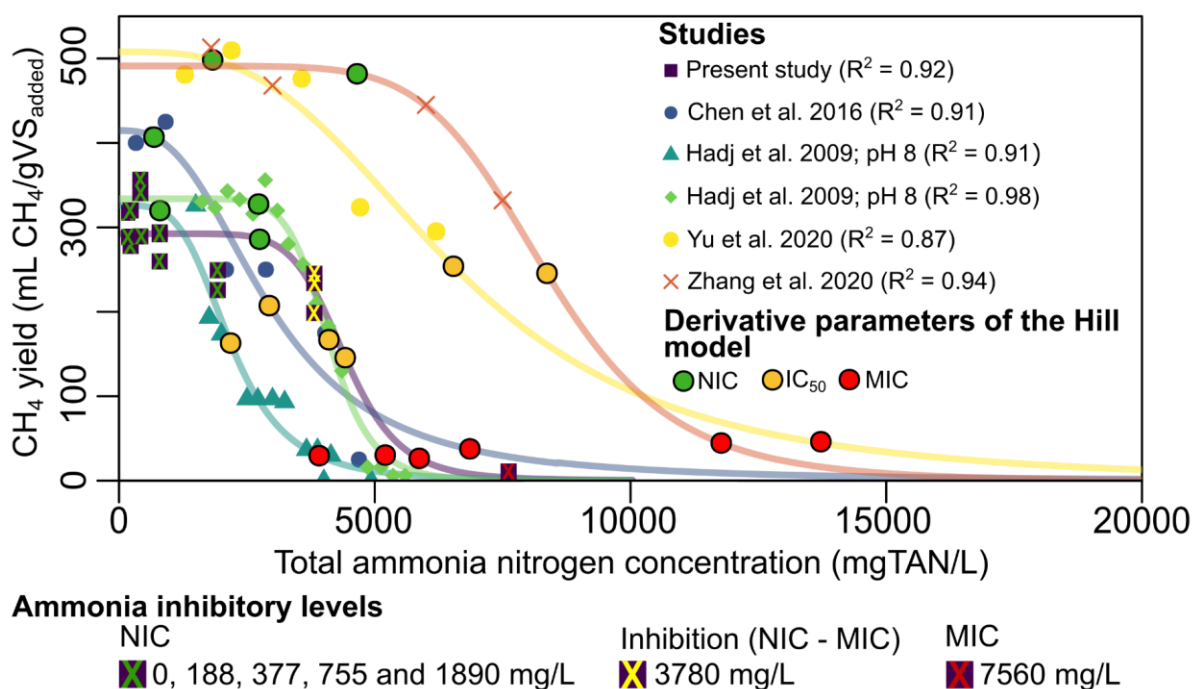


Figure 5.1. The validated Hill Model determined NIC and MIC, defining ammonia inhibitory levels. The coefficient of determination (R^2) was calculated for each dataset from the selected studies, confirming the high goodness of fit in profiling the effect of ammonia in FW/OFMSW anaerobic processes. In this experiment, TAN concentrations of 0, 188, 377, 755, and 1890 mg/L were categorized as NIC (green “X”), 3780 mg/L was classified as the inhibition level (yellow “X”), and 7580 mg/L was identified as MIC (red “X”).

Table 5.3. Kinetic and derivative parameters from Hill model across different studies

Feedstock	Feed regimen	Inoculum source	Ammonia source	Temperature (°C)	pH	IC ₅₀ (mg TAN/L)	NIC (mg TAN/L)	MIC (mg TAN/L)	Reference
FW	Semi-continuous	Sewage sludge from AD	NH ₄ Cl	37	7.2	2937	684	6859	Chen et al., 2016
OFMSW	Batch	Sewage sludge from AD	NH ₄ Cl	37	7.0 ^(a) – 8.0 ^(b)	4103 ^(a) , 2181 ^(b)	2727 ^(a) , 799 ^(b)	5204 ^(a) , 3912 ^(b)	Hadj et al., 2009
FW	Batch	Sludge from AD fed with FW	NH ₄ Cl	37	7.3 – 7.4	6538	1830	13721	Yu et al., 2021
FW	Batch	Sludge from AD fed with FW	NH ₄ Cl	37	7.5	8367	4654	11773	Zhang et al., 2020
FW	Batch	Granules from AD fed with organic wastes of flour industry	NH ₄ Cl	37	8	4381	2702	5805	In this study

AD = Anaerobic digestion; FW = Food waste; OFMSW = Organic food municipal solid waste; IC₅₀ = half maximal inhibitory concentration; NIC = non inhibitory concentration; MIC = minimum inhibitory concentration.

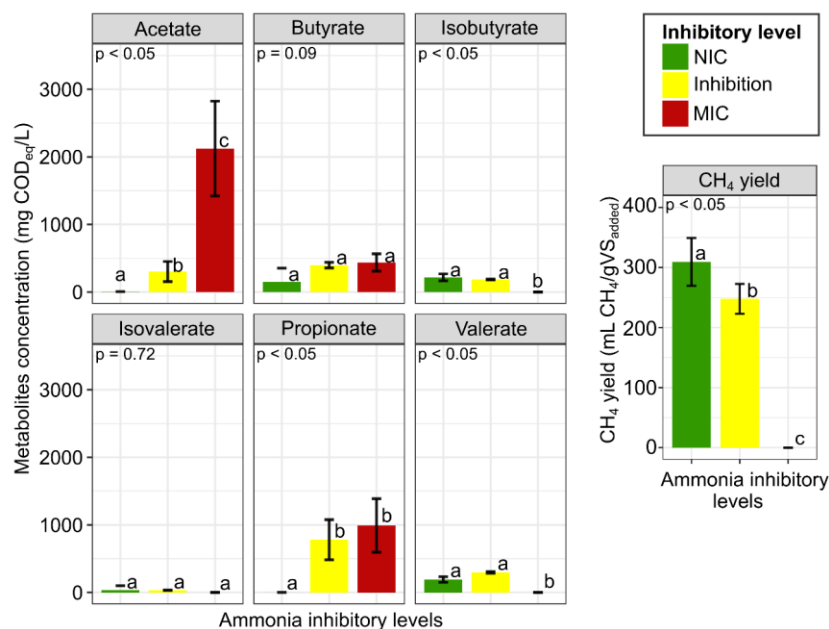


Figure 5.2. The bar plot illustrates the concentration of AD by-products within each determined ammonia inhibition level. The bar plot exemplifies how the concentration of specific volatile fatty acids (VFAs) or CH₄ yield differed significantly ($p < 0.05$) among the inhibition level, as determined by ANOVA. Pairwise comparisons were executed using the Tukey test. Lowercase letters within the bar plots indicate groups with statistically significant differences.

5.4.2. Variation in microbiome diversity across ammonia inhibitory levels

The metagenomic analysis identified 2197 genera and 2253 genes. Alpha diversity indices varied with ammonia inhibitory levels, depending on taxonomic or functional levels (Fig. 5.3). At the genus level, diversity measures such as q1 and Pielou indices significantly increased in the inhibition level ($p < 0.10$), while no significant differences were observed at the MIC level ($p > 0.10$) compared to the NIC level (Fig. 5.3a). However, q0 and q2 showed no significant differences ($p > 0.10$). Under inhibitory conditions, a higher abundance of syntrophic acetate-oxidizing bacteria (SAOB), rather than their richness, may contribute to a more evenly distributed microbial community (Hill et al., 2003; Yu et al., 2020). These aspects indicate an acclimated microbial community that modified its structure within the same genera to maintain CH₄ production (Ruiz-Sánchez et al., 2018; Yu et al., 2021).

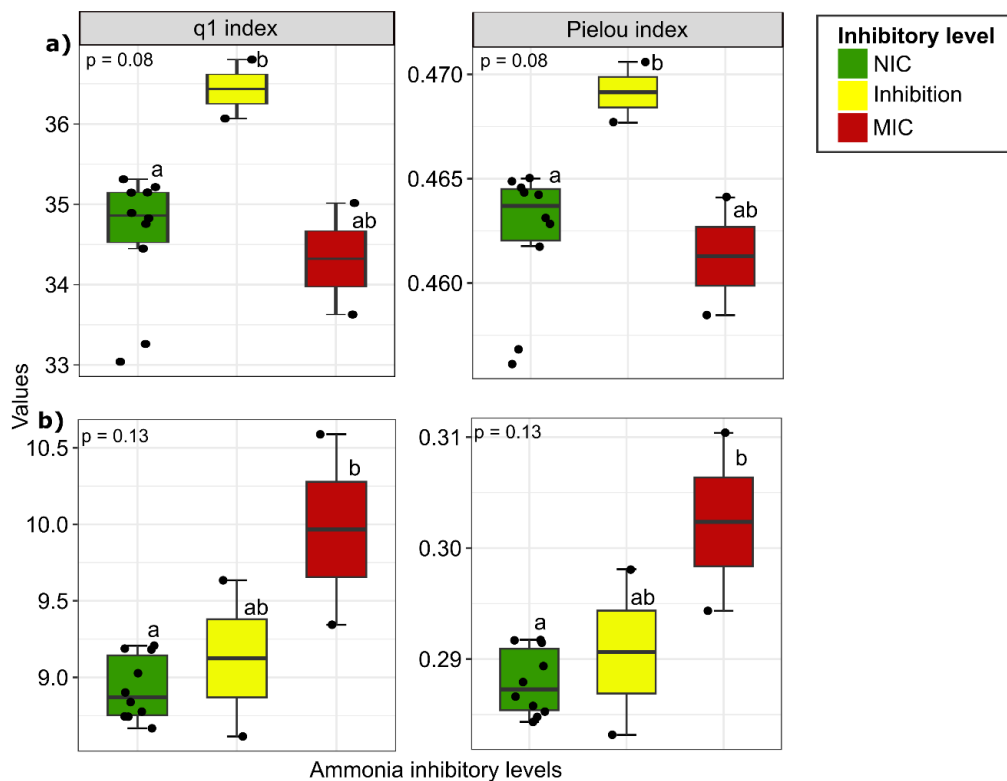


Figure 5.3. Distribution of key alpha indices through ammonia inhibitory levels based on q1 and Pielou at a) genera and b) genes level. Boxplots illustrate median, quartiles, and extreme values, with significance assessed using the Kruskal-Wallis test ($p < 0.10$) and pairwise comparisons using Wilcoxon rank sum tests ($p < 0.10$). Lowercase letters within the boxes indicate groups with statistically significant differences.

At functional level q1 and Pielou indices (Fig. 5.3b) showed significantly higher values in the MIC level ($p < 0.10$) compared to the NIC level, while remaining insignificant ($p > 0.10$) at the inhibition level. Additionally, q0 and q2 indices showed no significant differences ($p > 0.10$). Ammonia concentrations above 6000 mg/L may boost hydrolytic and fermentative activities, potentially increasing the gene abundance for these microbial activities, resulting in a uniform functional structure (Ma et al., 2021; Zhang et al., 2020). This characterizes the establishment of a functional microbial community resistant to high ammonia concentrations, although community is not related to CH₄ production.

NMDS analysis, employing Bray-Curtis and Jaccard metrics, showed varied responses depending on taxonomic or functional levels (Fig. 5.4). Ammonia presence modified the abundance of certain genera (Fig. 5.4a), demonstrating its selective power in shaping diverse microbial communities (Hardy et al., 2021). Despite a conserved gene composition due to inoculum redundancy (Fig. 5.4b), the abundance of genes linked to key metabolic pathways varied depending on ammonia inhibitory level (Zhang et al., 2022). These findings align with results in the subsequent section, underscoring the limitations of ordination methods in detecting global gene composition differences.

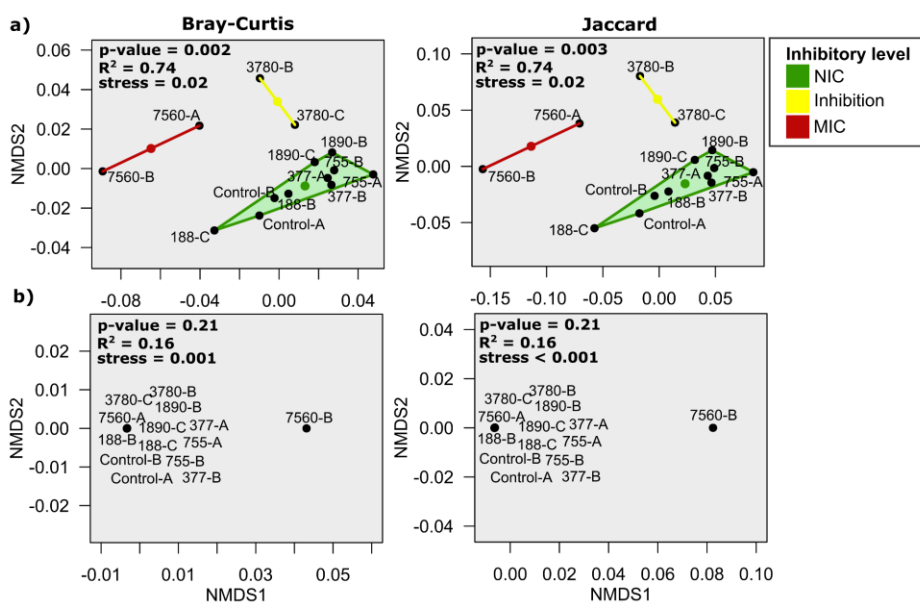


Figure 5.4. NMDS plots showing sample distributions based on Bray-Curtis and Jaccard dissimilarity indices at the (a) genus and (b) gene levels. Clusters are categorized according to defined ammonia inhibitory levels, with each cluster representing ammonia concentrations grouped by the analysis, including replicates (A, B). ANOSIM results, including p-values, R², and stress values, are provided to assess the statistical significance of clustering among inhibitory levels.

5.4.3. Significant abundance change using a dual approach

A set of 27 genera and 20 genes showed significant abundance changes using two different significance test approaches (Fig. 5.5). Among the 13 genera and 14 genes with a robust fold change ($FC \geq 2$) and high area under the curve ($AUC \geq 0.85$), a strong ability to discriminate ammonia inhibitory levels was observed (Fig 5.7). Meanwhile, the selected MIs group related with 14 genera and 6 genes which showed traditional significant differences despite having a lower fold change ($FC < 2$), demonstrated adequate discriminatory capacity ($AUC \geq 0.80$). Genera and genes that consistently differentiate between ammonia inhibition levels and align with findings from other studies can be considered as potential suitable MIs (He et al., 2017; Li et al., 2018; Poirier et al., 2020; Yu et al., 2020; Zhang et al., 2022). Therefore, this section focuses only on genera and genes considered as potential suitable MIs that also achieved a predominant abundance in comparative sets, an essential criterion for generalizing the detection method for future applications (Li et al., 2018).

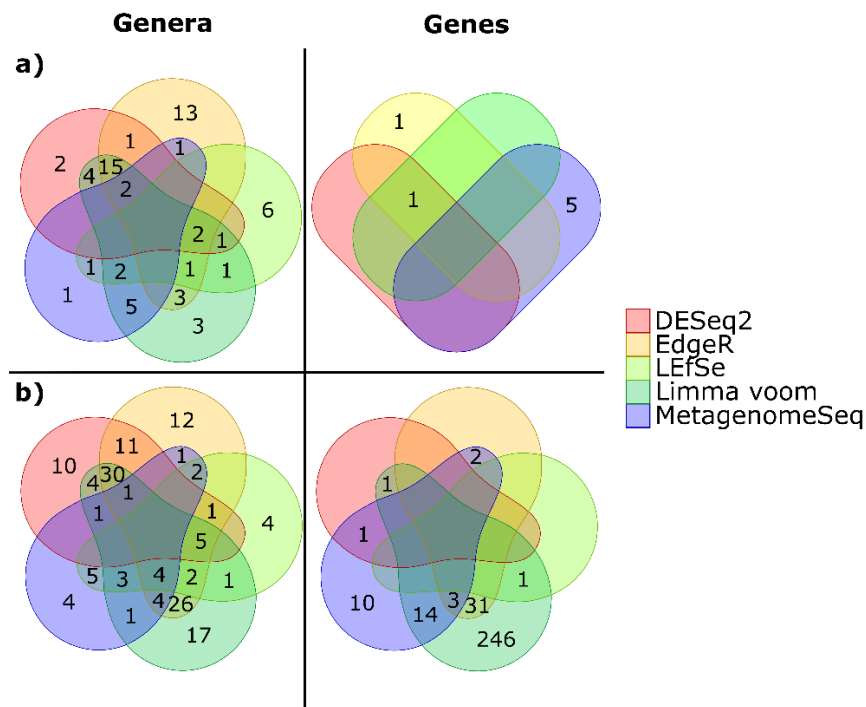


Figure 5.5. Venn diagrams illustrate the number of genera and genes shared between differential analyses. Each method, marked by a unique color, identified significantly differentially abundant genera and genes (adjusted $p < 0.05$). DESeq2 (red), EdgeR (yellow), LefSe (lime green), Limma voom (green), and MetagenomeSeq (blue) were used. a) NIC vs inhibition level: DESeq2: 27 genera, 1 gene; EdgeR: 38 genera, 2 genes; LefSe: 14 genera, 0 genes; Limma voom: 39 genera, 1 gene and; MetagenomeSeq: 14 genera, 1 gene. b) NIC vs MIC level: DESeq2: 63 genera, 2 genes; EdgeR: 99 genera, 36 genes; LefSe: 27 genera, 1 gene; Limma voom: 99 genera, 296 genes; MetagenomeSeq: 26 genera, 30 genes.

5.4.3.1. NIC level vs inhibition level

At the NIC level, increased abundance of *Sphaerochaeta* (Fig 5.7a) and the *hdrA* (Ferredoxin:CoB-CoM heterodisulfide reductase subunit A, K22480) and *mcrB* (methyl-coenzyme M reductase II subunit beta, K00401) genes (Fig 5.7c) may discriminate inhibited samples when their abundance decrease ($AUC \geq 0.90$). The key genus has sensibility to ammonia inhibition in other AD systems. The fermentative *Sphaerochaeta* display significant responses up to > 4 g TAN/L, indicating ammonia inhibition (He et al., 2017). Meanwhile, variations in the key genes reflect changes in microbial metabolism related to the effect of ammonia. The reduction of *mcrB* and *hdrA* genes may suggest a shift from acetoclastic to hydrogenotrophic methanogenesis, a common metabolic event when ammonia concentration reaches inhibitory levels (Yu et al., 2020; Zhang et al., 2022).

Conversely, in the inhibition level increased the abundance of genera *Anaerosalibacter*, *Clostridium Syntrophobacter*, and *Ruminococcus*, demonstrating high power classificatory ($AUC \geq 0.90$) to distinguish from the NIC level (Fig 5.7a). Only *Ruminococcus* was identified as a keystone with significant changes (Fig. 5.6). The increase in these genera may be revealed when ammonia reaches inhibitory levels. Particularly, hydrolytic bacteria like *Anaerosalibacter* and *Ruminococcus* thrive under inhibitory ammonia conditions, promoting growth during inhibited-AD (He et al., 2017; Poirier et al., 2020). Furthermore, as *Ruminococcus* was considered a keystone, it may be crucial for maintaining microbial interactions when the AD process shifts towards fermentation (Chen et al., 2016; Pan et al., 2021). Genera such as *Clostridium* and *Syntrophobacter*, which include SAOB and syntrophic propionate-oxidizing bacteria (SPOB), suggest CH_4 production via a hydrogenotrophic pathway. This methanogenic activity predominates under inhibitory ammonia levels (Yu et al., 2020; Zhang et al., 2022).

5.4.3.2. NIC level vs MIC level

The archaea *Methanomassiliicoccus*, *Methanosarcina*, and *Methanoculleus* (Fig. 5.7b) along the *acs* (acetyl-coenzyme A synthetase, K01895) and *mcrB* genes (Fig. 5.7d) presented higher abundance in NIC level than MIC level and highlighted with high discriminatory capacity ($AUC \geq 1.00$). H_2 -dependent methanogens and SAOB maintain AD at inhibitory ammonia levels, serving as key indicators when ammonia reaches MIC levels. Hydrogenotrophic methanogens such as *Methanosarcina* and *Methanoculleus*, and methylotrophic *Methanomassiliicoccus*, can persist at TAN concentrations up to 6000 mg/L (Ruiz-Sánchez et al., 2018). However, when the

environment shifts to high VFA (~3000 mg/L) and ammonia (~15 g TAN/L) concentrations, hydrogenotrophic methanogens become unviable (Goux et al., 2015; Hardy et al., 2021). This shift correlates with reduced *mcrB* and *acs* gene counts, indicating a disruption in syntrophic interactions for acetate/H₂ consumption, potentially leading to AD collapse (Hardy et al., 2021; Yu et al., 2020; Zhang et al., 2022).

In MIC level increased *Treponema* and *Ruminococcus* genera (Fig. 5.7b), and *fhs* (formate-tetrahydrofolate ligase, K01938) genes (Fig. 5.7d) demonstrating high accuracy in distinguishing them from the NIC level (AUC ≥ 1.00). The rise of fermentative microorganisms may indicate ammonia presence at MIC levels, promoting an environment dominated by VFAs. *Treponema*, a known homoacetogen, has been positively associated with VFA accumulation (Li et al., 2016). Also, an increase in the abundance of *Ruminococcus* has been observed during an over-acidification issue (~ 30 gVFA/L) in a semi-continuous process (Jo et al., 2018). An increased *fhs* gene count alongside acetate production may indicate homoacetogenic activity. However, this metabolic pathway requires careful consideration, as it can produce high acetate concentrations (~2000 mg/L) to scavenge H₂ (Li et al., 2016; Moestedt et al., 2020; Wei et al., 2020).

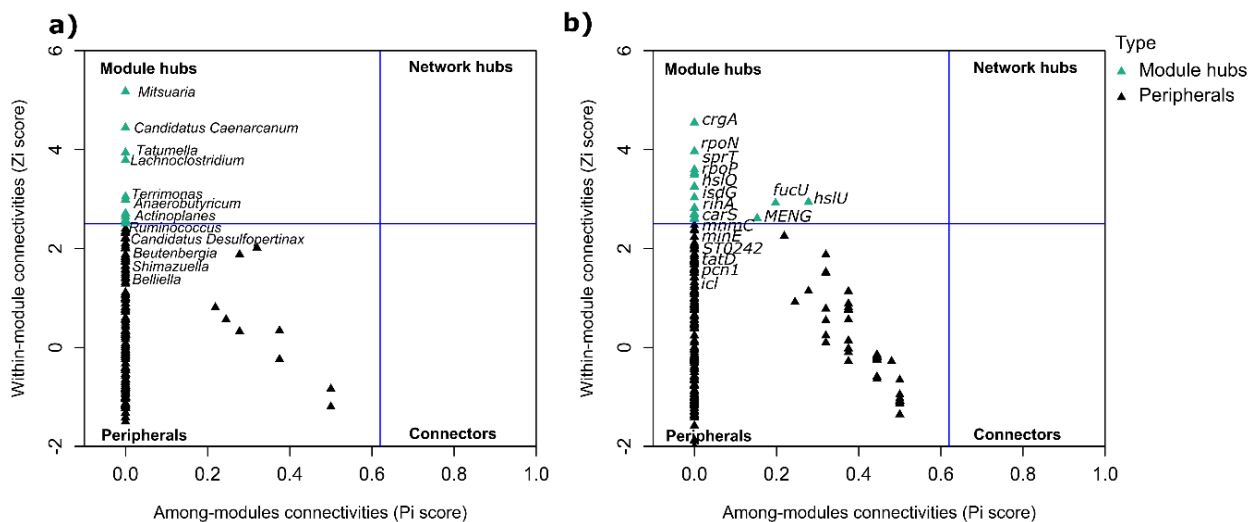


Figure 5.6. The plots show the distribution of genera and genes based on their topological properties within a microbial network determined in NIC level. Plot (a) displays the genus level, while plot (b) presents the gene level. The horizontal blue lines represent Zi score thresholds, and vertical blue lines denote Pi score thresholds, facilitating the identification of network roles. Module hubs are indicated by teal green triangles, and peripherals by black triangles.

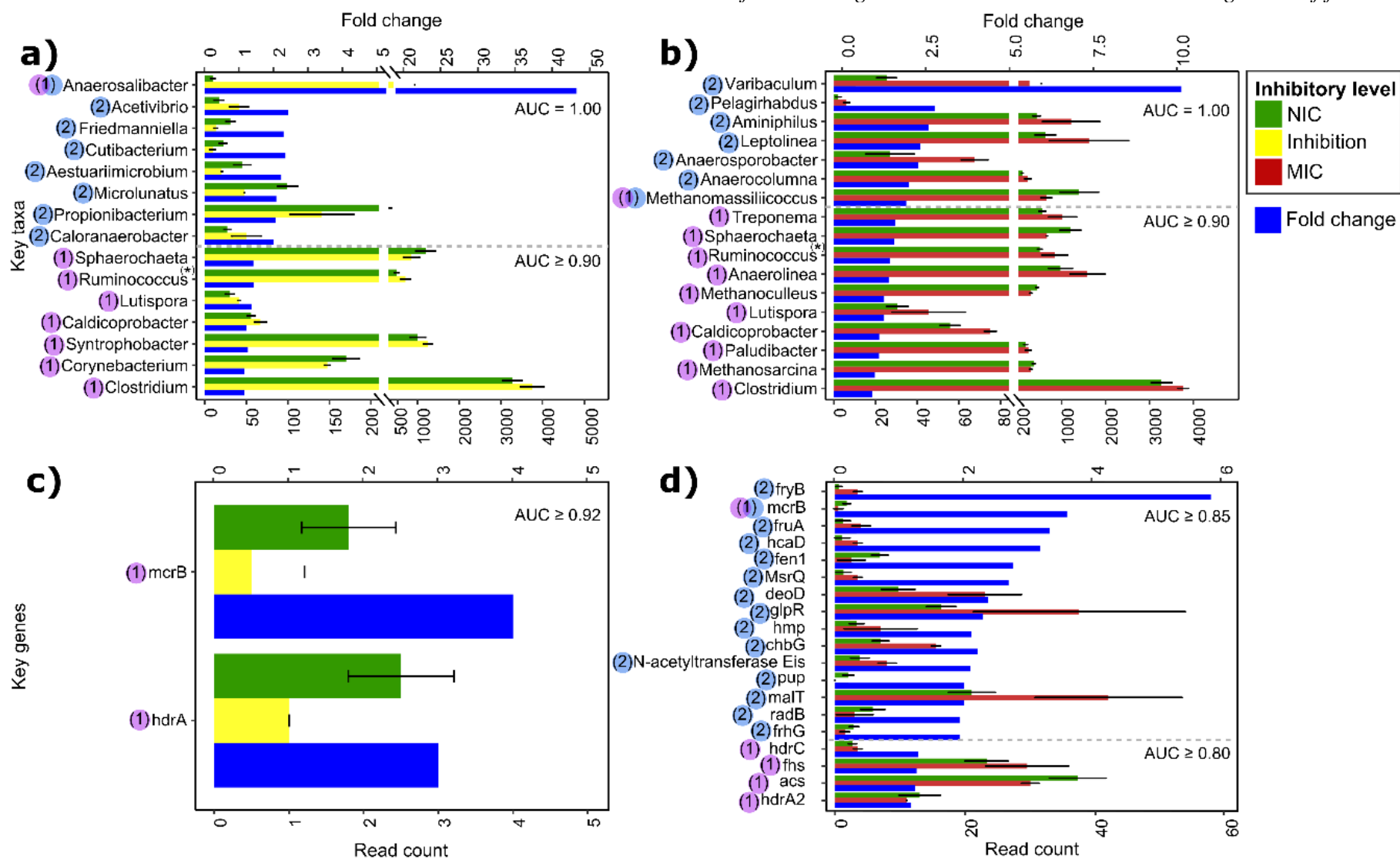


Figure 5.7. The bar plots show genera and genes with significant differences in ammonia inhibitory levels. (a) Key genera and (c) key genes from the NIC vs. inhibition comparison, and (b) key genera and (d) key genes from the NIC vs. MIC comparison. Purple circles indicate traditional significant differences ($p < 0.10$, Wilcoxon rank sum tests). Sky blue circles represent robust FC ($FC \geq 2$). The dashed gray line separates AUC values for key genera and genes: those with robust FC are above the line, and those with traditional significant differences are below. The numbering inside the circles distinguishes the source of genera and genes: 1) Potential suitable MI according to previous reports; 2) Non-suitable MI identified in the microbiome of current experiment. (*) Indicate keystone attributes.

5.4.4. Potential early warning attribute

A set of 10 key genera and 10 key genes with a significant abundance change in response to inhibitory levels, also exhibited a potential early warning response, as indicated by the z-score analysis (Fig. 5.8). This response was indicated by a sudden variation ($z\text{-score} \geq 1$) before reaching the inhibitory threshold (< 2702 mg TAN/L). Notably, some of these genera and genes have shown consistent responses in other AD systems, supporting their utility for predicting operational issues, as detailed in the following paragraphs.

In the case of *Sphaerochaeta* have been proposed as potential early warning indicators for foam detection, an issue that might be triggered by ammonia accumulation (He et al., 2017). Other key genera and genes have shown early shifts in their abundances, days before the manifestation of ammonia inhibition-related issues. *Methanomassiliicoccus* and *Syntrophobacter* abundances declined 8 to 11 d before over-acidification (Goux et al., 2015; He et al., 2018). Abrupt changes in *Anaerolinea* and *Methanosarcina* abundance occurred about 2 d before CH₄ production ceases (He et al., 2018). The relative fluorescence intensity of coenzyme F₄₂₀, a cofactor existent in methanogens and associated to *frh* gene, decreased around 20 d before over-acidification (Shamurad et al., 2020). The *hdr* gene showed a positive trend approximately 20 days before instability (Li et al., 2024). The upregulation of the *acs* gene appears to provide an early warning, at least 23 d before the onset of ammonia inhibition (Yu et al., 2020). These findings indicate that early warning signs are supported by key genera and genes involved in syntrophic and methanogenesis activities. Additionally, these signs suggest that changes in the microbiome occur before VFA accumulation or a decrease in CH₄ yield, covering the gaps left by physicochemical indicators in monitoring AD system (Li et al., 2018; Wu et al., 2021).

CHAPTER 5. Suitable microbial indicators for detecting ammonia inhibition in anaerobic digestion of food wastes

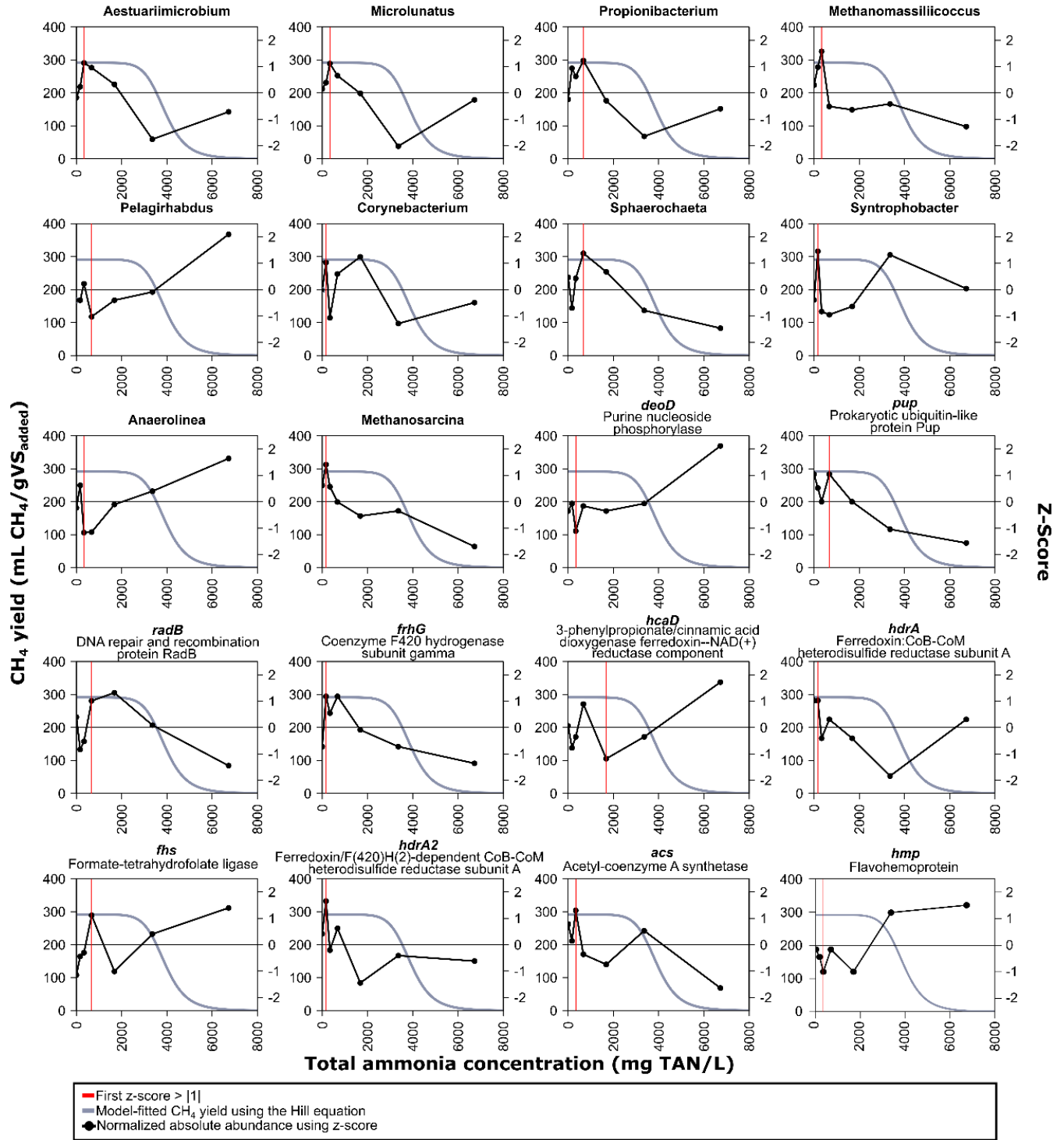


Figure 5.8. Z-score behavior of key genera and genes for each evaluated ammonia concentration alongside the predicted CH₄ yield according to the Hill model. The model predictions are represented by the gray curve. Normalized absolute abundance, depicted by the black line, traces the z-scores for each key genus or gene. The red line identifies the initial significant change (z-score > |1|) in absolute abundance before ammonia inhibition occurs, suggesting potential early warning signs.

5.4.5. Key metabolic role attribute

Metabolic changes in the microbiome due to ammonia effects were analyzed using two RDA analyses with taxonomic and functional data. These analyses confirmed that acetate and propionate were positively related to ammonia but negatively related to CH₄ yield (Fig. 5.9). The accumulation of these VFAs in FW digesters with ammonia buildup is attributed to changes in microbial metabolism (Hardy et al., 2021; Zhang et al., 2022). This effect typically initiates with disruptions in methanogenic and acetogenic stages, followed by enhancements in acidogenic and hydrolytic stages (Chen et al., 2016). KEGG pathways/modules analysis, using z-scores, confirmed variations in the metabolism of proteins, carbohydrates, VFAs, ammonia, and methane (Fig. 5.10). Additionally, reconstructed MAGs ($\geq 50\%$ completeness, $\leq 10\%$ contamination) associated these metabolic pathways with MIs (Fig. 5.11). Significant correlations between MI abundance and AD by-products further validated the metabolic roles of MIs in the experiment (Fig 5.12).

At a NIC level of 377 mg TAN/L, the acetoclastic methanogenesis pathway (M00357) involving *Methanosarcina* (Bin284) and *acs* gene was favored, suggesting acetate consumption for CH₄ production (Zhang et al., 2022). Increasing TAN concentration to 755 mg/L favored the Wood-Ljungdahl pathway (W-L, M00377), which involves the *fhs* gene. This indicates that H₂/CO₂ played a dual role: either being consumed to produce acetate by homoacetogenic bacteria or being produced for acetate consumption by SAOB (Ruiz-Sánchez et al., 2018; Zhang et al., 2022). The positive correlations between the *fhs* gene and acetate suggest that this gene could be an indicator of the utilization of the W-L pathway for homoacetogenesis.

At 1890 mg TAN/L, near the NIC threshold (2702 mg TAN/L), the glycine cleavage system (GCS, M00621) dominated, emphasizing the role of SAOB in acetate degradation (Ruiz-Sánchez et al., 2018; Yu et al., 2020). Both identified SAO pathways (W-L and GCS) were associated with *Anaerolinea* (Bin288), *Syntrophobacter* (Bin91) and *Sphaerochaeta* (Bin136 and Bin184). These shifts in acetate metabolism led to H₂-dependent methanogenesis, favoring methylotrophic methanogenesis (M00356) linked to *Methanomassiliicoccus* (Bin10 and Bin92) and hydrogenotrophic methanogenesis (M00567) linked to *Methanosarcina* (Bin284). Negative correlations between *Methanosarcina*, *Methanomassiliicoccus*, *Sphaerochaeta*, and acetate, along with positive correlations with CH₄ yield, indicate their roles in methanogenesis and SAO activity.

This contrasts with *Anaerolinea* potential involvement in acetate production. Therefore, these MIs can signal relevant metabolic changes in the microbiome before significant changes in physicochemical variables (e.g. ammonia, CH₄ yield, and VFA), highlighting their early warning attribute.

At 3780 mg TAN/L, ammonia levels reached the inhibition threshold, leading to a decline in the denitrification process (M00529). The disruption of this pathway, involving *Anaerolinea* (Bin185), *Leptolinea* (Bin185), *Varibaculum* (Bin244), and *Syntrophobacter* (Bin91), likely increased H₂ partial pressure by reducing nitrate usage, thereby hindering propionate degradation (Li et al., 2015). This change, combined with increased nitrification (M00528), suggests that high nitrite availability may impact AD microorganisms (Hartop et al., 2017). Although methylotrophic methanogenesis, encoded by *Methanomassiliicoccus* (Bin92 and Bin10) and supported by syntrophic pathways like W-L or GCS, maintains AD, the decrease in methanogenesis enzymes (map00680) indicates a global decline in the methanogenic population. Negative correlations between *Methanoculleus*, *Methanomassiliicoccus* and *Methanosarcina* with ammonia evidenced this. Additionally, the increased phosphate acetyltransferase-acetate kinase pathway (M00579), encoded by *Anaerocolumna* (Bin259), *Anaerosporobacter* (Bin259), and *Aminiphilus* (Bin186), suggests sustained acetate production from acetyl-CoA (Yu et al., 2020). These taxa correlate positively with acetate and ammonia, indicating their role as acetogens resistant to stress conditions. The MIs may describe crucial disruptions in microbiome functionality due to ammonia, indicating the likelihood of propionate and acetate accumulation.

At a MIC level of 7580 mg TAN/L, increased chitin disaccharide deacetylase activity, involving the key gene *chbG*, and potentially generated by *Anaerocolumna* (Bin155) and *Anaerosporobacter* (Bin155), indicated a preference for carbohydrate hydrolysis over methanogenesis (Verma & Mahadevan, 2012). Additionally, overall carbohydrate metabolism (map00010) increased, linked to microorganisms such as *Anaerolinea* (Bin288, Bin185), *Leptolinea* (Bin288, Bin185), *Varibaculum* (Bin244, Bin185), *Anaerocolumna* (Bin155, Bin259), and *Anaerosporobacter* (Bin155, Bin259). These genera and the *chbG* gene showed positive correlations with VFAs and ammonia, suggesting a fermentative role under MIC conditions. Other ammonia-associated fermentative activities also increased, including protein metabolism (map04974), amino acid metabolism linked to the key gene *hcaD* (3-phenylpropionate/cinnamic acid dioxygenase

ferredoxin--NAD(+) reductase component, K00529), and purine metabolism (map00230) linked to the key gene *deoD* (purine nucleoside phosphorylase, K03784). Both genes showed positive correlations with ammonia. These findings support that fermentative activities are favorable under ammonia conditions where CH₄ production is challenging and VFA production remains unaffected (Chen et al., 2016).

The high concentration of propionate under MIC levels likely arises via the lactate pathway, found in *Anaerocolumna* (Bin25, Bin155, Bin259), *Anaerosporobacter* (Bin25, Bin155, Bin259), *Anaerolinea* (Bin185), and *Aminiphilus* (Bin186) (Xu et al., 2024). These microorganisms showed positive correlations with propionate and negative correlations with CH₄ yield inferred this role. Simultaneously, decreased propionate (map00640) and butyrate (map00650) metabolisms linked to *Syntrophobacter* (Bin91) suggest that ammonia reaching MIC deteriorates syntrophic oxidation of these VFAs (Zhang et al., 2022). At this ammonia level, the complete deterioration of all three methanogenic pathways halted CH₄ production. The *mcrB* gene displayed negative correlations with ammonia, indicating a global inhibitory effect of ammonia on methanogenic activity. Therefore, these MIC conditions could provide insights into the main hydrolytic, acidogenic, syntrophic VFA oxidation, and methanogenesis activities affected by ammonia, indicating a shift from a methanogenic to a fermentative process.

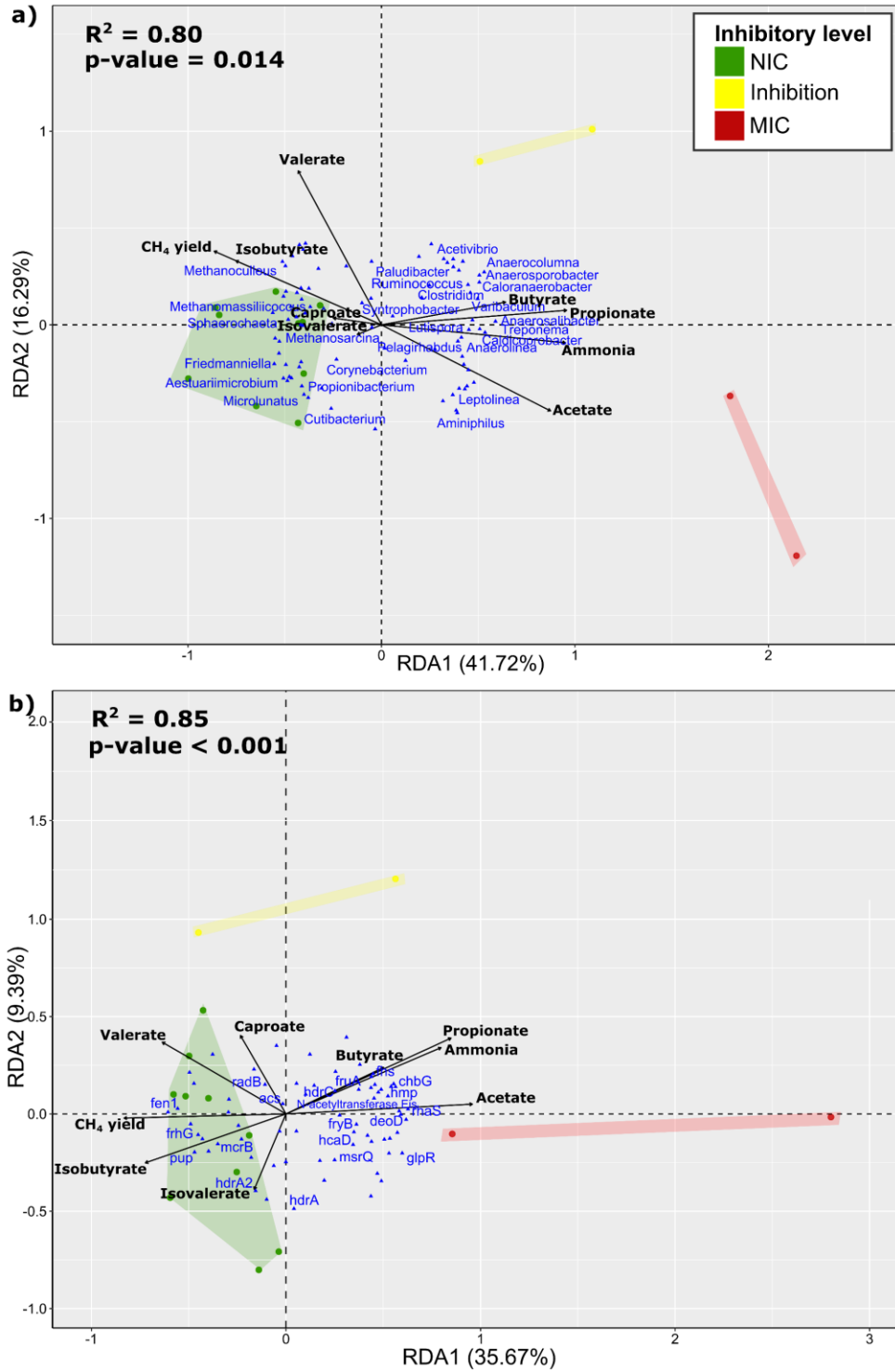


Figure 5.9. The RDA illustrates the response in absolute abundance of (a) genera and (b) genes in relation to AD by-products. The percentage of the total variation explained by each RDA axis is shown in parenthesis (35 – 41%). The redundancy statistic value (R^2) reflects the degree of correlation between the explanatory and response variables, ranging from 0.80 – 0.85 indicating a well-fitted model. The p-value from the ANOVA permutation tests, used to assess the RDA model, is also provided ($p < 0.05$). Samples categorized as NIC, inhibition, and MIC are represented by colored dots in green, yellow, and red, respectively.

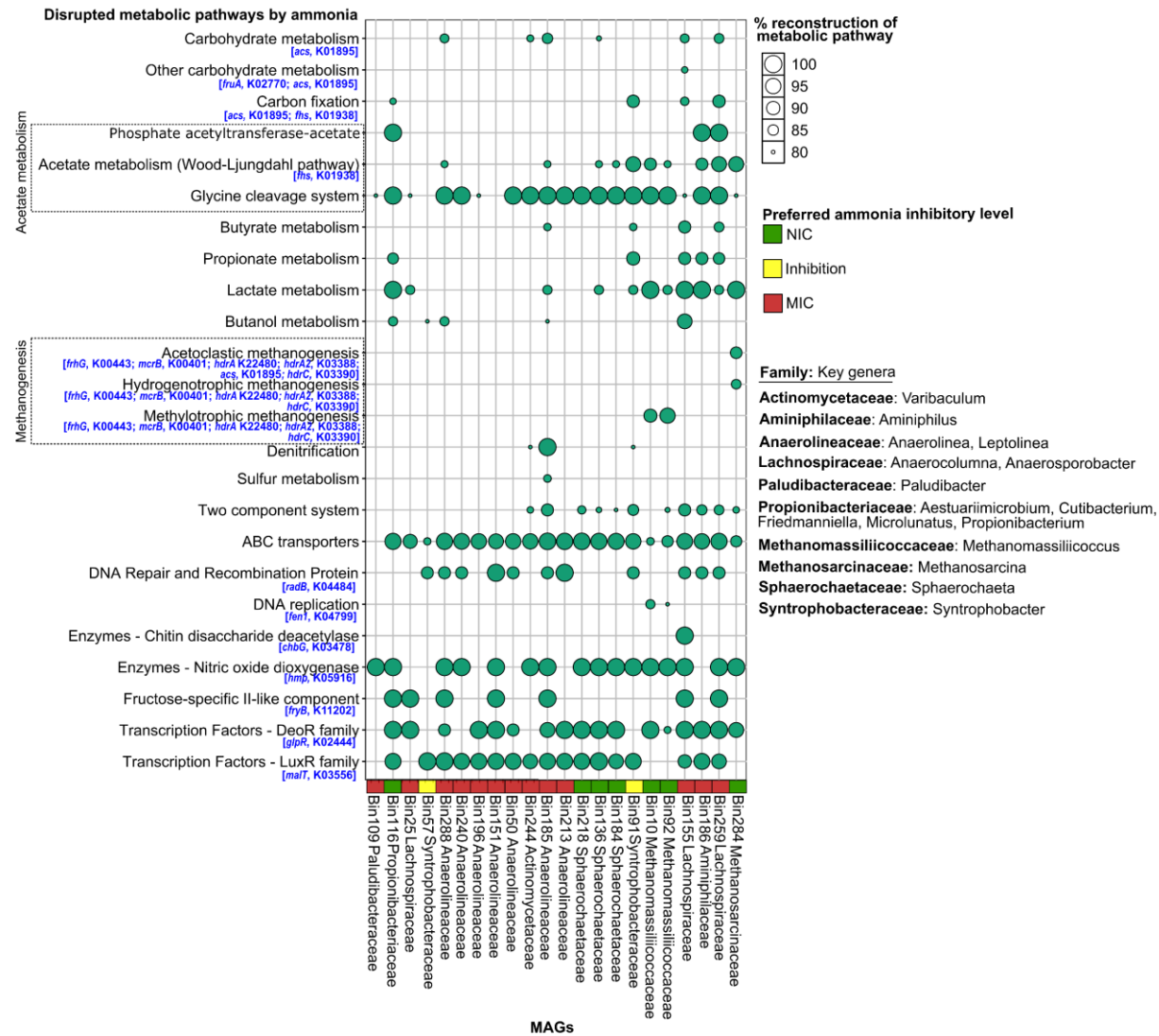


Figure 5.11. The heatmaps show the disrupted metabolic pathways by ammonia and constructed MAG at family level. The size of the circles represents the KO coverage percentage for the respective metabolic pathways. Key genes linked to these pathways are highlighted in blue. Green, yellow, and red squares indicate the preferred inhibitory level for each key genus within its respective taxonomic family.

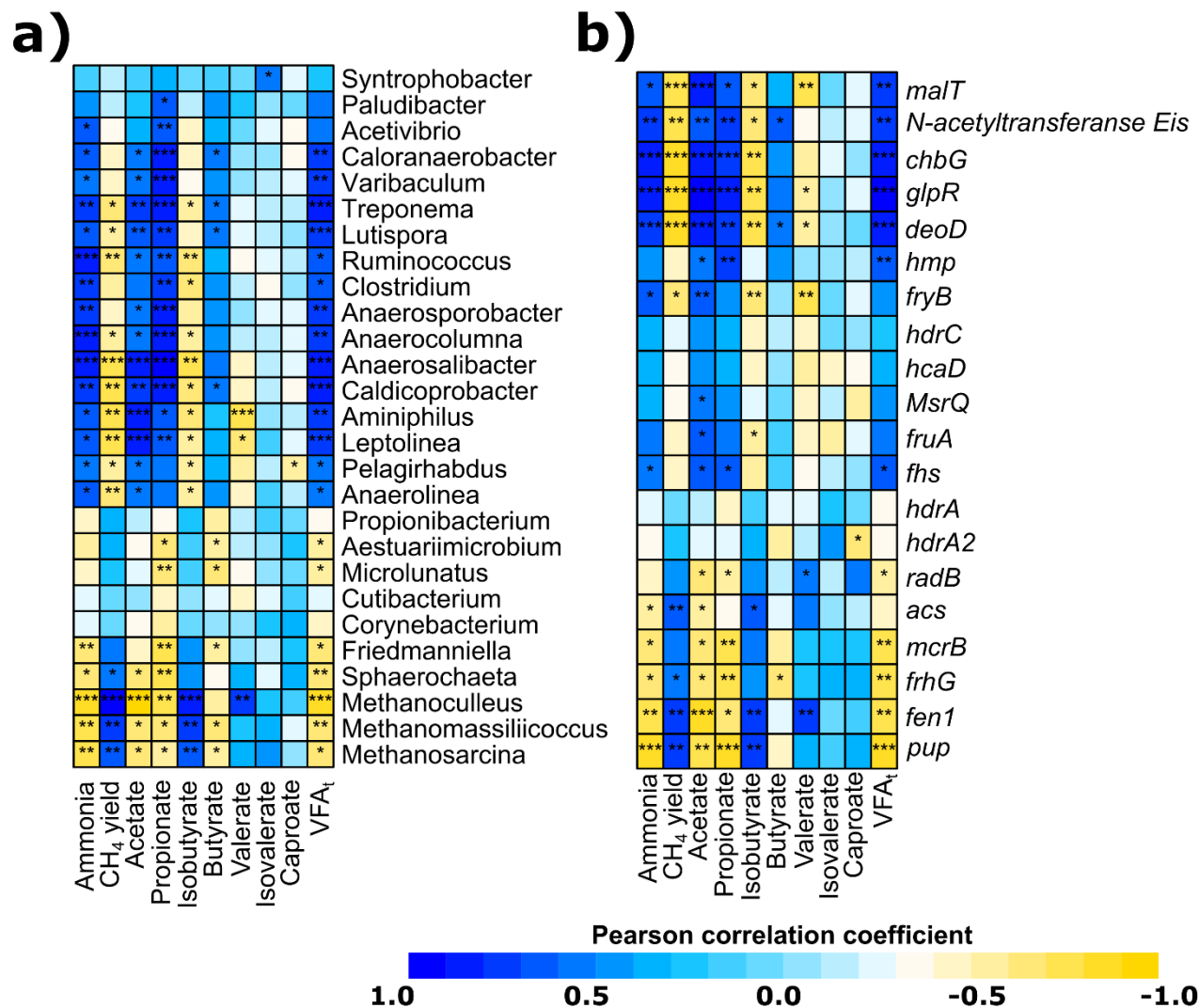


Figure 5.12. The heatmap depicts the correlations between the a) key genera and b) key genes and AD by-products. Significant correlations, determined by Pearson correlation coefficient are denoted with *, **, and *** to represent $p < 0.05$, $p < 0.01$, and $p < 0.001$, respectively.

5.4.6. Future applications of suitable MIs

Anaerolinea, *Sphaerochaeta*, *Syntrophobacter*, *Methanomassiliicoccus*, *Methanosarcina*, *fhs*, and *acs* were identified as suitable MIs due to their multiple attributes. These MIs could help differentiate conditions with a positive ammonia effect (NIC) from those with negative effects of low (NIC – MIC) or high (MIC) impact on CH₄ yield, as observed with a FC between 1.22 and 2.15 in their abundance. A sudden variation in MI count with a z-score $\geq |1|$ could indicate early warning signs of ammonia inhibition. This early response is supported by the presence of crucial metabolic pathways in the MAG of these MIs, which are disrupted by ammonia content, potentially occurring before excessive propionate or acetate accumulation or a decrease in CH₄ yield (Wu et al., 2021).

Given that suitable MIs might provide consistent responses in other mesophilic FW digesters, their implementation in microbial management seems imminent (Hardy et al., 2021; Ruiz-Sánchez et al., 2018; Zhang et al., 2022). These MIs can be validated through experiments focusing on microbial-based management using three approaches: detecting key challenges (retrospective management), monitoring processes (prospective management), and verifying countermeasure feasibility (proactive management) (Carballa et al., 2015). In these cases, MIs can be used to test different algorithms typically used in control systems (e.g., model-adaptive control, fuzzy logic, or artificial neural networks) to predict the status of AD. This approach would enable the development of strategies around physical actions that ensure process stability and maximize efficiency, facilitating modernization from a biological perspective (Nguyen et al., 2015).

5.5. Conclusion

Standardizing ammonia inhibition levels in the AD process fed with FW and conducting an integrative statistical analysis enabled the identification of potential MIs. Attributes such as consistent responses, significant abundance changes, early warning signs, and key metabolic roles led to the identification of *Anaerolinea*, *Sphaerochaeta*, *Syntrophobacter*, *Methanomassiliicoccus*, *Methanosarcina*, *fhs*, and *acs* as suitable MIs. These MIs are recommended for further validation in similar processes to advance microbial management concepts. This analytical approach can also be applied to identify MIs for other inhibitory compounds across various biological systems, thus enhancing biological process optimization.

CHAPTER 6. Evaluation of microbial indicators for ammonia inhibition detection in anaerobic sequencing batch reactors

6.1. Abstract

Microbial indicators are valuable biological metrics for detecting inhibitory effects of ammonia. However, variations in feedstock and inoculum composition may bias the responses of microbial indicators. This study implemented short-term monitoring of four processes differentiated by semi-continuous ammonia addition (0–3.78 g TAN/L) within an anaerobic sequencing batch reactor system. This approach evaluated the response of 14 microbial indicators across three inhibitory levels: non-inhibitory (< 2.51 g TAN/L), low-inhibitory (2.51–11.07 g TAN/L), and high inhibitory (11.07–26.23 g TAN/L). Based on significant responses to these levels, indicators were classified into two groups: stepped response indicators and extreme response indicators. Stepped response indicators, such as *Anaerolineaceae* and the *acs* gene, exhibited a gradual negative response to increasing ammonia levels (non-inhibitory → low-inhibitory → high-inhibitory), reflecting a decline in syntrophic relationships within the microbiome. Extreme response indicators, including *Aminobacterium*, *Clostridium sensu stricto* (subgenera 1, 15, 7, and 8), *Methanosarcina*, *Syntrophobacter*, *Methanomassiliicoccus*, and the *fhs* gene, exhibited significant changes only between non-inhibitory and high-inhibitory levels. Such a response indicates a vulnerability in the syntrophic oxidation of acetate and propionate, highlighting the need for maintaining H₂-dependent methanogenesis and the risk of volatile fatty acid accumulation. The use of microbial indicators revealed distinct metabolic profiles that differentiated microbiomes with similar VFA concentrations and methane production, offering a clear advantage over conventional physicochemical indicators. From a strategic perspective, these microbial indicators are poised to significantly enhance the management and optimization of food waste digesters by providing a more nuanced understanding of microbial metabolism in response to ammonia inhibitory levels.

Reference to the work in preparation

Jonathan Cortez-Cervantes, Iván Moreno-Andrade, Claudia Etchebere, Julián Carrillo-Reyes.
Evaluation of microbial indicators for ammonia inhibition detection in anaerobic sequencing batch reactors to be submitted to Bioresource Technology

6.2. Introduction

Ammonia inhibition is a common operational challenge in FW digesters (Wang et al., 2018). Even under favorable conditions (< 3 g VS/L-d), a sudden increase in protein content in FW can release high ammonia concentrations, potentially causing digester failure by acidification (Peng et al., 2018; Zhang et al., 2022). Industrial FW digesters often incorporate monitoring systems for physicochemical indicators like biogas production, pH, temperature, and ammonia levels to ensure the stability of AD (Wu et al., 2021). However, monitoring these parameters alone may not reliably detect when ammonia negatively impacts the AD inoculum (Jiang et al., 2019). This is because ammonia favors the selective enrichment of phylogenetically related microbiomes that perform AD under deterministic mechanisms (Cardona et al., 2022). Although this selective enrichment suggests possible inoculum acclimation to stress conditions (~ 3 g TAN/L), medium-term observations (150 days) indicated the accumulation of volatile fatty acids (VFAs), which ultimately reduces digester performance (Peng et al., 2018; Xu et al., 2018).

Recent studies have investigated the use of microbial indicators (MIs) to assess AD performance, even for detecting key challenges like ammonia inhibition (Cortez-Cervantes et al., 2024; Poirier et al., 2020). Commonly, ammonia selects for a microbiome characterized by VFA degradation through syntrophic relationships, such as hydrogenotrophic methanogenesis, while displacing acetoclastic methanogenesis (Hardy et al., 2021; Zhang et al., 2022). This shift in microbial structure tends to persist, as ammonia selects for phylogenetically related microorganisms (Cardona et al., 2022). Thus, to identify MIs with universal responses to ammonia inhibition in anaerobic processes fed with similar feedstocks is considered feasible (Li et al., 2018). However, uncontrollable factors, such as compositional changes in the feedstock and microbial acclimation, may alter MI responses, potentially biasing their effectiveness in detecting ammonia effects (Theuerl et al., 2018; Yan et al., 2019).

Previous results have proposed potential MIs to elucidate metabolic changes associated with ammonia inhibition levels in FW digesters (see chapter 5). When ammonia exceeds the non-inhibitory concentration ($\text{NIC} > 2.70$ g TAN/L), an increase in *Syntrophobacter* and a decrease in *Sphaerochaeta* suggest that the syntrophic requirements for propionate oxidation (SPO) might surpass those for syntrophic acetate oxidation (SAO). Additionally, the co-presence of the genes *acs* (acetyl-CoA synthetase gene, K01895) and *fhs* (formate—tetrahydrofolate ligase, K01938)

could indicate whether acetate is being utilized via acetoclastic methanogenesis or the Wood-Ljungdahl pathway respectively. When ammonia crosses the minimum inhibitory concentration (MIC > 5.80 g TAN/L), a reduction in *Methanomassiliicoccus* and *Methanosarcina*, along with an increase in fermentative bacteria like *Anaerolinea*, may indicate that the inoculum is unable to sustain AD. Other MIs, such as *Aminobacterium*, *Clostridium*, HA73, T78, *Corynebacterium*, *Lactobacillus*, and *Prevotella*, were reliable for evaluating FW digester performance (Cortez-Cervantes et al., 2024). These microorganisms were linked with carbohydrate and amino acid fermentation and syntrophic activities, which are metabolism frequently affected by inhibitory ammonia levels (Cortez-Cervantes et al., 2024; Zhang et al., 2022). Despite proposing potential MIs, their evaluation in real-world systems, subject to FW variability and microbiome changes over time, has yet to be confirmed.

This chapter aims to evaluate the response of reliable and suitable MIs to detect ammonia, by monitoring an anaerobic sequencing batch reactor (AnSBR) system under perturbations. The AnSBR system comprised four processes, differentiated by the semi-continuous addition of ammonia concentrations at 0, 0.37, 0.75, and 3.75 g TAN/L at the end of each operating cycle. Each process was subjected to disturbances related to compositional variation in FW such as changes in feedstock batch and variations in the organic loading rate (OLR). These factors allowed obtain a database of diverse ammonia concentrations, obtaining an inhibitory profile characterized by three levels: non-inhibitory, low-inhibitory, and high-inhibitory. The ability of the collected MIs to distinguish ammonia inhibitory levels was determined using a center log ratio (CLR) transformation and non-parametric significance test. Additionally, MI profiles based on z-score elucidated a key metabolic behavior of each process. This approach allowed differentiation of microbiomes that appeared similar based on physicochemical indicators, such as volumetric methane production rate (VMPR) and methane (CH₄) yield, highlighting the sensitivity of microbial indicators. As a result, microbial indicators demonstrated greater specificity in detecting ammonia inhibition. Since these indicators are considered reproducible, they could be easily integrated into models for developing new monitoring systems for FW digester systems.

6.3. Material and methods

6.3.1. Feedstocks sources and activated inoculum

Three sources of FW, labeled FW-1, FW-2, and FW-3, were separately collected in 20 L plastic containers from different food markets in Santiago de Queretaro, Mexico. FW was mainly composed by fruits and vegetables. Each feedstock batch was homogenized using an electric blender. To maintain a consistent physicochemical composition, each FW sample was stored in 1.75 L self-sealing bags at -20°C until use. The total solids (TS, g TS/g) and volatile solids (VS, g VS/g) content for each feedstock batch 0.08 ± 0.001 and 0.05 ± 0.001 , 0.12 ± 0.001 and 0.10 ± 0.001 , and 0.09 ± 0.001 , for FW-1, FW-2, and FW-3, respectively.

For inoculum preparation, 20 L of granular sludge was obtained from a mesophilic anaerobic process at a flour industry and stored at 4°C . To remove residual organic matter, 2.5 L of granular sludge was placed in an open 3 L container at room temperature for 3 d. The sludge was then characterized, yielding 0.07 ± 0.001 g VS/g and 0.05 ± 0.001 g VS/g. Inoculum activation was conducted in batch-fed AD systems using three 1 L glass reactors with a working volume of 0.85 L. Each reactor was set to an S_0/X_0 ratio of 0.15, using FW-1 as feedstock, and granular sludge as the initial inoculum, along with acetate and butyrate at 100 mg/L and 50 mg/L, respectively. These VFAs were chosen to activate acetoclastic methanogens, hydrogenotrophic methanogens, and syntrophic bacteria, crucial for CH_4 production. Reactors were mixed at 144 rpm and maintained at 35°C for 17 d. through hotplate stirrers. Final inoculum characterization showed 0.04 ± 0.001 g TS/g and 0.03 ± 0.001 g VS/g.

6.3.2. Operation of the AnSBR system

Different AnSBR systems were operated to evaluate MIs for detecting ammonia inhibition under multiple perturbations related to FW composition (Fig. 6.1). The systems were divided into four different processes, P0, P0.37, P0.75, and P3.78, corresponding to semi-continuous ammonia additions of 0, 0.37, 0.75, and 3.78 g TAN/L, respectively, at the end of each operation cycle. Each process was run by triplicate. The selected concentration range was chosen based on previous experiments (Chapter 5), where $\text{TAN} \leq 0.75$ g/L caused metabolic variations without significantly affecting CH_4 yield being NIC, while $\text{TAN} \geq 3.78$ g/L exhibited inhibitory effects on AD using the same inoculum.

Experimental setup consisted in 12 AnSBR glass reactors of 0.6 L of total volume, a working volume of 0.36 L, and a head space of 0.24 L. The exchange volume was 50%. The AnSBR reactors were operated using an AMPTS II system (Automatic Methane Potential System, Bioprocess Control, Sweden) for the measurement of biogas online. The hydraulic retention time (HRT) was 10.1 d where each operating cycle included filling (5 min), reaction (5 d), settling (1 h), and draw (5 min). Filling and drawing between cycles were performed manually. Start-up conditions were S_0/X_0 0.5 g VS/g VS, 10 g VS/L of acclimated inoculum, and feeding with 20 g VS/L FW-1. NH_4Cl (50 g/L stock solution) was added as an ammonia source, adjusting the concentration per process. Each reactor was provided with 4 g NaHCO_3/L , NaOH (5 N) to adjust the pH 8.2, and distilled water to fill until the working volume. Anaerobic conditions were established by purging with N_2 injection. The reactors were placed in a 37°C water bath with intermittent mixing (144 rpm, 60s ON/120s OFF) and continuous gas production measurement (mL/h) for 35 d.

Each process was exposed to simulated disturbances, accounting for factors that altered substrate composition, such as variations in feedstock batches (FW-1, FW-2, and FW-3) and changing OLR at 1 and 2 g VS/L-d. The AnSBR system operated in three phases: phase I used FW-1 at 1 g VS/L-d (cycles 1–2); phase II used FW-2 at 2 g VS/L-d (cycles 3–4); and phase III used FW-3 at 1 g VS/L-d (cycles 5–7). Physicochemical characterization, including VFAs, ammonia, biogas composition, volumetric methane production rate (VMPR, Eq 6.1) and CH_4 yield (Eq 6.2) was determined at the end of each cycle. Microbial community characterization was conducted during cycles 1, 3, and 6, corresponding to each perturbation phase (P0, P0.75, and P3.78). Samples were collected at the point of maximum methane production (3, 12, and 27 days) (Figure 6.1).

$$\text{VMPR} = \frac{\text{Volume of CH}_4 \text{ produced}}{\text{Reactor volume} \times \text{Operation time}} \quad \text{Eq. 6.1}$$

Where VMPR is the volumetric methane production rate ($\text{mL CH}_4/\text{L}_{\text{reactor}}\text{-d}$), volume of CH_4 produce is the total amount of methane generated during the cycle or day (mL CH_4), reactor volume is the working volume of the reactor (0.18 L) and operation time is the duration of the cycle in days (5 d)

$$\text{CH}_4 \text{ yield} = \left(\frac{\text{Volume of CH}_4 \text{ produced}}{\text{Mass of VS added}} \right) \quad \text{Eq. 6.2}$$

Where CH_4 yield is the methane yield ($\text{mL CH}_4/\text{gVS}_{\text{added}}$), volume of CH_4 produced is the total amount of methane generated during the cycle (mL) and mass of VS added is the amount of volatile solids (VS) added to the reactor during the cycle (g).

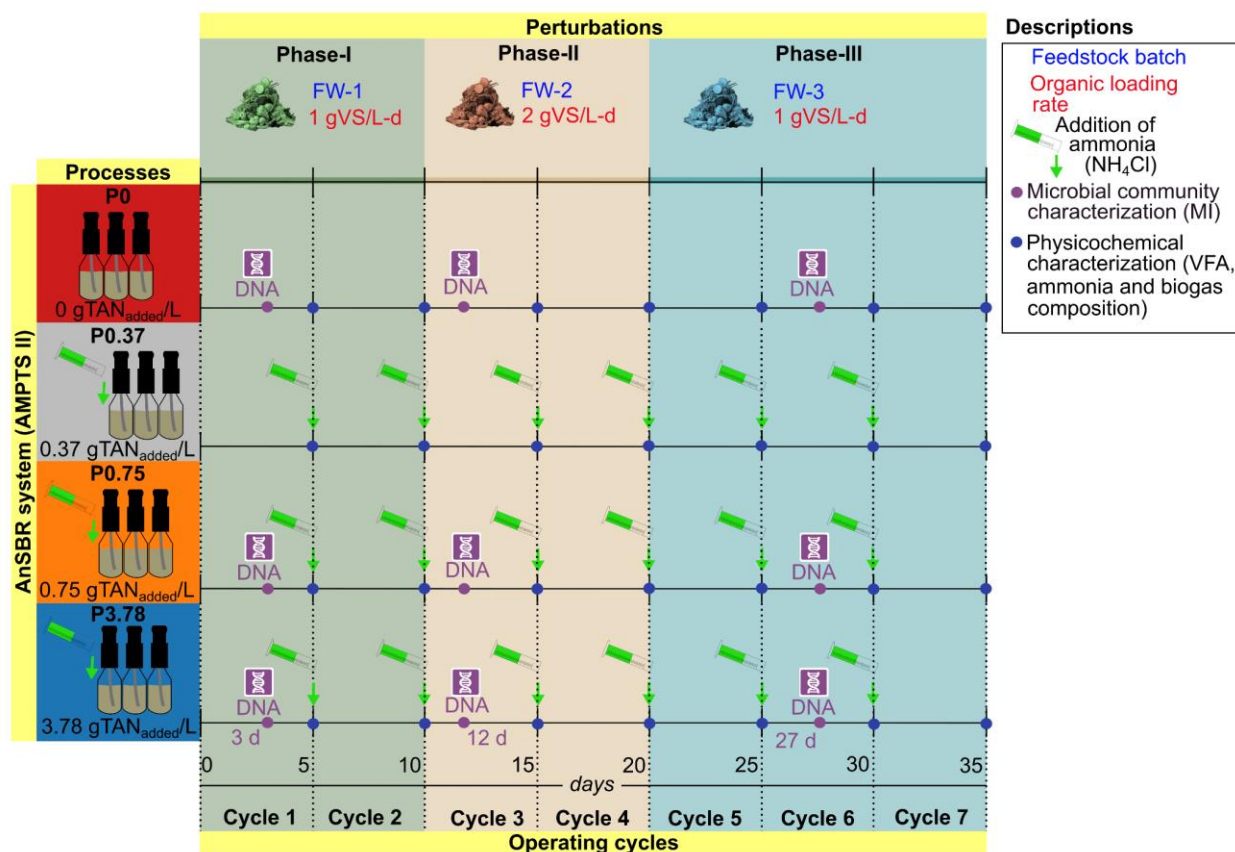


Figure 6.1. Operation of the AnSBR system divided into four processes based on the semi-continuous addition at certain ammonia concentration. Each process involved perturbations from changes in feedstock batches and variations in OLR. Samples for physicochemical characterization were collected at the end of each operating cycle. Biomass samples for microbial community characterization were collected on days corresponding to the approximate maximum methane production rates (days 3, 12, and 27) observed during cycles 1, 3, and 6.

6.3.3. Determination of ammonia inhibitory levels

The measured NH_3 was corrected using a correction factor considered the operating conditions (pH 8 at 35 °C) applied to the system, using the Henderson-Hasselbalch equation (Eq. 6.3):

$$\text{pH} = \text{pK}_a + \log_{10} \frac{[\text{NH}_3]}{[\text{NH}_4^+]} \quad \text{Eq. 6.3}$$

Where pH represents the operational pH (8.2), and pK_a is the negative log of the acid dissociation constant (K_a) for NH₄⁺, determined at 25 °C (K_a = 5.6 x 10⁻¹⁰) and 35°C (K_a = 1.1 x 10⁻¹⁰).

Subsequently, total ammonia nitrogen (TAN) was calculated by rearranging the equation from Yan et al. (2019) (Eq. 6.4):

$$\text{TAN} = \text{FAN}_c \left(1 + \frac{10^{-\text{pH}}}{\text{K}_a} \right) \quad \text{Eq. 6.4}$$

In this equation, TAN is the total ammonia nitrogen (g/L), FAN is the corrected free ammonia (g/L), K_a is the dissociation constant at 35 °C (as defined in Eq. 6.3), and pH is the operational pH. Consequently, NH₄⁺ was determined by rearranging TAN = NH₃ + NH₄⁺.

Ammonia inhibitory levels were determined based on kinetic parameters linked to an inhibition model. The Hill equation (Eq. 6.4) was employed to generate a model curve describing the inhibitory profile of ammonia on methane production. The model input data consisted of VMPR values relative to ammonia concentration (g TAN/L), using all observed data from the AnSBR system. Model validation comprised extracting the residuals and applying the Shapiro-Wilk test to confirm the non-normality of the residuals (p > 0.05). The coefficient of determination (R²) was used to assess the goodness of fit of the model.

$$\mu = \mu_m + (\mu_0 - \mu_m) \frac{1}{\left(1 + \left(\frac{\text{IC}_{50}}{S} \right)^n \right)} \quad \text{Eq. 6.4}$$

Where μ was the VMPR (mL CH₄/L_r-d), μ_m was the maximum VMPR (mL CH₄/L_r-d), μ₀ was the minimum VMPR (mL CH₄/L_r-d), S was the ammonia concentration (g TAN/L), IC₅₀ was the ammonia concentration when μ_m/2, and n was an empirical coefficient.

The IC₅₀ and n values from the validated Hill model were used to calculate the non-inhibitory concentration (NIC, Eq. 6.5) and the minimum inhibitory concentration (MIC, Eq. 6.6) of ammonia (Lambert & Pearson, 2000). These concentrations categorized the AnSBR system

samples according to the inhibitory effect of ammonia, identifying three inhibitory levels: non-inhibitory ($< \text{NIC}$), low inhibitory ($\text{NIC} - \text{IC}_{50}$), and high inhibitory ($\text{IC}_{50} - \text{MIC}$).

$$\text{NIC} = 10^{\left(\log_{10} \text{IC}_{50} - \frac{1.718}{n}\right)} \quad \text{Eq. 6.5}$$

$$\text{MIC} = 10^{\left(\log_{10} \text{IC}_{50} + \frac{1}{n}\right)} \quad \text{Eq. 6.6}$$

The "nlsML" function from the "minpack.lm" package was used to estimate the IC_{50} and n parameters of the Hill model, as well as the R^2 determination (Elzhov et al., 2016). The "shapiro.test" function from the "stats" package was applied to assess the residual distribution of the model.

6.3.4. DNA extraction and full-length 16S amplicon sequencing analysis

Taxonomic and functional characterization of the microbial community was performed using full-length 16S amplicon sequencing of 27 samples, collected during 3 selected cycles and 3 different processes, for each triplicated test. A 2 mL volume of mixed liquor and stored at -20°C until processing. DNA extraction was conducted using the DNeasy PowerSoil Pro Kit (Qiagen, Germany) following the protocol provided by the manufacturer. DNA quality was assessed with a 260/280 absorbance ratio (> 1.80) using a NANODrop 2000c (Thermo Scientific, USA). The universal primer set 27F (AGRGTTYGATYMTGGCTCAG) and 1492R (RGYTACCTTGTTACGACTT) was selected for full-length 16S amplicon sequencing to characterize bacteria populations, and Arch21F (TCCGGTTGATCCYGCCGG) and A1401R (CRGTGWGTRCAAGGRGCA) set of primers for archaea. Library preparation and sequencing were performed using the PacBio Sequel platform at the Integrated Microbiome Resource Lab (IMR), Dalhousie University (Halifax, Canada).

The 16S rRNA gene sequences were analyzed separately for archaeal and bacterial communities. Taxonomic characterization was performed using raw circular consensus sequencing (CCS) PacBio data in demultiplexed fastq format, processed with Qiime2 (v2024.5) following the provider's guidelines ([https://github.com/LangilleLab/microbiome_helper/wiki/PacBio-CCS-Amplicon-SOP-v2-\(qiime2-2022.2\)](https://github.com/LangilleLab/microbiome_helper/wiki/PacBio-CCS-Amplicon-SOP-v2-(qiime2-2022.2))). This analysis generated ASV count and sequence tables, which were subsequently used for functional characterization with PICRUSt2 following the

standard method (<https://github.com/picrust/picrust2/wiki/Full-pipeline-script>). The outputs of the bioinformatics tools included ASV count tables, corresponding taxonomic classifications, and predicted genes annotated with KEGG orthology (KO) for each selected sample.

6.3.5. Diversity analysis

To assess microbial diversity, absolute abundances of ASVs and KOs for bacteria and archaea were combined to evaluate both taxonomic and functional diversity in each sample. For consistent comparison across processes, random subsampling without replacement was applied. In this analysis, the minimum sequence counts assigned to ASV (7223 inferred sequences) and KO (6684099 predicted genes) in the merged data were used as the sampling depth. Rarefaction curves confirmed that the selected sampling depth captured the raw richness in the samples. Unique ASVs or KOs present in only one sample were removed to filter rarefied data and eliminate artifacts (Chong et al., 2020).

Alpha diversity was determined to evaluate diversity profiles within ammonia inhibitory levels. Hill numbers such as q0 (richness), q1 (Shannon index) and q2 (Simpson index), and Pielou evenness were determined. Significant differences within and between inhibitory levels were identified using Kruskal-Wallis ($p < 0.05$) and Wilcoxon rank-sum tests with Benjamini-Hochberg p-value adjustment ($p < 0.10$) respectively. The “hill_div” and “estimate_richness” functions from the “hilldiv” and “vegan” packages were used to determine Hill numbers, while significance tests were performed using the “kruskal.test” and “pairwise.wilcox.test” functions from the R base package. Alpha indices were visualized with the “ggplot” function from the “ggplot2” package.

Beta diversity was assessed to evaluate taxonomic and functional differentiation between ammonia inhibitory levels. Rarefied ASV and KO data were transformed using the Hellinger method to standardize composition and improve ordination analysis (Legendre & Gallagher, 2001). Bray-Curtis’s dissimilarity was calculated to evaluate compositional differences between samples. Nonmetric Multidimensional Scaling (NMDS) technique was used to generate ordination scores, which represent the relative dissimilarity of samples in a reduced-dimensional space. Dissimilarity differences between microbial communities across inhibitory levels were assessed with ANOSIM ($p < 0.05$) with 999 permutations. The Hellinger transformation was performed using the “decostand” function, the distance matrix was obtained with the “vegdist” function, NMDS

solutions were derived with the "metaMDS" function, and data visualization was achieved using the "ordihull" function, all contained within the "vegan" package.

6.3.6. Statistical analysis for evaluation of MIs

The 14 potential MIs identified in Sections 3 and 5, including *Aminobacterium*, *Clostridium* (subgenera sensu stricto 1, 7, 8, 15), HA73, T78, *Corynebacterium*, *Lactobacillus*, *Prevotella*, *Syntrophobacter*, *Sphaerochaeta*, *Anaerolinea*, *Methanomassiliicoccus*, *Methanosarcina*, *acs*, and *fhs*, were evaluated. Archaeal and bacterial data were processed separately. The absolute abundances of ASVs were collapsed at the genus level, and KOs were filtered to remove artifacts (see Section 6.3.4). This filtered data served as input for statistical analysis. The ability of potential MIs to differentiate ammonia inhibitory levels and construct metabolic profiles across each operational cycle was assessed.

To assess the ability to differentiate ammonia inhibitory levels, the data was transformed to CLR values, accounting for the compositional nature of microbial abundance data. This transformation normalizes the data by taking the log of the relative abundance of each genus/KO and centering it by the geometric mean of all genera/KOs within each sample (Hu & Satten, 2023). The CLR values of each MI were grouped and compared across and within inhibitory levels using Kruskal-Wallis ($p < 0.05$) and Wilcoxon rank-sum tests with Benjamini-Hochberg p-value adjustment ($p < 0.10$). The CLR transformation was performed using the "decostand" function in the "vegan" package, with data visualized through the "ggplot" function from the "ggplot2" package. Significance tests were detailed in Section 6.3.4.

To evaluate the differentiation of microbiomes, MI profiles were constructed based on variations in the rarefied abundance in each operating cycles in the selected processes. The rarefied data to each set was obtained according to random subsampling without replacement in each data set (see section 6.3.4). For each AnSBR process, the average genera or KO counts were calculated across replicates, forming a matrix of values. To create the MI profiles, the z-score was calculated using equation 6.7 and visualized in a heatmap.

$$Z\text{-score} = \frac{x - \mu}{\sigma} \quad \text{Eq. 6.7}$$

where x represents the genus or KO rarefied abundance, and μ the average and σ denote the standard deviation. The z-score transformation was performed using the "sapply" function from the R base package, while data visualization through the "pheatmap" function from the "pheatmap" package.

6.3.7. Analytic methods

The composition of biogas (H_2 , CH_4 , and CO_2) was determined using gas chromatography (SRI Instruments Model 8610 C, Champaign, IL, USA) equipped with a thermal conductivity detector and two stainless steel columns (2 m long; 0.79 mm in diameter). The injector, column, and detector temperatures were set at 90, 110, and 150 °C, respectively. Nitrogen served as the carrier gas at a flow rate of 20 mL/min. Gas volume was reported under standard temperature and pressure conditions (0 °C and 1013.25 hPa). Volatile fatty acids (VFA), lactate, caproate and butanol were quantified using high-performance liquid chromatography (HPLC, Agilent Technologies model 1260, CA, USA). The HPLC was equipped with an AMINEX HPX-87 H column and two detectors: a diode-array detector and a refractive index detector (Bio-Rad, CA, USA) at a detection wavelength of 210 nm. A 5 mM H_2SO_4 solution was used as the eluent at a flow rate of 0.6 mL/min with the column maintained at 50 °C (Villanueva-Galindo et al., 2024). TS, NH_3 , and VS were measured according to standard methods (APHA, 2005).

6.4. Results and discussion

6.4.1. Physicochemical characterization of ammonia inhibitory levels

The AnSBR system provided an ammonia inhibitory profile on AD, which remained consistent despite variations in OLR and feedstock changes (Fig. 6.2). Three inhibitory levels were identified: non-inhibitory at < 2.51 g TAN/L, low-inhibitory at $2.51 - 11.07$ g TAN/L, and high-inhibitory at $11.07 - 26.23$ g TAN/L (Fig. 6.2a). Each level showed distinct physicochemical responses based on inhibitory effect of ammonia. Comparing non-inhibitory to low-inhibitory levels revealed significant changes ($p < 0.05$) with TAN ($\text{NH}_4^+ - \text{NH}_3$) increasing by 226% (Fig. 6.2d), propionate increasing by 304% (Fig. 6.2e), and CH_4 yield decreasing by 20% (Fig. 6.2c). These results suggest that low inhibitory levels of ammonia lead to propionate accumulation and a reduction in CH_4 yield, which are common indicators of deteriorated microbial activity due to ammonia. (Zhang et al., 2022).

Comparing non-inhibitory and high-inhibitory levels, VMPR (Fig. 6.2b) and CH_4 yield decreased significantly by 68–70% ($p < 0.05$). Additionally, TAN and VFAs, including acetate, butyrate, and propionate, increased by over 710% ($p < 0.05$). Similar trends were observed between low-inhibitory and high-inhibitory levels. These results indicate greater differences in physicochemical variables as ammonia concentration increased. At high-inhibitory levels, ammonia likely created a stressful environment, negatively impacting syntrophic VFA degradation and acetoclastic methanogenesis, leading to pronounced variations in metabolic responses (Capson-Tojo et al., 2020; Zhang et al., 2022). Therefore, NIC, IC_{50} , and MIC thresholds allowed for the assessment of ammonia effects irrespective of variations in FW composition, providing valuable categories for evaluating MIs.

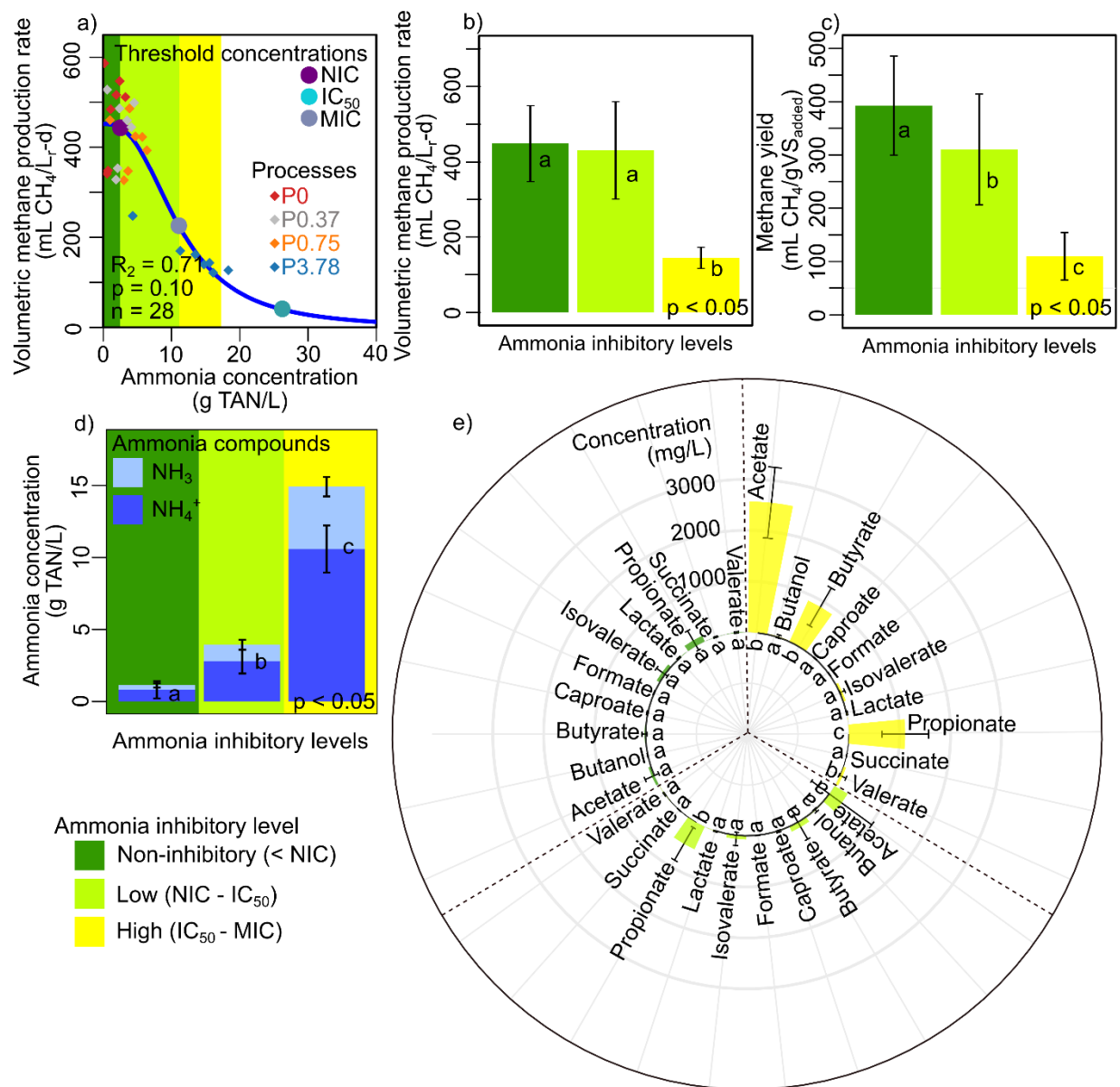


Figure 6.2. Physicochemical characterization of samples from the AnSBR system grouped by ammonia inhibitory levels. a) The Hill model was applied using the average VMPR and ammonia concentration data from each replicate of processes P0, P0.37, P0.75, and P3.78. The model was evaluated using the Shapiro-Wilk test, which revealed the normality of the residuals ($p > 0.05$). The coefficient of determination (R^2) indicated the fit of the model. The bar plots display significant differences in b) VMPR considering average data per cycle, c) CH₄ yield considering average data per cycle, d) final ammonia concentration, and e) VFA concentration among the ammonia inhibitory levels. ANOVA ($p < 0.05$) and Tukey's test ($p < 0.05$) were used for within-group and between-group comparisons, respectively.

6.4.2. Physicochemical characterization of operating cycles

Significant differences ($p < 0.05$) in physicochemical parameters were observed across AnSBR processes during each operating cycle (Fig. 6.3), including CH_4 yield (Fig. 6.3a), VMPR (Fig. 6.3b), TAN (Fig. 6.3c), and VFA concentrations (Fig. 6.3d). However, the processes P0, P0.37, and P0.75, which had ammonia added at non-inhibitory levels (< 0.75 g TAN/L), showed significant similarities ($p > 0.05$) in CH_4 yield, VMPR, acetate, butyrate, and propionate from cycle 5 onward. In contrast, process P3.75, with ammonia added at a low-inhibitory level (3.75 g TAN/L), remained significantly different ($p < 0.05$) from P0, P0.37, and P0.75 throughout all cycles. These distinctions were aligned with ammonia inhibitory levels, demonstrating consistent physicochemical responses over time. This confirms the effectiveness of NIC, IC_{50} , and MIC in categorizing ammonia effects in semi-continuous processes.

In phase I, during cycle 1, ammonia concentrations differed significantly ($p < 0.05$) between P0, P0.37, and P0.75 (0.16 ± 0.01 to 0.71 ± 0.01 g TAN/L) yet remained non-inhibitory levels. Thus, no significant differences ($p > 0.05$) were observed in VMPR (535 ± 63 mL CH_4 /L-d) and CH_4 yield (525 ± 63 mL CH_4 /g VS_{added}). Conversely, in P3.78, ammonia reached low-inhibitory levels (2.94 ± 0.83 g TAN/L), significantly reducing ($p < 0.05$) VMPR (273 ± 15 mL CH_4 /L-d) and CH_4 yield (247 ± 11 mL CH_4 /g VS_{added}). In cycle 2, P0, P0.37, and P0.75 reached low-inhibitory levels (3.24 ± 0.14 to 6.38 ± 0.54 g TAN/L), increasing propionate (288 ± 225 mg COD_{eq} /L) and decreasing CH_4 yield (505 ± 8 to 393 ± 42 mL CH_4 /g VS_{added}). In P3.78, ammonia reached high-inhibitory levels (11.29 ± 0.01 g TAN/L), significantly decreasing VMPR (169 ± 20 mL CH_4 /L-d) and increasing acetate (1693 ± 301 mg COD_{eq} /L). These results suggest that the inhibitory levels were consistent with the physicochemical responses observed in the reactors.

In phase II, cycle 3 had a transition to FW-2 batch and an increase in OLR to 2 g VS/L-d. During these conditions the processes P0, P0.37, and P0.75 significantly converged in the ammonia concentration (4.85 ± 1.65 g TAN/L, $p > 0.05$) remaining within the low-inhibitory threshold. However, the slight overall increase in ammonia reduced CH_4 yield (258 ± 36 mL CH_4 /g VS_{added}) and increased acetate and propionate concentrations (34 ± 59 mg COD_{eq} /L and 718 ± 290 mg COD_{eq} /L, respectively). A similar decline was observed in P3.78, where ammonia concentrations remained at high-inhibitory levels but increased (18.32 ± 0.85 g TAN/L, $p < 0.05$). This led to reductions in VMPR (127 ± 6 mL CH_4 /L-d) and CH_4 yield (69 ± 3 mL CH_4 /g VS_{added}), along with

increased acetate (2753 ± 129 mg COD_{eq}/L) and propionate (718 ± 290 mg COD_{eq}/L). In cycle 4, trends in VMPR, CH₄ yield, acetate, and butyrate partially mirrored those in cycle 3 across all processes. This phase assessed the worst-case scenario for maintaining AD in the AnSBR system, demonstrating that increased OLR could lead to higher ammonia levels in inhibited processes. However, ammonia inhibitory levels proved to be of limited use in demonstrating the effect of ammonia on microbial metabolism.

In phase III, which included cycles 5, 6, and 7, the switch to FW-3 batches and a return to an OLR of 1 g VS/L-d improved performance compared to phase II. CH₄ yields increased for P0, P0.37, and P0.75 (332 ± 8 to 351 ± 1 mL CH₄/g VS_{added}). Acetate (0 ± 1 to 21 ± 18 mg COD_{eq}/L), butyrate (3 ± 6 to 24 ± 41 mg COD_{eq}/L), and propionate (15 ± 18 to 269 ± 180 mg COD_{eq}/L) decreased significantly ($p < 0.05$). Despite similar physicochemical responses, ammonia levels varied in cycles 6 and 7. P0.75 maintained low-inhibitory levels (3.02 ± 0.41 to 3.63 ± 0.05 g/L TAN), while P0 and P0.37 remained non-inhibitory (0.54 ± 0.02 and 2.11 ± 0.01 g/L TAN, respectively). These findings suggest that non-inhibitory ammonia concentrations do not significantly impact short-term performance (35 days), but uncontrolled ammonia could accumulate in biomass over the medium term (100-150 days) (Jiang et al., 2019; Peng et al., 2018; Zhang et al., 2022). Meanwhile, P3.78 remained at high-inhibitory levels ($> 13.47 \pm 0.19$ g TAN/L), leading to slight increases in CH₄ yield (103 ± 22 to 161 ± 46 mL CH₄/g VS_{added}) and decreases in acetate (1637 ± 944 to 2880 ± 828 mg COD_{eq}/L), butyrate (887 ± 449 to 1302 ± 641 mg COD_{eq}/L), and propionate (326 ± 99 to 1276 ± 7 mg COD_{eq}/L). This highlights that multiple metabolic changes occur within inhibitory levels, which are not easily observable using physicochemical variables.

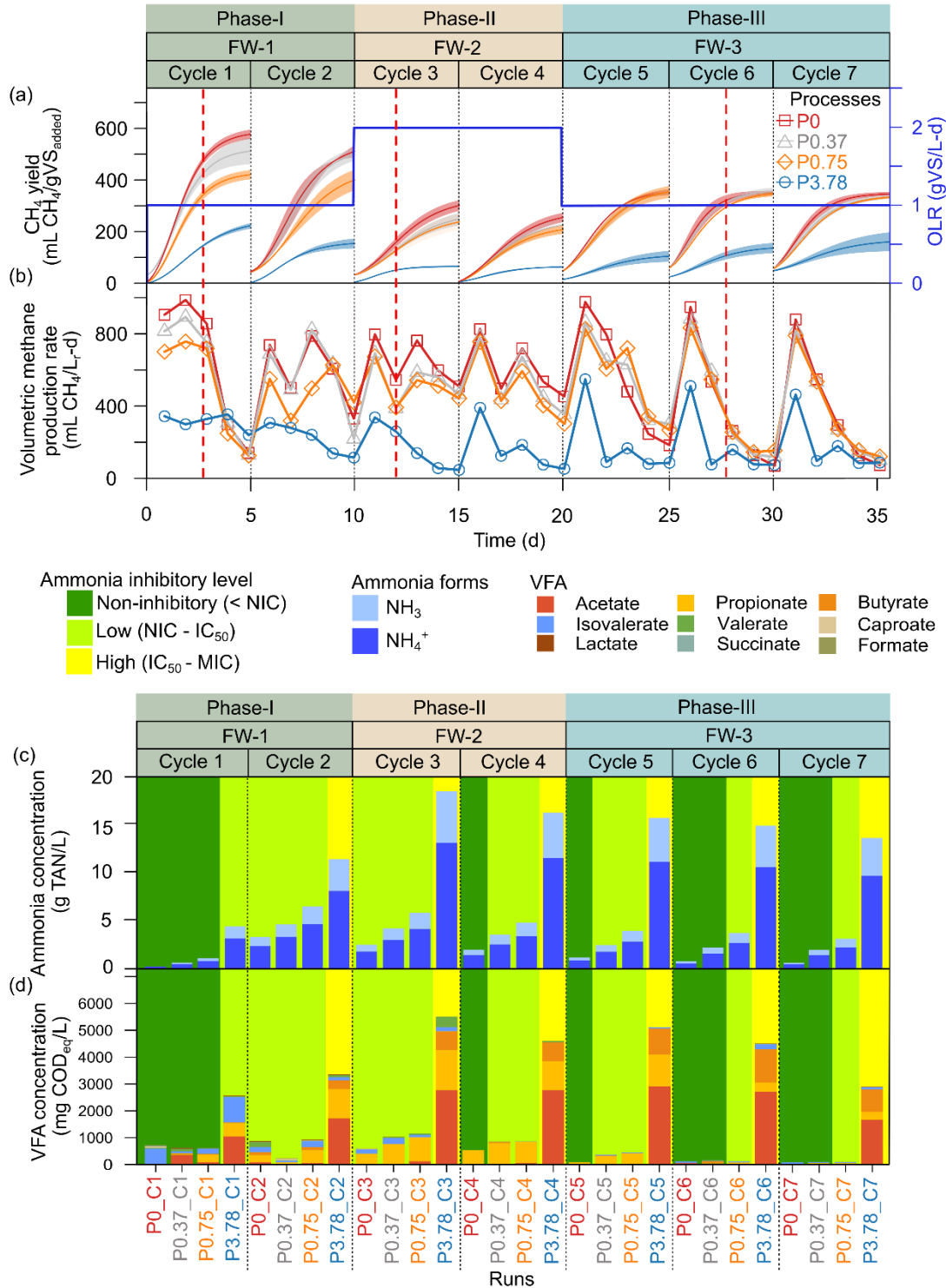


Figure 6.3. Response variables of the AnSBR system per operating cycle (cycles 1-7) during the semi-continuous addition of different ammonia concentrations (0, 0.75, 0.37, and 3.78 g TAN/L), variability of OLR (1 and 2 g VS/L-d), and different feedstock sources (FW1, FW2, and FW3). (a) Cumulative CH₄ yield and (b) VMPR considering average data per day. The red dashed line indicates the sample collection point for microbial community analysis. (c) Ammonia and (d) VFA accumulation corresponding to each ammonia concentration and its inhibitory level.

6.4.3. Microbial diversity across ammonia inhibitory levels

Significant changes in taxonomic and predicted functional profiles of microbial communities were observed across different ammonia inhibitory levels (Fig. 6.4). Among the alpha diversity metrics evaluated, only q_0 showed significant differences ($p < 0.05$) between these levels. Interestingly, q_0 showed contrasting trends depending on whether genera or gene data were used.

A significant decrease ($p < 0.01$) in ASV richness was observed when comparing non-inhibitory to high-inhibitory levels (Fig. 6.4a), while predicted KO richness significantly increased ($p < 0.05$) (Fig. 6.4b). The lower ASV richness at high-inhibitory levels may result from ammonia creating a deterministic environment that assembles phylogenetically similar and resistant microorganisms (Cardona et al., 2022). Such harsh conditions suppress the growth of sensitive key microorganisms, including acetoclastic methanogens, making the process vulnerable to future instabilities (Hong Zhang et al., 2022). Thus, this inhibitory stress may favor the expression of genes for new metabolic pathways, allowing resistant microorganisms to maintain their functionality and potentially enhance the functional diversity of the AD microbiome. For example, *Clostridium* typically engages in polysaccharide hydrolysis and homoacetogenesis under non-inhibitory conditions, but in ammonia-inhibited digesters, they may also contribute to syntrophic acetate oxidation (Allison & Martiny, 2009; Amha et al., 2017; Hardy et al., 2021; Zhang et al., 2022; Ziganshin et al., 2013).

Beta diversity analysis using Bray-Curtis's distance revealed a significant differentiation ($p < 0.05$) in microbial diversity across ammonia inhibitory levels. Microbial communities at high inhibitory levels exhibited distinct taxonomic (Fig. 6.4c) and predicted functional profiles (Fig. 6.4d) compared to those at low and non-inhibitory levels, which showed greater similarity. These results suggest that, regardless of factors such as changes in feedstock batches, variations in feedstock composition due to OLR fluctuations, or microbial residence time, ammonia exerts strong selective pressure on the microbial community.

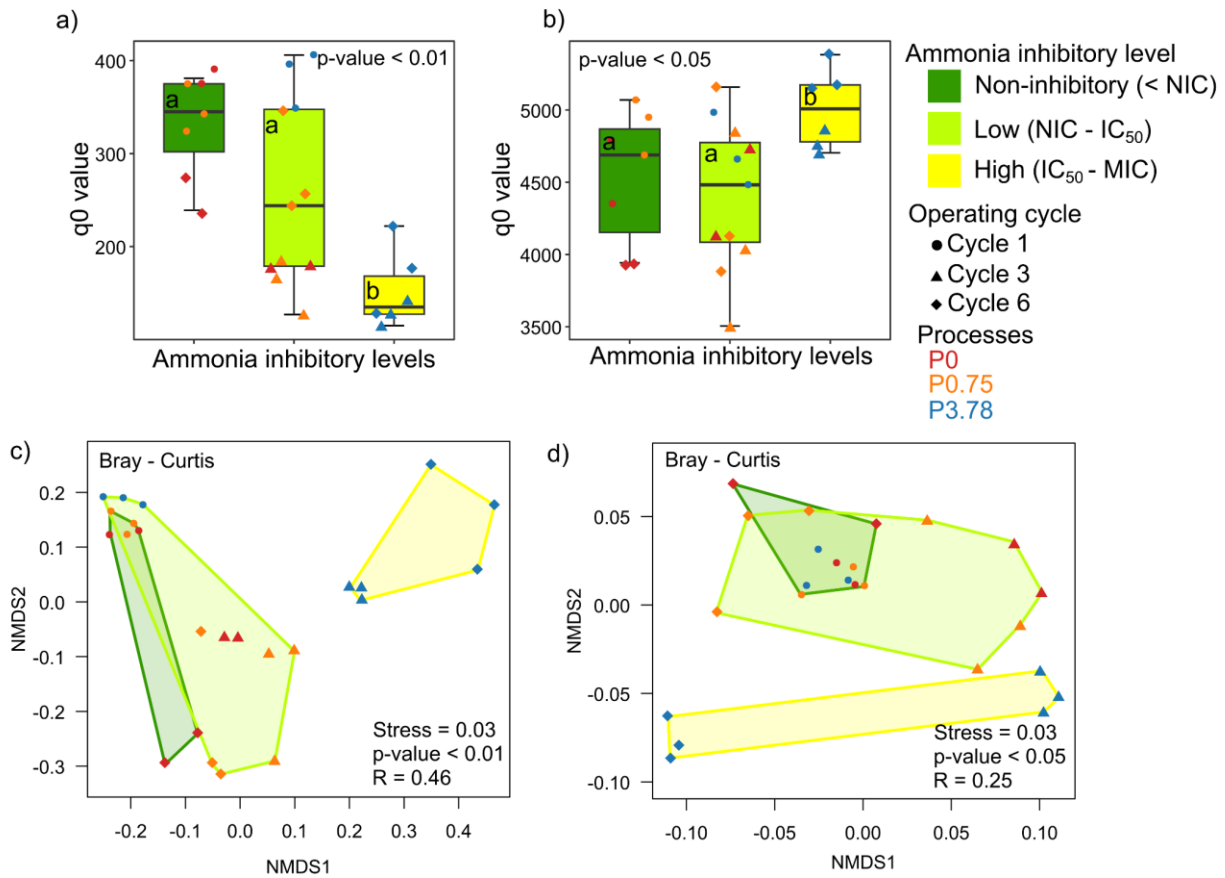


Figure 6.4. Microbial diversity across ammonia inhibitory levels defined by processes in selected operating cycles. Box plots of q0 value and NMDS ordination plots of Hellinger-transformed Bray–Curtis’s dissimilarity matrices obtained from ASV (a, c) and predicted KO (b, d) abundances. Significant differences in the alpha diversity metric (only q0 value) are shown by p-value (Kruskal-Wallis test), while lowercase letters in the box plots indicate inhibitory levels that were similar or different (Wilcoxon rank-sum test with Benjamini-Hochberg p-value adjustment, $p < 0.10$). Significant differences in beta diversity are supported by the p-value (ANOSIM, $p < 0.05$) and good NMDS fit (0.03). The influence of ammonia in clustering microbial communities was confirmed by the R statistic (0.25 – 0.46).

6.4.4. Response of MIs to ammonia inhibitory levels

A total of 8 MIs exhibited significant differences ($p < 0.10$) across varying levels of ammonia inhibition (Fig. 6.5). These MIs were classified into two categories based on their response patterns: stepped response indicators and extreme response indicators. Stepped response indicators showed a gradual increase or decrease in abundance, with significant changes at each incremental level of the inhibitory compound (non-inhibitory \rightarrow low-inhibitory \rightarrow high-inhibitory). In contrast, extreme response indicators exhibited significant changes only between non-inhibitory and high-inhibitory levels of ammonia. This sensitivity to ammonia, irrespective of variations in

feedstock composition in FW digesters, suggests that these MI could serve as universal indicators, a crucial gap in understanding the effect of ammonia during AD.

Among extreme response indicators, *Aminobacterium*, *Clostridium* (including subgenera *sensu stricto* 1, 15, 7, and 8), and *Methanosarcina* significantly increased in abundance ($p < 0.05$) under high ammonia concentrations. The ammonia at inhibitory levels is reported to enhance protein and amino acid hydrolysis, thereby sustaining ammoniacal nitrogen production (Zhang et al., 2022). Consistent with this, the rise of ammonia-resistant microorganisms like *Aminobacterium* suggests that amino acid degradation may still occur (Wang et al., 2018). In addition, the ammonia-inhibited digesters maintain syntrophic oxidation of VFAs is crucial to prevent over-acidification (Li et al., 2018; Zhang et al., 2022). Ammonia-induced possibly selective pressure on microbiome assembly may lead to an increase in *Clostridium sensu stricto*, indicating potential VFA degradation deficiencies due to a loss of VFA-degrading microbial richness (Cardona et al., 2022; Wang et al., 2024). *Methanosarcina*, a resilient archaeon commonly found in ammonia-inhibited FW digesters, maintained methanogenesis due to its metabolic flexibility in utilizing acetate, H_2 , and methylated compounds (Wang et al., 2018). However, when *Methanosarcina* assumes a dominant role in CH_4 production, it may indicate a replacement of acetoclastic archaea, indicating deficiencies in AD (Hardy et al., 2021).

Other extreme response indicators with contrasting responses included *Syntrophobacter*, *Methanomassiliicoccus*, and the *fhs* gene, all showing significant decreases at the high-inhibitory level. These results suggest that ammonia severely disrupted syntrophic pathways, particularly acetogenesis and H_2 -dependent methanogenesis. The decline in *Syntrophobacter* populations and *fhs* gene likely indicates impaired in syntrophic propionate and acetate degradation (via Wood-Ljungdahl pathway) respectively (Müller et al., 2016; Zhang et al., 2022). A similar reduction in *Methanomassiliicoccus* suggests a decrease in methylotrophic methanogenesis, leading to reduced CH_4 production (Hardy et al., 2021; Ruiz-Sánchez et al., 2018). Therefore, these extreme response indicators imply that ammonia has already caused a severe shift in the microbiome, moving away from an authentic microbiome to achieve better performance in AD.

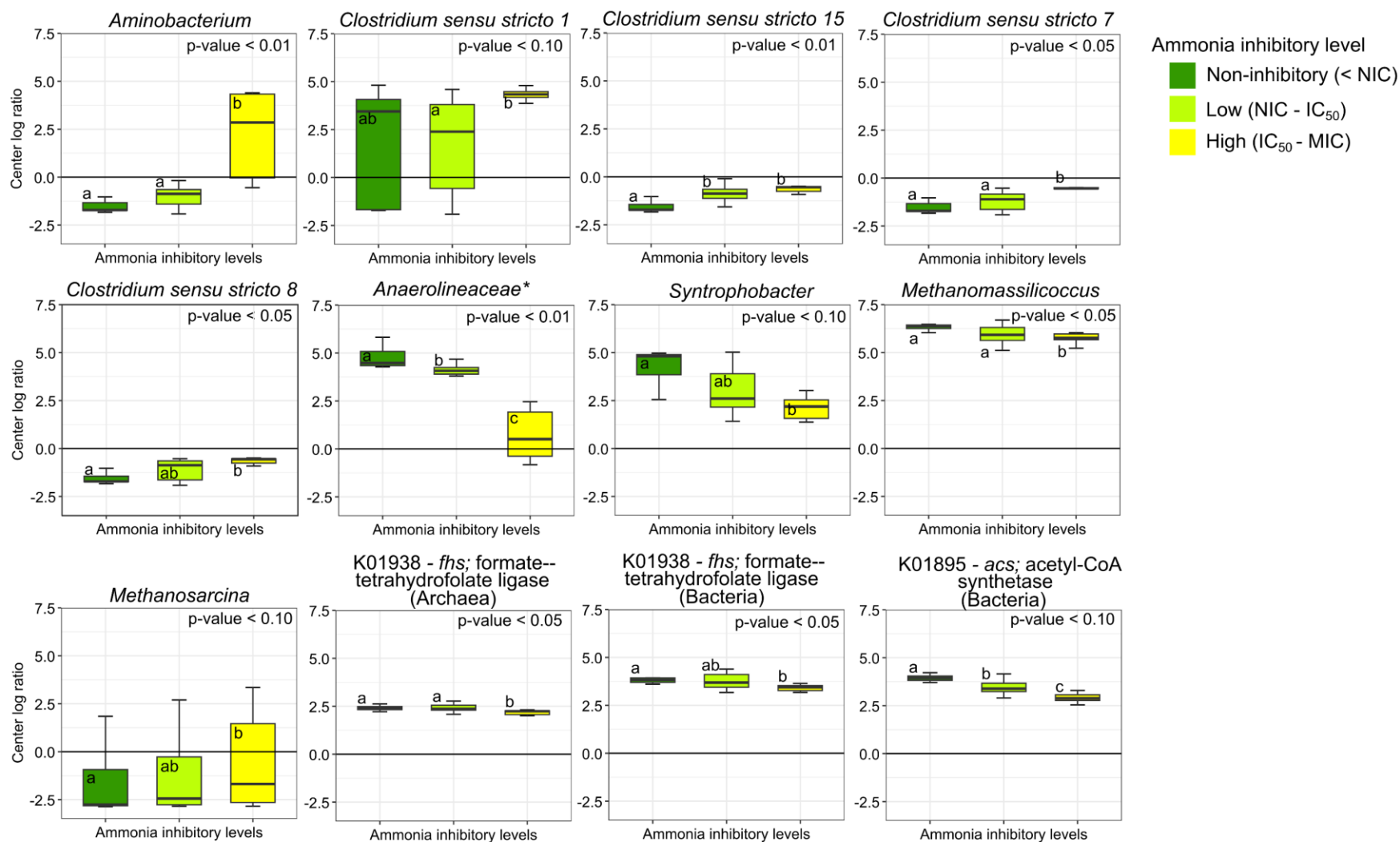


Figure 6.5. Significant responses of MIs for identifying different ammonia inhibitory levels. The distribution of CLR values illustrates the behavior of MIs across ammonia inhibitory levels using boxplots. Significant differences in the MIs are shown by p-value (Kruskal-Wallis test), while lowercase letters in the plots indicate the study groups that were similar or different (Wilcoxon rank-sum test with Benjamini-Hochberg p-value adjustment, $p < 0.10$). (*) indicates ASVs related to unclassified genera, such as T78 belonging to the *Anaerolineaceae* family.

The stepped response indicators were associated with *Anaerolineaceae* and *acs* gene (only in bacteria), showing a gradual decline ($p > 0.10$) in relative abundance as ammonia inhibitory levels increased. Although the *acs* gene was not linked to reduced acetoclastic methanogenesis (archaea group, $p > 0.10$), it suggests potential damage to the SAO pathway, particularly the Wood-Ljungdahl pathway in bacteria (Yu et al., 2020). Lesser-known genera within *Anaerolineaceae* (e.g., T78) play a significant ecological and metabolic role as potential syntrophic bacteria (Bovio-Winkler et al., 2021; Cortez-Cervantes et al., 2024). This highlights the need for further investigation into their role in FW digesters. These MIs showed greater sensitivity to ammonia effects and higher abundances, which likely contribute to maintaining a suitable microbiome for AD. Therefore, preserving microorganisms associated with these MIs may be beneficial for optimizing the AD microbiome.

6.4.5. MI profiles in the AnSBR processes

The evaluation of MIs in each AnSBR process provided profiles that offer insights into overall biological aspects about the metabolic behavior of microbiome (Fig. 6.6). This is crucial, as relying solely on physicochemical indicators may lead to misinterpretations about the status of process. For instance, in cycle 6, where VMPR and CH₄ yield recovery was observed in P0 and P0.75, a decrease in *Syntrophobacter* and the *acs* gene suggest deficiencies in SPO and SAO pathways in both processes. Additionally, in the same cycle, MIs such as *Methanosarcina*, *Aminobacterium*, *Sphaerochaeta*, and *Clostridium sensu stricto* in P0.75 and P3.75 indicated that ammonia selected resistant members. This microbiome likely faces thermodynamic limitations, reduced the abundance of key microorganisms, and a shift towards favoring fermentative activities over digestive ones (Peng et al., 2018; Yan et al., 2019; Zhang et al., 2022).

The MI profiles also revealed metabolic shifts, providing insights into the status of microbiome under ambiguous conditions. In the same cycle 6, processes P0 and P0.75 showed similar VMPR, CH₄ yields, and VFA concentrations. Under such responses, microbial community of P0.75 likely acclimated better to ammonia stress than P0. Despite similar physicochemical responses, MI profiles indicated that P0.75 experienced a loss of key microorganisms such as *Anaerolineaceae*, along with the emergence of potentially non-beneficial *Aminobacterium* and a stress-adapted SAOB like *Sphaerochaeta* (see Chapter 5). This highlights that MI profiles can differentiate microbiome conditions even when physicochemical responses appear similar.

CHAPTER 6. Evaluation of microbial indicators for ammonia inhibition detection in anaerobic sequencing batch reactors

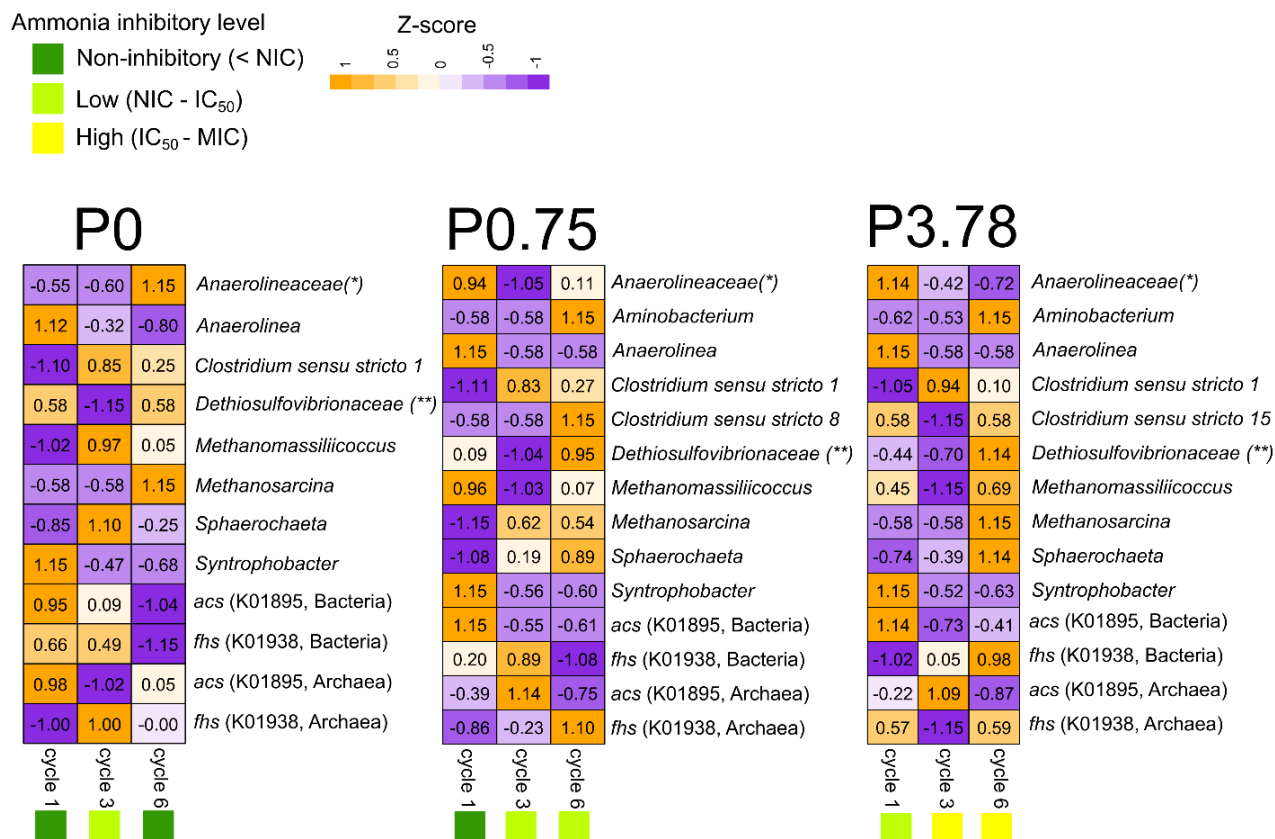


Figure 6.6. Profiles of MIs based on standardized abundance in each AnSBR processes across selected operating cycles (cycles 1, 3, and 6) and classified by ammonia inhibitory level. The z-score distributions illustrate MI behavior across operating cycles in the processes using heatmaps. (*) indicates ASVs associated with unclassified genera, such as T78 from the *Anaerolineaceae* family (**) indicates ASVs linked to unique genera (*Desulfovibrio*) within the *Dethiosulfovibrionaceae* family, the same family related to HA73.

6.5. Conclusion

MIs effectively identified the impact of ammonia in an AnSBR system fed with food waste, despite variations in feedstock composition. MIs were categorized into two groups based on their sensitivity to ammonia inhibitory levels: stepped response indicators and extreme response indicators.

Stepped response indicators, such as *Anaerolineaceae* and the *acs* gene, showed progressive sensitivity to ammonia, affecting syntrophic relationships and acetate degradation at low inhibitory levels. Extreme response indicators, including *Aminobacterium*, *Clostridium sensu stricto* (subspecies 1, 15, 7, and 8), *Methanosarcina*, *Syntrophobacter*, *Methanomassiliicoccus*, and the *fhs* gene, differentiated only between non-inhibitory and high-inhibitory levels. These indicators suggested a decline in SPO and SAO activities, a reliance on H₂-dependent methanogenesis, and the presence of resistant fermentative microorganisms, indicating microbiome vulnerability at high inhibitory levels.

MIs effectively distinguished microbiomes with similar physicochemical responses, such as VMPR and CH₄ yield, highlighting the advantages of MIs over traditional physicochemical indicators. MIs accurately assessed the impact of ammonia, regardless of feedstock composition variations or shifts in the microbial community over time. Developing and implementing monitoring techniques that incorporate these valuable indicators is essential to enhance the detection of effects of ammonia and facilitate recovery processes, ultimately preventing inhibition.

CHAPTER 7. General conclusions and future perspectives

The current research aimed to identify microbial indicators for monitoring anaerobic processes fed with organic solid waste. The statistical framework used successfully defined key attributes that, when applied in multi-omics and multi-experimental contexts, validated the reliability of these indicators. These MIs effectively addressed challenges related to CH₄ yield and ammonia inhibition in a reproducible manner. Furthermore, they provided early warnings of inhibitory compounds and were linked to key microbial metabolisms.

Given these attributes, the MIs show significant potential for implementation in monitoring systems, integration into mathematical algorithms or models, and evaluation of recovery strategies that address critical challenges. These components are essential for designing and developing new control systems based on biological information. Such systems will provide the necessary tools to maximize efficiency and ensure long-term stability of OSW digesters.

Perspectives and recommendations.

Considering the steps for applying the microbial management concept in AD, this thesis serves as a foundation for initiating experiments focused on the three areas of microbial-based management in AD (Fig. 7.1). Future applications of MIs are recommended to follow a sequential approach: first, evaluating their ability to detect key challenges (retrospective management); second, developing monitoring processes (prospective management); and finally, verifying the feasibility of countermeasures (proactive management) (Carballa et al., 2015; Wei et al., 2020). Following this structured process, the implementation of microbial-based management primarily depends on financial viability. Overhead costs (e.g., genetic material extraction, molecular protocols, repairs, and data analysis personnel) should be carefully considered to ensure the appropriate application of MIs (Cordier et al., 2020; Wu et al., 2019). This approach will lead to the proper and profitable use of MIs, ensuring stable and efficient processes without economic losses, thus contributing to the modernization of AD systems.

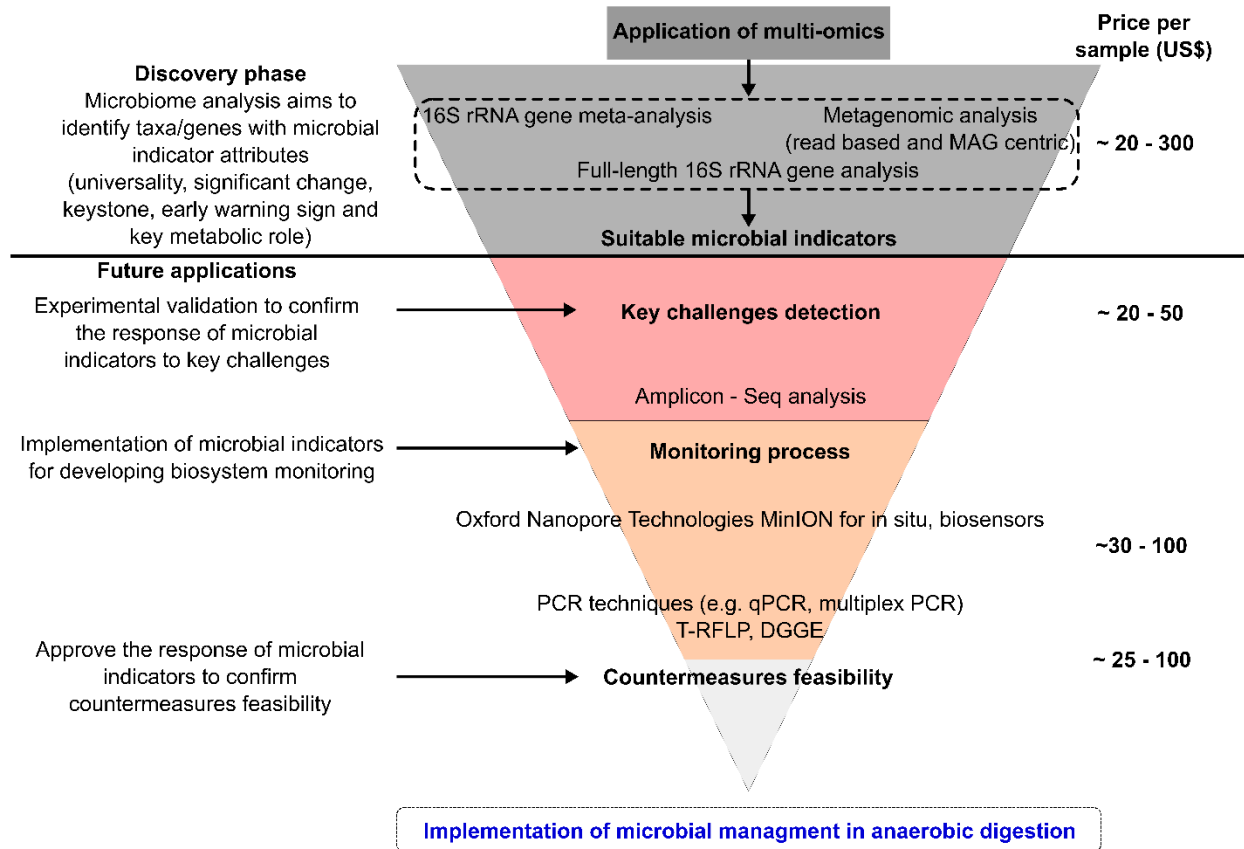


Figure 7.1. Steps for the progressive implementation of MIs within with microbial management concept. Evaluating MI attributes across taxa and genes, irrespective of the omics tool used, appears ideal for achieving consistent responses. Future MI applications involve designing experimental assays to understand their response in detecting key challenges, monitoring processes, and assessing the feasibility of countermeasures. This figure was adapted from the concept by Terzin et al. (2024) and Carballa et al., (2015).

7.1. Retrospective management: Key challenges detection

Sampling collections with taxonomic and functional information from key challenges offer a practical option for applying a statistical framework to identify suitable MIs (Ou et al., 2021). This approach pertains to retrospective management, where the process undergoes evaluation (e.g., health or operational issues), performance is elucidated regarding potential causes, and corrective measures may be implemented upon issue identification (Carballa et al., 2015). Previously, this concept was applied to propose methods for identifying inhibitory ammonia levels. Beyond this approach, MIs also hold potential for developing simplified AI-machine learning models through experimental assays or meta-analyses. These models could enable highly accurate categorical predictions using a small number of microorganisms (Wijaya et al., 2023). Once developed, the model will only require a microcomputer and a data analyst to evaluate the microbiome in real systems.

In a practical application, considering that suitable MIs may provide several weeks of lead time to anticipate perturbations, microbiome assessments should align with the recommended sampling frequency of at least once every two weeks for external tests (Wu et al., 2021). For this type of management, the most informative and cost-effective option for collecting taxonomic information is 16S rRNA sequencing (\$20 – \$50), while metagenomic sequencing offers higher resolution but is more expensive (\$100 – \$300) and not always necessary (Liu et al., 2021). Once taxonomic information is obtained, the model can be applied to discern operational issues from favorable states. If an issue is detected, the appropriate countermeasure can be selected to restore CH₄ production.

7.2. Prospective management: Process monitoring

Monitoring is a continuous and systematic procedure involving the periodic surveillance of indicators to verify process status and predict instability events, ensuring long-term operational efficiency (Wu et al., 2021). It is linked with prospective management, involving continuous data collection to analyze reliable patterns providing insight into the future state of the process (Carballa et al., 2015). Previously, the identified MIs were capable of detecting ammonia inhibition through short-term monitoring and provided a more detailed description of the AD process compared to physicochemical indicators such as CH₄ production, ammonia, or VFA concentrations. Upon detecting these adverse trends, solutions like bioaugmentation could be implemented to restore AD performance. Upon detecting this adverse trend, solutions such as bioaugmentation could be proposed to restore AD (Basak et al., 2021). Therefore, designing a real-time monitoring biosystem with rapid and effective screening devices enables timely corrective actions to prevent AD collapse, offering an alternative to conventional monitoring systems currently in use.

Currently, there are devices and techniques that may be attractive for monitoring MI. For instance, to monitor key taxa and genes, acquiring devices such as the Oxford Nanopore Technologies MinION (\$1999, <https://nanoporetech.com/>) or biosensors (e.g. microbial electrolysis cells the cost is \$40 – 80) could be cost-effective (Innard & Chong, 2022; Wu et al., 2019). Alternatively, the low per-sample cost and quick turnaround of PCR techniques (approximately \$25) make them a prudent option (Johnston-Monje & Lopez Mejia, 2020). For key diversity indexes, fingerprinting techniques like terminal restriction length polymorphism (T-RFLP, \$100 - \$200 per sample) or purchasing equipment for denaturing gradient gel electrophoresis (DGGE, \$500) could be applied

(De Vrieze, 2020; Johnston-Monje & Lopez Mejia, 2020). These technologies can deliver results within hours, and when combined with the early warning capabilities of MIs, a minimum sampling frequency of once per week may ensure economic feasibility for their applications (Wu et al., 2021). Based on these responses, promising models could be designed, such as those supported by artificial intelligence, to enhance AD state prediction (Wijaya et al., 2023).

7.3. Proactive management: Countermeasures feasibility

Understanding the responses of MIs to identify or predict the status of AD could lead to inferring a process diagnosis. It is compelling to evaluate precise countermeasures aligned with the indicator response (Innard & Chong, 2022). This approach seems suited to proactive management by implementing preventive actions to avoid negative process impacts (Carballa et al., 2015). For example, if microorganisms with metabolic capacity to produce biosurfactants like *Lactobacillus* were suggested as suitable MIs, they could significantly predict foam formation (He et al., 2017). Subsequently, the operator could decide on corrective measures such as applying an anti-foaming agent (e.g., rapeseed oil) (Kougiyas et al., 2015). Another approach would be to validate improvement actions to increase CH₄ production. For instance, an increase in *Methanosarcina* may validate the effectiveness of trace element supplementation (Zhang et al. 2019). Undoubtedly, MIs emerge as an extension in the modernization of anaerobic systems, enhancing the reliability of these processes.

7.4. Integration of microbial management into the design of new control strategies

The development of MIs with reproducibility and reliability presents a key opportunity to advance control systems based on microbial management in FW digesters (Fig. 7.2). Future research should focus on designing novel monitoring systems, identifying new MIs to address emerging challenges, and integrating control algorithms to enhance system performance. Additionally, evaluating the effectiveness of actuators in counteracting specific challenges will be essential for optimizing process control. Once implemented, these control systems will enable the optimization of microbial metabolism using MI data, offering significant potential for maintaining long-term stability in FW digesters. This approach paves the way for further exploration of adaptive control strategies that enhance operational resilience and efficiency.

Based on the results of this research, a relatively simple automated control system for managing ammonia inhibition can be developed for FW digesters. The proposed system involves continued

monitoring of key physicochemical indicators, such as ammonia concentration, biogas production, pH, and temperature, complemented by MIs. Due to the sensitivity and early-warning capabilities of MIs, they can be employed either through retrospective management, using conventional and cost-effective techniques like qPCR or 16S rRNA sequencing, or through the design of new monitoring systems that provide rapid detection using affordable biosensors. The data collected would be processed by a controller based on one or more models, which would determine if the process is inhibited. The actuator would then execute physical actions to counteract the problem, such as reducing the organic load or applying bioaugmentation. After implementing the corrective measures, the response of the indicators would be reassessed to confirm the effectiveness of the solution.

The findings of this research highlight key considerations for advancing microbial management strategies in AD using the proposed MIs. Key questions include: What is the most reliable and cost-effective detection method for MIs? What model is best suited for integrating these indicators into control systems? What recovery strategies are most effective for addressing inhibition, and how do they align with MI responses? How much time is required to observe MI responses? Can AD processes be effectively controlled using only MIs? Addressing these questions through future research will be essential to incorporating MIs and improving conventional control systems.

MIs represent a significant step toward modernizing AD and other bioprocesses that demand increased efficiency and long-term stability. Their integration will play a pivotal role in achieving the industrial consolidation of these bioprocesses, offering valuable insights for process optimization and resilience.

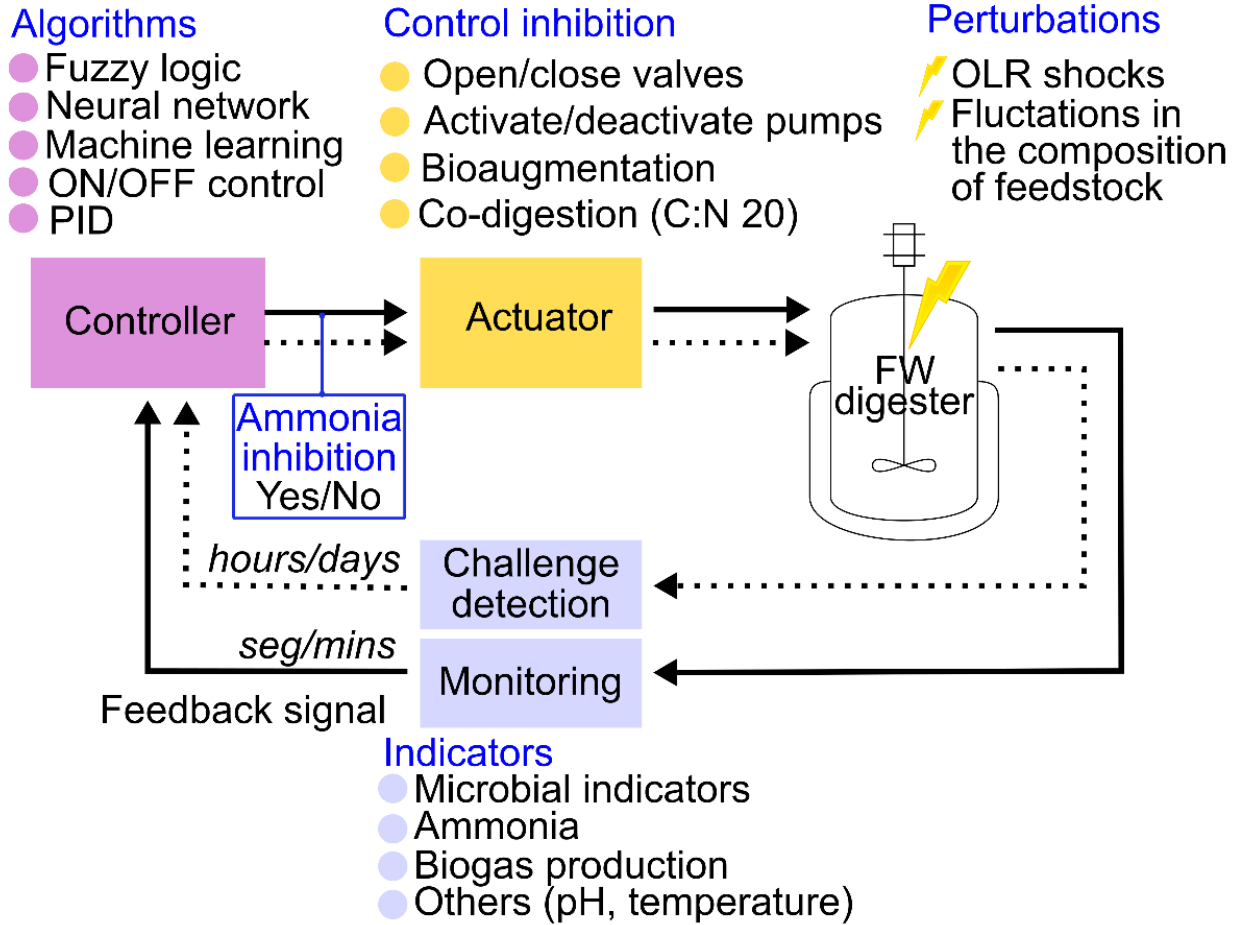


Figure 7.2. Future control systems utilizing MIs, integrating the three key areas of microbial management to address, for instance, ammonia inhibition in FW digesters. The proposed set of indicators could be used to develop new control systems, ensuring long-term stability of AD. This figure was adapted from the concept by Nguyen et al. (2015).

PRODUCTS DERIVED FROM THIS THESIS

Research papers

- Cortez-Cervantes, Jonathan, Iván Moreno-Andrade, Ana E. Escalante, Daniel de los Cobos-Vasconcelos, and Julián Carrillo-Reyes. 2024. “Identifying Reliable Microbial Indicators in Anaerobic Digestion of Organic Solid Waste: Insights from a Meta-Analysis.” **Journal of Environmental Chemical Engineering** 12(5).
<https://doi.org/10.1016/j.jece.2024.113392>
- Cortez-Cervantes, Jonathan, Iván Moreno-Andrade, Pabel Cervantes-Avilés, Julián Carrillo-Reyes. “Suitable microbial indicators for ammonia inhibition detection in food wastes anaerobic digestion.” **Submitted to Chemosphere**.
- Cortez-Cervantes, Jonathan, Iván Moreno-Andrade, Claudia Etchebehere, Julián Carrillo-Reyes. “Evaluation of microbial indicators for ammonia inhibition detection in anaerobic sequencing batch reactors.” **to be submitted to Bioresource Technology**.

Book chapters

- Moreno-Andrade, I., Salazar-Batres, K. J., Villanueva-Galindo, E., Cortez-Cervantes, J. F., Jimenez-Ocampo, U., Carrillo-Reyes, J., & Vargas, A. (2022). Biohydrogen from Food Waste. In: Kuddus, M., Yunus, G., Ramteke, P.W., Molina, G. (eds) **Organic Waste to Biohydrogen. Clean Energy Production Technologies**. Springer, Singapore.
https://doi.org/10.1007/978-981-19-1995-4_2
- Carrillo-Reyes, J., Valdez-Vazquez, I., Vital-Jácome, M., Vargas, A., Navarro-Díaz, M., Cortez-Cervantes, J., & Chango-Cañola, A. P. (2024). Microbial Communities in Dark Fermentation, Analytical Tools to Elucidate Key Microorganisms and Metabolic Profiles. In V. Alcaraz Gonzalez, R. A. Flores Estrella, A. Haarstrick, & V. Gonzalez Alvarez (Eds.), **Wastewater Exploitation: From Microbiological Activity to Energy** (pp. 107–132). Cham: Springer Nature Switzerland. https://doi.org/10.1007/978-3-031-57735-2_7

Conference proceedings

- Poster presentation at the **4th International Conference for Bioresource Technology for Bioenergy, Bioproducts & Environmental Sustainability**, with the project titled "*Biomarkers discriminate operational status based on ammonia concentration in anaerobic digestion processes fed with OFMSW*" held from May 14–15, 2023, in Riva del Garda, Italy.
- Oral presentation at the **XIV Latin American Workshop and Symposium on Anaerobic Digestion**, with the project titled "*Meta-analysis reveals potential bioindicators for anaerobic digestion of organic solid wastes*" held from June 23–27, 2023, in Santiago de Querétaro, Querétaro, Mexico.
- Poster presentation at the **18th IWA World Conference on Anaerobic Digestion**, with the project titled "*Systematic microbiome data analysis: identifying potential reproducible early warning indicators for ammonia inhibition,*" held from June 3–5, 2024, in Istanbul, Turkey.

REFERENCES

- Agyeman, F. O., Han, Y., & Tao, W. (2021). Elucidating the kinetics of ammonia inhibition to anaerobic digestion through extended batch experiments and stimulation-inhibition modeling. *Bioresource Technology*, 340. <https://doi.org/10.1016/j.biortech.2021.125744>
- Alavi-Borazjani, S. A., Capela, I., & Tarelho, L. A. C. (2020). Over-acidification control strategies for enhanced biogas production from anaerobic digestion: A review. *Biomass and Bioenergy*, 143(June), 105833. <https://doi.org/10.1016/j.biombioe.2020.105833>
- Alberdi, A., & Gilbert, M. T. P. (2019). Hilldiv: An R package for the integral analysis of diversity based on Hill numbers. *BioRxiv*.
- Allison, S. D., & Martiny, J. B. H. (2009). Resistance, resilience, and redundancy in microbial communities. *In the Light of Evolution*, 2, 149–166. <https://doi.org/10.17226/12501>
- Amani, T., Nosrati, M., & Sreerkrishnan, T. R. (2010). Anaerobic digestion from the viewpoint of microbiological, chemical, and operational aspects - A review. *Environmental Reviews*, 18, 255–278. <https://doi.org/10.1139/A10-011>
- Amha, Y. M., Corbett, M., & Smith, A. L. (2019). Two-Phase Improves Performance of Anaerobic Membrane Bioreactor Treatment of Food Waste at High Organic Loading Rates. *Environmental Science and Technology*, 53(16), 9572–9583. <https://doi.org/10.1021/acs.est.9b02639>
- Amha, Y. M., Sinha, P., Lagman, J., Gregori, M., & Smith, A. L. (2017). Elucidating microbial community adaptation to anaerobic co-digestion of fats, oils, and grease and food waste. *Water Research*, 123, 277–289. <https://doi.org/10.1016/j.watres.2017.06.065>
- Amir, A., Daniel, M., Navas-Molina, J., Kopylova, E., Morton, J., Xu, Z. Z., ... Knight, R. (2017). Deblur Rapidly Resolves Single-Nucleotide Community Sequence Patterns. *American Society for Microbiology*, 2(2), e00191-16. <https://doi.org/10.1128/mSystems.00191-16>
- Angelidaki, I., Alves, M., Bolzonella, D., Borzacconi, L., Campos, J. L., Guwy, A. J., ... Van Lier, J. B. (2009). Defining the biomethane potential (BMP) of solid organic wastes and energy crops: A proposed protocol for batch assays. *Water Science and Technology*, 59(5), 927–934. <https://doi.org/10.2166/wst.2009.040>
- Ao, T., Ran, Y., Chen, Y., Li, R., Luo, Y., Liu, X., & Li, D. (2020). Effect of viscosity on process stability and microbial community composition during anaerobic mesophilic digestion of Maotai-flavored distiller's grains. *Bioresource Technology*, 297(September 2019), 122460. <https://doi.org/10.1016/j.biortech.2019.122460>
- APHA. (2005). Standard Methods for the Examination of Water and Wastewater. *Standard Methods*, 541. <https://doi.org/ISBN 9780875532356>
- Banks, C. J., Heaven, S., Zhang, S., & Baier, U. (2018). Food waste digestion: Anaerobic digestion of food waste for a circular economy. In *IEA Bioenergy Task 37*.

- Basak, B., Patil, S. M., Saha, S., Kurade, M. B., Ha, G. S., Govindwar, S. P., ... Jeon, B. H. (2021). Rapid recovery of methane yield in organic overloaded-failed anaerobic digesters through bioaugmentation with acclimatized microbial consortium. *Science of the Total Environment*, 764(144219), 1–13. <https://doi.org/10.1016/j.scitotenv.2020.144219>
- Berg, G., Rybakova, D., Fischer, D., Cernava, T., Vergès, M. C. C., Charles, T., ... Schloter, M. (2020). Microbiome definition re-visited: old concepts and new challenges. *Microbiome*, 8(1), 1–22. <https://doi.org/10.1186/s40168-020-00875-0>
- Berry, D., & Widder, S. (2014). Deciphering microbial interactions and detecting keystone species with co-occurrence networks. *Frontiers in Microbiology*, 5(MAY), 1–14. <https://doi.org/10.3389/fmicb.2014.00219>
- Bokulich, N. A., Kaehler, B. D., Rideout, J. R., Dillon, M., Bolyen, E., Knight, R., ... Gregory Caporaso, J. (2018). Optimizing taxonomic classification of marker-gene amplicon sequences with QIIME 2's q2-feature-classifier plugin. *Microbiome*, 6(1). <https://doi.org/10.1186/s40168-018-0470-z>
- Bolger, A. M., Lohse, M., & Usadel, B. (2014). *Genome analysis Trimmomatic: a flexible trimmer for Illumina sequence data*. 30(15), 2114–2120. <https://doi.org/10.1093/bioinformatics/btu170>
- Bolyen, E., Rideout, J. R., Dillon, M. R., Bokulich, N. A., Abnet, C. C., Al-Ghalith, G. A., ... Caporaso, J. G. (2019). Reproducible, interactive, scalable and extensible microbiome data science using QIIME 2. *Nature Biotechnology*, 37(8), 852–857. <https://doi.org/10.1038/s41587-019-0209-9>
- Bovio-Winkler, P., Cabezas, A., & Etchebehere, C. (2021). Database Mining to Unravel the Ecology of the Phylum Chloroflexi in Methanogenic Full Scale Bioreactors. *Frontiers in Microbiology*, 11, 603234. <https://doi.org/10.3389/fmicb.2020.603234>
- Buttigieg, P. L., & Ramette, A. (2014). A guide to statistical analysis in microbial ecology: A community-focused, living review of multivariate data analyses. *FEMS Microbiology Ecology*, 90(3), 543–550. <https://doi.org/10.1111/1574-6941.12437>
- Cabrol, L., Marone, A., Tapia-Venegas, E., Steyer, J. P., Ruiz-Filippi, G., & Trably, E. (2017). Microbial ecology of fermentative hydrogen producing bioprocesses: Useful insights for driving the ecosystem function. *FEMS Microbiology Reviews*, 41(2), 158–181. <https://doi.org/10.1093/femsre/fuw043>
- Calusinska, M., Goux, X., Fossépré, M., Muller, E. E. L., Wilmes, P., & Delfosse, P. (2018). A year of monitoring 20 mesophilic full-scale bioreactors reveals the existence of stable but different core microbiomes in bio-waste and wastewater anaerobic digestion systems. *Biotechnology for Biofuels*, 11(1), 1–19. <https://doi.org/10.1186/s13068-018-1195-8>
- Cao, Y., Dong, Q., Wang, D., Zhang, P., Liu, Y., & Niu, C. (2022). microbiomeMarker: microbiome biomarker analysis toolkit. *Bioinformatics*, 38(16).

- Capson-Tojo, G., Moscoviz, R., Astals, S., Robles, & Steyer, J. P. (2020). Unraveling the literature chaos around free ammonia inhibition in anaerobic digestion. *Renewable and Sustainable Energy Reviews*, *117*, 109487. <https://doi.org/10.1016/j.rser.2019.109487>
- Carballa, M., Rigueiro, L., & Lema, J. M. (2015). Microbial management of anaerobic digestion: Exploiting the microbiome-functionality nexus. *Current Opinion in Biotechnology*, *33*, 103–111. <https://doi.org/10.1016/j.copbio.2015.01.008>
- Cardona, L., Mazéas, L., & Chapleur, O. (2022). Deterministic processes drive the microbial assembly during the recovery of an anaerobic digester after a severe ammonia shock. *Bioresource Technology*, *347*(November 2021). <https://doi.org/10.1016/j.biortech.2021.126432>
- Chatterjee, B., & Mazumder, D. (2019). Role of stage-separation in the ubiquitous development of Anaerobic Digestion of Organic Fraction of Municipal Solid Waste: A critical review. *Renewable and Sustainable Energy Reviews*, *104*(November 2018), 439–469. <https://doi.org/10.1016/j.rser.2019.01.026>
- Chen, H., Wang, W., Xue, L., Chen, C., Liu, G., & Zhang, R. (2016). Effects of Ammonia on Anaerobic Digestion of Food Waste: Process Performance and Microbial Community. *Energy and Fuels*, *30*(7), 5749–5757. <https://doi.org/10.1021/acs.energyfuels.6b00715>
- Chen, Y., Cheng, J. J., & Creamer, K. S. (2008). Inhibition of anaerobic digestion process: A review. *Bioresource Technology*. <https://doi.org/10.1016/j.biortech.2007.01.057>
- Chong, J., Liu, P., Zhou, G., & Xia, J. (2020). Using MicrobiomeAnalyst for comprehensive statistical, functional, and meta-analysis of microbiome data. *Nature Protocols*, *15*(3), 799–821. <https://doi.org/10.1038/s41596-019-0264-1>
- Cordier, T., Alonso-Sáez, L., Apothéloz-Perret-Gentil, L., Aylagas, E., Bohan, D. A., Bouchez, A., ... Lanzén, A. (2020). Ecosystems monitoring powered by environmental genomics: A review of current strategies with an implementation roadmap. *Molecular Ecology*, *30*(13), 2937–2958. <https://doi.org/10.1111/mec.15472>
- Cortez-Cervantes, J., Moreno-Andrade, I., Escalante, A. E., de los Cobos-Vasconcelos, D., & Carrillo-Reyes, J. (2024). Identifying reliable microbial indicators in anaerobic digestion of organic solid waste: Insights from a meta-analysis. *Journal of Environmental Chemical Engineering*, *12*(5). <https://doi.org/10.1016/j.jece.2024.113392>
- De Vrieze, J. (2020). The next frontier of the anaerobic digestion microbiome: From ecology to process control. *Environmental Science and Ecotechnology*, *3*, 100032. <https://doi.org/10.1016/j.ese.2020.100032>
- De Vrieze, J., Heyer, R., Props, R., Van Meulebroek, L., Gille, K., Vanhaecke, L., ... Boon, N. (2021). Triangulation of microbial fingerprinting in anaerobic digestion reveals consistent fingerprinting profiles. *Water Research*, *202*(July), 117422. <https://doi.org/10.1016/j.watres.2021.117422>

- Delignette-Muller, M. L., & Dutang, C. (2015). fitdistrplus: An R package for fitting distributions. *Journal of Statistical Software*, 64(4). <https://doi.org/10.18637/jss.v064.i04>
- Duan, X., Chen, Y., Feng, L., & Zhou, Q. (2021). Metagenomic analysis reveals nonylphenol-shaped acidification and methanogenesis during sludge anaerobic digestion. *Water Research*, 196, 117004. <https://doi.org/10.1016/j.watres.2021.117004>
- Elzhov, T. V., Mullen, K. M., Spiess, A.-N., & Maintainer, B. B. (2016). minpack.lm: R Interface to the Levenberg-Marquardt Nonlinear Least-Squares Algorithm Found in MINPACK, Plus Support for Bounds. *R Package Version 1.2-1*.
- Estaki, M., Jiang, L., Bokulich, N. A., McDonald, D., González, A., Kosciolk, T., ... Knight, R. (2020). QIIME 2 Enables Comprehensive End-to-End Analysis of Diverse Microbiome Data and Comparative Studies with Publicly Available Data. *Current Protocols in Bioinformatics*, 70(1), 1–46. <https://doi.org/10.1002/cpbi.100>
- Faust, K., Lahti, L., Gonze, D., de Vos, W. M., & Raes, J. (2015). Metagenomics meets time series analysis: Unraveling microbial community dynamics. *Current Opinion in Microbiology*, 25(May), 56–66. <https://doi.org/10.1016/j.mib.2015.04.004>
- Fernandes, A. D., Macklaim, J. M., Linn, T. G., Reid, G., & Gloor, G. B. (2013). ANOVA-Like Differential Expression (ALDEx) Analysis for Mixed Population RNA-Seq. *PLoS ONE*, 8(7). <https://doi.org/10.1371/journal.pone.0067019>
- Fernandez-Bayo, J. D., Simmons, C. W., & VanderGheynst, J. S. (2020). Characterization of digestate microbial community structure following thermophilic anaerobic digestion with varying levels of green and food wastes. *Journal of Industrial Microbiology and Biotechnology*, 47(12), 1031–1044. <https://doi.org/10.1007/s10295-020-02326-z>
- Freedman, D., & Diaconis, P. (1981). On the Histogram as a Density Estimator: L 2 Theory. In *Z. Wahrscheinlichkeitstheorie verw. Gebiete* (Vol. 57).
- Gaby, J. C., Zamanzadeh, M., & Horn, S. J. (2017). The effect of temperature and retention time on methane production and microbial community composition in staged anaerobic digesters fed with food waste. *Biotechnology for Biofuels*, 10(1), 1–14. <https://doi.org/10.1186/s13068-017-0989-4>
- Ganidi, N., Tyrrel, S., & Cartmell, E. (2009). Anaerobic digestion foaming causes - A review. *Bioresource Technology*, 100(23), 5546–5554. <https://doi.org/10.1016/j.biortech.2009.06.024>
- Gao, S., Huang, Y., Yang, L., Wang, H., Zhao, M., Xu, Z., ... Ruan, W. (2015). Evaluation the anaerobic digestion performance of solid residual kitchen waste by NaHCO₃ buffering. *Energy Conversion and Management*, 93, 166–174. <https://doi.org/10.1016/j.enconman.2015.01.010>
- Giordani, A., Brucha, G., Santos, K. A., Rojas, K., Hayashi, E., Alves, M. M. S., & Tommaso, G. (2021). Performance and Microbial Community Analysis in an Anaerobic Hybrid

- Baffled Reactor Treating Dairy Wastewater. *Water, Air, and Soil Pollution*, 232(10). <https://doi.org/10.1007/s11270-021-05348-0>
- Goux, X., Calusinska, M., Lemaigre, S., Marynowska, M., Klocke, M., Udelhoven, T., ... Delfosse, P. (2015). Microbial community dynamics in replicate anaerobic digesters exposed sequentially to increasing organic loading rate, acidosis, and process recovery. *Biotechnology for Biofuels*, 8(1). <https://doi.org/10.1186/s13068-015-0309-9>
- Groemping, U. (2019). Fractional Factorial Designs with 2-Level Factors. *Comprehensive R Archive Network (CRAN)*.
- Grohmann, A., Vainshtein, Y., Euchner, E., Grumaz, C., Bryniok, D., Rabus, R., & Sohn, K. (2018). Genetic repertoires of anaerobic microbiomes driving generation of biogas. *Biotechnology for Biofuels*, 11(1). <https://doi.org/10.1186/s13068-018-1258-x>
- Guo, B., Zhang, L., Sun, H., Gao, M., Yu, N., Zhang, Q., ... Liu, Y. (2022). Microbial co-occurrence network topological properties link with reactor parameters and reveal importance of low-abundance genera. *Npj Biofilms and Microbiomes*, 8(1), 1–13. <https://doi.org/10.1038/s41522-021-00263-y>
- Hadj, B. E., Astals, S., Galí, A., Mace, S., & Mata-Álvarez, J. (2009). Ammonia influence in anaerobic digestion of OFMSW. *Water Science and Technology*, 59(6), 1153–1158. <https://doi.org/10.2166/wst.2009.100>
- Han, J., Kamber, M., & Pei, J. (2012). Data Preprocessing. In *Data Mining* (pp. 83–124). Elsevier. <https://doi.org/10.1016/b978-0-12-381479-1.00003-4>
- Hao, L., Michaelsen, T. Y., Singleton, C. M., Dottorini, G., Kirkegaard, R. H., Albertsen, M., ... Dueholm, M. S. (2020). Novel syntrophic bacteria in full-scale anaerobic digesters revealed by genome-centric metatranscriptomics. *ISME Journal*, 14(4), 906–918. <https://doi.org/10.1038/s41396-019-0571-0>
- Hardy, J., Bonin, P., Lazuka, A., Gonidec, E., Guasco, S., Valette, C., ... Gralnick, J. A. (2021). Similar Methanogenic Shift but Divergent Syntrophic Partners in Anaerobic Digesters Exposed to Direct versus Successive Ammonium Additions. *Microbiology Spectrum*, 9(2), e00805-21. <https://doi.org/10.1128/Spectrum.00805-21>
- Hartop, K. R., Sullivan, M. J., Giannopoulos, G., Gates, A. J., Bond, P. L., Yuan, Z., ... Richardson, D. J. (2017). The metabolic impact of extracellular nitrite on aerobic metabolism of *Paracoccus denitrificans*. *Water Research*, 113, 207–214. <https://doi.org/10.1016/j.watres.2017.02.011>
- He, J., Wang, X., Yin, X. bo, Li, Q., Li, X., Zhang, Y. fei, & Deng, Y. (2018). Insights into biomethane production and microbial community succession during semi-continuous anaerobic digestion of waste cooking oil under different organic loading rates. *AMB Express*, 8(1). <https://doi.org/10.1186/s13568-018-0623-2>

- He, Q., Li, L., Zhao, X., Qu, L., Wu, D., & Peng, X. (2017). Investigation of foaming causes in three mesophilic food waste digesters: Reactor performance and microbial analysis. *Scientific Reports*, 7(1), 1–10. <https://doi.org/10.1038/s41598-017-14258-3>
- Hill, T. C. J., Walsh, K. A., Harris, J. A., & Moffett, B. F. (2003). Using ecological diversity measures with bacterial communities. *FEMS Microbiology Ecology*, 43(1), 1–11. [https://doi.org/10.1016/S0168-6496\(02\)00449-X](https://doi.org/10.1016/S0168-6496(02)00449-X)
- Holliger, C., Alves, M., Andrade, D., Angelidaki, I., Astals, S., Baier, U., ... Wierinck, I. (2016). Towards a standardization of biomethane potential tests. *Water Science and Technology*, 74(11). <https://doi.org/10.2166/wst.2016.336>
- Hu, Y. J., & Satten, G. A. (2023). Compositional analysis of microbiome data using the linear decomposition model (LDM). *Bioinformatics*, 39(11), 1–5. <https://doi.org/10.1093/bioinformatics/btad668>
- Huerta, B., Segura, Y., & Valcárcel, Y. (2024). Effluent biomonitoring. In P. Wexler (Ed.), *Encyclopedia of Toxicology* (4th ed.). Elsevier Inc. <https://doi.org/10.1016/b978-0-12-824315-2.00326-2>
- Innard, N., & Chong, J. P. J. (2022). The challenges of monitoring and manipulating anaerobic microbial communities. *Bioresource Technology*, 344. <https://doi.org/10.1016/j.biortech.2021.126326>
- Janssen, S., Mcdonald, D., Gonzalez, A., Navas-Molina, J. A., Jiang, L., Xu, Z. Z., ... Knight, R. (2018). Phylogenetic Placement of Exact Amplicon Sequences. *MSystems*, 3(3), e00021-18.
- Jiang, Y., McAdam, E., Zhang, Y., Heaven, S., Banks, C., & Longhurst, P. (2019). Ammonia inhibition and toxicity in anaerobic digestion: A critical review. *Journal of Water Process Engineering*, 32(April), 100899. <https://doi.org/10.1016/j.jwpe.2019.100899>
- Jo, Y., Kim, J., Hwang, K., & Lee, C. (2018). A comparative study of single- and two-phase anaerobic digestion of food waste under uncontrolled pH conditions. *Waste Management*, 78, 509–520. <https://doi.org/10.1016/j.wasman.2018.06.017>
- Johnson, R., & Waterfield, J. (2004). Making words count: the value of qualitative research. *Physiotherapy Research International : The Journal for Researchers and Clinicians in Physical Therapy*, 9(3), 121–131. <https://doi.org/10.1002/pri.312>
- Johnston-Monje, D., & Lopez Mejia, J. (2020). Botanical microbiomes on the cheap: Inexpensive molecular fingerprinting methods to study plant-associated communities of bacteria and fungi. *Applications in Plant Sciences*, 8(4), 1–12. <https://doi.org/10.1002/aps3.11334>
- Khafipour, A., Jordaan, E. M., Flores-Orozco, D., Khafipour, E., Levin, D. B., Sparling, R., & Cicek, N. (2020). Response of Microbial Community to Induced Failure of Anaerobic Digesters Through Overloading With Propionic Acid Followed by Process Recovery.

- Frontiers in Bioengineering and Biotechnology*, 8(December), 1–15.
<https://doi.org/10.3389/fbioe.2020.604838>
- Kim, D., Kim, H., Kim, J., & Lee, C. (2019). Co-feeding spent coffee grounds in anaerobic food waste digesters: Effects of co-substrate and stabilization strategy. *Bioresource Technology*, 288(May). <https://doi.org/10.1016/j.biortech.2019.121594>
- Kleyböcker, A., Liebrich, M., Verstraete, W., Kraume, M., & Würdemann, H. (2012). Early warning indicators for process failure due to organic overloading by rapeseed oil in one-stage continuously stirred tank reactor, sewage sludge and waste digesters. *Bioresource Technology*, 123, 534–541. <https://doi.org/10.1016/j.biortech.2012.07.089>
- Kolde, R. (2012). Package 'pheatmap'. *Bioconductor*.
- Kong, X., Liu, J., Yue, X., Li, Y., & Wang, H. (2019). Fe0 inhibits bio-foam generating in anaerobic digestion reactor under conditions of organic shock loading and re-startup. *Waste Management*, 92, 107–114. <https://doi.org/10.1016/j.wasman.2019.05.020>
- Kougias, P. G., Boe, K., Einarsdottir, E. S., & Angelidaki, I. (2015). Counteracting foaming caused by lipids or proteins in biogas reactors using rapeseed oil or oleic acid as antifoaming agents. *Water Research*, 79, 119–127.
<https://doi.org/10.1016/j.watres.2015.04.034>
- Kougias, Panagiotis G., Treu, L., Campanaro, S., Zhu, X., & Angelidaki, I. (2016). Dynamic functional characterization and phylogenetic changes due to Long Chain Fatty Acids pulses in biogas reactors. *Scientific Reports*, 6(March), 1–10. <https://doi.org/10.1038/srep28810>
- Labatut, R. A., & Pronto, J. L. (2018). Sustainable Waste-to-Energy Technologies : Anaerobic Digestion. In *Sustainable Food Waste-to-Energy Systems*. Elsevier Inc.
<https://doi.org/10.1016/B978-0-12-811157-4.00004-8>
- Lambert, R. J. W., & Pearson, J. (2000). Susceptibility testing: Accurate and reproducible minimum inhibitory concentration (MIC) and non-inhibitory concentration (NIC) values. *Journal of Applied Microbiology*, 88(5), 784–790. <https://doi.org/10.1046/j.1365-2672.2000.01017.x>
- Law, C. W., Chen, Y., Shi, W., & Smyth, G. K. (2014). Voom: Precision weights unlock linear model analysis tools for RNA-seq read counts. *Genome Biology*, 15(2).
<https://doi.org/10.1186/gb-2014-15-2-r29>
- Lee, J., Shin, S. G., Han, G., Koo, T., & Hwang, S. (2017). Bacteria and archaea communities in full-scale thermophilic and mesophilic anaerobic digesters treating food wastewater: Key process parameters and microbial indicators of process instability. *Bioresource Technology*, 245(June), 689–697. <https://doi.org/10.1016/j.biortech.2017.09.015>
- Legendre, P., & Gallagher, E. D. (2001). Ecologically meaningful transformations for ordination of species data. *Oecologia*, 129(2), 271–280. <https://doi.org/10.1007/s004420100716>

- Li, C., Hao, L., Lü, F., Duan, H., Zhang, H., & He, P. (2022). Syntrophic Acetate-Oxidizing Microbial Consortia Enriched from Full-Scale Mesophilic Food Waste Anaerobic Digesters Showing High Biodiversity and Functional Redundancy. *MSystems*, 7(5).
<https://doi.org/10.1128/msystems.00339-22>
- Li, Dinghua, Liu, C.-M., Luo, R., Sadakane, K., & Lam, T.-W. (2015). MEGAHIT: an ultra-fast single-node solution for large and complex metagenomics assembly via succinct de Bruijn graph. *Bioinformatics*, 10, 1674–1676. <https://doi.org/10.1093/bioinformatics/btv033>
- Li, Dong, Chen, L., Liu, X., Mei, Z., Ren, H., Cao, Q., & Yan, Z. (2017). Instability mechanisms and early warning indicators for mesophilic anaerobic digestion of vegetable waste. *Bioresource Technology*, 245(13), 90–97. <https://doi.org/10.1016/j.biortech.2017.07.098>
- Li, L., He, Q., Ma, Y., Wang, X., & Peng, X. (2016). A mesophilic anaerobic digester for treating food waste: Process stability and microbial community analysis using pyrosequencing. *Microbial Cell Factories*, 15(1), 1–11. <https://doi.org/10.1186/s12934-016-0466-y>
- Li, L., Peng, X., Wang, X., & Wu, D. (2018). Anaerobic digestion of food waste: A review focusing on process stability. *Bioresource Technology*, 248(174), 20–28.
<https://doi.org/10.1016/j.biortech.2017.07.012>
- Li, Q., Li, Y. Y., Qiao, W., Wang, X., & Takayanagi, K. (2015). Sulfate addition as an effective method to improve methane fermentation performance and propionate degradation in thermophilic anaerobic co-digestion of coffee grounds, milk and waste activated sludge with AnMBR. *Bioresource Technology*, 185, 308–315.
<https://doi.org/10.1016/j.biortech.2015.03.019>
- Li, Yang, Zhang, Y., Xu, Z., Quan, X., & Chen, S. (2015). Enhancement of sludge granulation in anaerobic acetogenesis by addition of nitrate and microbial community analysis. *Biochemical Engineering Journal*, 95, 104–111. <https://doi.org/10.1016/j.bej.2014.12.011>
- Li, Yanzeng, Zhang, S., Chen, Z., & Huang, W. (2024). Biogas slurry reflux enhances the organic loading rate of high-solid anaerobic digestion of kitchen waste by alleviating fatty acids accumulation. *Chemical Engineering Journal*, 482(October 2023), 149072.
<https://doi.org/10.1016/j.cej.2024.149072>
- Liu, Y. X., Qin, Y., Chen, T., Lu, M., Qian, X., Guo, X., & Bai, Y. (2021). A practical guide to amplicon and metagenomic analysis of microbiome data. *Protein and Cell*, 12(5), 315–330.
<https://doi.org/10.1007/s13238-020-00724-8>
- Love, M. I., Huber, W., & Anders, S. (2014a). Moderated estimation of fold change and dispersion for RNA-seq data with DESeq2. *Genome Biology*, 15(12).
<https://doi.org/10.1186/s13059-014-0550-8>
- Love, M. I., Huber, W., & Anders, S. (2014b). Moderated estimation of fold change and dispersion for RNA-seq data with DESeq2. *Genome Biology*, 15(12).
<https://doi.org/10.1186/s13059-014-0550-8>

- Luo, L., & Wong, J. W. C. (2019). Enhanced food waste degradation in integrated two-phase anaerobic digestion: Effect of leachate recirculation ratio. *Bioresource Technology*, 291(May), 121813. <https://doi.org/10.1016/j.biortech.2019.121813>
- Lv, N., Zhao, L., Wang, R., Ning, J., Pan, X., Li, C., ... Zhu, G. (2020). Novel strategy for relieving acid accumulation by enriching syntrophic associations of syntrophic fatty acid-oxidation bacteria and H₂/formate-scavenging methanogens in anaerobic digestion. *Bioresource Technology*, 313(June), 123702. <https://doi.org/10.1016/j.biortech.2020.123702>
- Ma, S., Jiang, F., Huang, Y., Zhang, Y., Wang, S., Fan, H., ... Deng, Y. (2021). A microbial gene catalog of anaerobic digestion from full-scale biogas plants. *GigaScience*, 10(1), 1–10. <https://doi.org/10.1093/gigascience/giaa164>
- Ma, X., Yu, M., Yang, M., Zhang, S., Gao, M., Wu, C., & Wang, Q. (2020). Effect of liquid digestate recirculation on the ethanol-type two-phase semi-continuous anaerobic digestion system of food waste. *Bioresource Technology*, 313, 123534. <https://doi.org/10.1016/j.biortech.2020.123534>
- Mao, C., Feng, Y., Wang, X., & Ren, G. (2015). Review on research achievements of biogas from anaerobic digestion. *Renewable and Sustainable Energy Reviews*, 45, 540–555. <https://doi.org/10.1016/j.rser.2015.02.032>
- Martínez-Porchas, M., Villalpando-Canchola, E., & Vargas-Albores, F. (2016). Significant loss of sensitivity and specificity in the taxonomic classification occurs when short 16S rRNA gene sequences are used. *Heliyon*, 2(9). <https://doi.org/10.1016/j.heliyon.2016.e00170>
- McMurdie, P. J., & Holmes, S. (2013). Phyloseq: An R Package for Reproducible Interactive Analysis and Graphics of Microbiome Census Data. *PLoS ONE*. <https://doi.org/10.1371/journal.pone.0061217>
- Menzel, P., Ng, K. L., & Krogh, A. (2016). Fast and sensitive taxonomic classification for metagenomics with Kaiju. *Nature Communications*, 7. <https://doi.org/10.1038/ncomms11257>
- Mirza, F. N., Malik, A. A., Couzens, C., & Omer, S. B. (2020). Influenza-negative influenza-like illness (fnILI) Z-score as a proxy for incidence and mortality of COVID-19. *Journal of Infection*, 81(5), 793–796. <https://doi.org/10.1016/j.jinf.2020.08.046>
- Moestedt, J., Müller, B., Nagavara Nagaraj, Y., & Schnürer, A. (2020). Acetate and Lactate Production During Two-Stage Anaerobic Digestion of Food Waste Driven by *Lactobacillus* and *Aeriscardovia*. *Frontiers in Energy Research*, 8(June), 1–15. <https://doi.org/10.3389/fenrg.2020.00105>
- Moreno-Andrade, I., Moreno, G., & Quijano, G. (2020). Theoretical framework for the estimation of H₂S concentration in biogas produced from complex sulfur-rich substrates. *Environmental Science and Pollution Research*, 27(14), 15959–15966. <https://doi.org/10.1007/s11356-019-04846-3>

- Mugnai, G., Borruso, L., Mimmo, T., Cesco, S., Luongo, V., Frunzo, L., ... Villa, F. (2021). Dynamics of bacterial communities and substrate conversion during olive-mill waste dark fermentation: Prediction of the metabolic routes for hydrogen production. *Bioresource Technology*, 319, 124157. <https://doi.org/10.1016/J.BIORTECH.2020.124157>
- Müller, B., Sun, L., Westerholm, M., & Schnürer, A. (2016). Bacterial community composition and fhs profiles of low- and high-ammonia biogas digesters reveal novel syntrophic acetate-oxidising bacteria. *Biotechnology for Biofuels*, 9(1), 1–18. <https://doi.org/10.1186/s13068-016-0454-9>
- Muller, E. E. L., Faust, K., Widder, S., Herold, M., Martínez Arbas, S., & Wilmes, P. (2018). Using metabolic networks to resolve ecological properties of microbiomes. *Current Opinion in Systems Biology*, 8, 73–80. <https://doi.org/10.1016/j.coisb.2017.12.004>
- Nakakubo, R., Møller, H. B., Nielsen, A. M., & Matsuda, J. (2008). Ammonia inhibition of methanogenesis and identification of process indicators during anaerobic digestion. *Environmental Engineering Science*, 25(10), 1487–1496. <https://doi.org/10.1089/ees.2007.0282>
- Navarro-Díaz, M., Martinez-Sanchez, M. E., Valdez-Vazquez, I., & Escalante, A. E. (2020). A framework for integrating functional and microbial data: The case of dark fermentation H₂ production. *International Journal of Hydrogen Energy*, 45(56), 31706–31718. <https://doi.org/10.1016/j.ijhydene.2020.08.189>
- Nearing, J. T., Douglas, G. M., Hayes, M. G., MacDonald, J., Desai, D. K., Allward, N., ... Langille, M. G. I. (2022). Microbiome differential abundance methods produce different results across 38 datasets. *Nature Communications*, 13(1). <https://doi.org/10.1038/s41467-022-28034-z>
- Nguyen, D., Gadhamshetty, V., Nitayavardhana, S., & Khanal, S. K. (2015). Automatic process control in anaerobic digestion technology: A critical review. *Bioresource Technology*, 193, 513–522. <https://doi.org/10.1016/j.biortech.2015.06.080>
- Nguyen, L. N., Nguyen, A. Q., & Nghiem, L. D. (2019). Microbial Community in Anaerobic Digestion System : Progression in Microbial Ecology. In *Energy, Environment, and Sustainability* (pp. 331–355). Singapore: Springer. https://doi.org/10.1007/978-981-13-3259-3_15
- Oksanen, A. J., Blanchet, F. G., Friendly, M., Kindt, R., Legendre, P., Mcglinn, D., ... Wagner, H. (2020). *Vegan: Community Ecology Package*. Retrieved from <https://cran.r-project.org/package=vegan>
- Ou, F. S., Michiels, S., Shyr, Y., Adjei, A. A., & Oberg, A. L. (2021). Biomarker Discovery and Validation: Statistical Considerations. *Journal of Thoracic Oncology*, 16(4), 537–545. <https://doi.org/10.1016/j.jtho.2021.01.1616>

- Pan, A. Y. (2021). Statistical analysis of microbiome data: The challenge of sparsity. *Current Opinion in Endocrine and Metabolic Research*, *19*, 35–40. <https://doi.org/10.1016/j.coemr.2021.05.005>
- Pan, Z., Chen, Y., Zhou, M., McAllister, T. A., & Guan, L. L. (2021). Microbial interaction-driven community differences as revealed by network analysis. *Computational and Structural Biotechnology Journal*, *19*, 6000–6008. <https://doi.org/10.1016/j.csbj.2021.10.035>
- Pasalari, H., Gholami, M., Rezaee, A., Esrafil, A., & Farzadkia, M. (2021). Perspectives on microbial community in anaerobic digestion with emphasis on environmental parameters: A systematic review. *Chemosphere*, *270*. <https://doi.org/10.1016/j.chemosphere.2020.128618>
- Patil, S. M., Kurade, M. B., Basak, B., Saha, S., Jang, M., Kim, S.-H., & Jeon, B.-H. (2021). Anaerobic co-digester microbiome during food waste valorization reveals Methanosaeta mediated methanogenesis with improved carbohydrate and lipid metabolism. *Bioresource Technology*, *332*, 125123. <https://doi.org/10.1016/j.biortech.2021.125123>
- Paulson, J. N., Colin Stine, O., Bravo, H. C., & Pop, M. (2013). Differential abundance analysis for microbial marker-gene surveys. *Nature Methods*, *10*(12), 1200–1202. <https://doi.org/10.1038/nmeth.2658>
- Pavi, S., Kramer, L. E., Gomes, L. P., & Miranda, L. A. S. (2017). Biogas production from co-digestion of organic fraction of municipal solid waste and fruit and vegetable waste. *Bioresource Technology*, *228*, 362–367. <https://doi.org/10.1016/j.biortech.2017.01.003>
- Peng, X., Zhang, S. Y., Li, L., Zhao, X., Ma, Y., & Shi, D. (2018). Long-term high-solids anaerobic digestion of food waste: Effects of ammonia on process performance and microbial community. *Bioresource Technology*, *262*(174), 148–158. <https://doi.org/10.1016/j.biortech.2018.04.076>
- Peng, Y., Li, L., Yuan, W., Wu, D., Yang, P., & Peng, X. (2022). Long-term evaluation of the anaerobic co-digestion of food waste and landfill leachate to alleviate ammonia inhibition. *Energy Conversion and Management*, *270*(174). <https://doi.org/10.1016/j.enconman.2022.116195>
- Pielou, E. C. (1966). The measurement of diversity in different types of biological collections. *Journal of Theoretical Biology*, *13*(C), 131–144. [https://doi.org/10.1016/0022-5193\(66\)90013-0](https://doi.org/10.1016/0022-5193(66)90013-0)
- Poirier, S., Bize, A., Bureau, C., Bouchez, T., & Chapleur, O. (2016). Community shifts within anaerobic digestion microbiota facing phenol inhibition: Towards early warning microbial indicators? *Water Research*, *100*, 296–305. <https://doi.org/10.1016/j.watres.2016.05.041>
- Poirier, S., Déjean, S., Midoux, C., Lê Cao, K. A., & Chapleur, O. (2020). Integrating independent microbial studies to build predictive models of anaerobic digestion inhibition by ammonia and phenol. *Bioresource Technology*, *316*(August), 123952. <https://doi.org/10.1016/j.biortech.2020.123952>

- Qiao, W., Takayanagi, K., Li, Q., Shofie, M., Gao, F., Dong, R., & Li, Y. Y. (2016). Thermodynamically enhancing propionic acid degradation by using sulfate as an external electron acceptor in a thermophilic anaerobic membrane reactor. *Water Research*, *106*, 320–329. <https://doi.org/10.1016/j.watres.2016.10.013>
- Quast, C., Pruesse, E., Yilmaz, P., Gerken, J., Schweer, T., Yarza, P., ... Glöckner, F. O. (2013). The SILVA ribosomal RNA gene database project: Improved data processing and web-based tools. *Nucleic Acids Research*, *41*, D590-6. <https://doi.org/10.1093/nar/gks1219>
- Rahman, M. S., Hoque, M. N., Puspo, J. A., Islam, M. R., Das, N., Siddique, M. A., ... Sultana, M. (2021). Microbiome signature and diversity regulates the level of energy production under anaerobic condition. *Scientific Reports*, *11*(1), 1–23. <https://doi.org/10.1038/s41598-021-99104-3>
- Rajagopal, R., Massé, D. I., & Singh, G. (2013). A critical review on inhibition of anaerobic digestion process by excess ammonia. *Bioresource Technology*, *143*, 632–641. <https://doi.org/10.1016/j.biortech.2013.06.030>
- Ramette, A. (2007, November). Multivariate analyses in microbial ecology. *FEMS Microbiology Ecology*, Vol. 62, pp. 142–160. <https://doi.org/10.1111/j.1574-6941.2007.00375.x>
- Rigby, R. A., Stasinopoulos, D. M., & Lane, P. W. (2005). Generalized additive models for location, scale and shape. *Journal of the Royal Statistical Society. Series C: Applied Statistics*, *54*(3), 507–554. <https://doi.org/10.1111/j.1467-9876.2005.00510.x>
- Robinson, M. D., McCarthy, D. J., & Smyth, G. K. (2009). edgeR: A Bioconductor package for differential expression analysis of digital gene expression data. *Bioinformatics*, *26*(1), 139–140. <https://doi.org/10.1093/bioinformatics/btp616>
- Rui, J., Li, J., Zhang, S., Yan, X., Wang, Y., & Li, X. (2015). The core populations and co-occurrence patterns of prokaryotic communities in household biogas digesters. *Biotechnology for Biofuels*, *8*(1), 1–15. <https://doi.org/10.1186/s13068-015-0339-3>
- Ruiz-Sánchez, J., Campanaro, S., Guivernau, M., Fernández, B., & Prenafeta-Boldú, F. X. (2018). Effect of ammonia on the active microbiome and metagenome from stable full-scale digesters. *Bioresource Technology*, *250*, 513–522. <https://doi.org/10.1016/j.biortech.2017.11.068>
- Sánchez-Arias, M., Riojas-Rodríguez, H., Catalán-Vázquez, M., Terrazas-meraz, M. A., & Rosas, I. (2019). Socio-environmental assessment of a landfill using a mixed study design : A case study from México. *Waste Management*, *85*, 42–59. <https://doi.org/10.1016/j.wasman.2018.12.012>
- Seemann, T. (2014). *Genome analysis Prokka: rapid prokaryotic genome annotation*. *30*(14), 2068–2069. <https://doi.org/10.1093/bioinformatics/btu153>

- Segata, N., Izard, J., Waldron, L., Gevers, D., Miropolsky, L., Garrett, W. S., & Huttenhower, C. (2011). Metagenomic biomarker discovery and explanation. *Genome Biology*, *12*(6), R60. <https://doi.org/10.1186/gb-2011-12-6-r60>
- SEMARNAT. (2020). *Diagnóstico Básico para la Gestión Integral de Residuos*. Mexico. Retrieved from <https://www.gob.mx/cms/uploads/attachment/file/554385/DBGIR-15-mayo-2020.pdf>
- Shade, A. (2017). Diversity is the question, not the answer. *ISME Journal*, *11*(1), 1–6. <https://doi.org/10.1038/ismej.2016.118>
- Shamurad, B., Sallis, P., Petropoulos, E., Tabraiz, S., Ospina, C., Leary, P., ... Gray, N. (2020). Stable biogas production from single-stage anaerobic digestion of food waste. *Applied Energy*, *263*(February), 13. <https://doi.org/10.1016/j.apenergy.2020.114609>
- Shi, X., Lin, J., Zuo, J., Li, P., Li, X., & Guo, X. (2017). Effects of free ammonia on volatile fatty acid accumulation and process performance in the anaerobic digestion of two typical bio-wastes. *Journal of Environmental Sciences*, *55*, 49–57. <https://doi.org/10.1016/j.jes.2016.07.006>
- Sieber, J. R., Mcinerney, M. J., & Gunsalus, R. P. (2012). Genomic Insights into Syntrophy : The Paradigm for Anaerobic Metabolic Cooperation. *Annual Review of Microbiology*, *66*(1), 429–452. <https://doi.org/10.1146/annurev-micro-090110-102844>
- Sing, T., Sander, O., Beerenwinkel, N., & Lengauer, T. (2005). ROCr: Visualizing classifier performance in R. *Bioinformatics*, *21*(20). <https://doi.org/10.1093/bioinformatics/bti623>
- Skovmand, L. H., Xu, C. C. Y., Servedio, M. R., Nosil, P., Barrett, R. D. H., & Hendry, A. P. (2018). Keystone Genes. *Trends in Ecology and Evolution*, *33*(9), 689–700. <https://doi.org/10.1016/j.tree.2018.07.002>
- Sun, H., Ni, P., Angelidaki, I., Dong, R., & Wu, S. (2019). Exploring stability indicators for efficient monitoring of anaerobic digestion of pig manure under perturbations. *Waste Management*, *91*, 139–146. <https://doi.org/10.1016/j.wasman.2019.05.008>
- Svensson, K., Paruch, L., Gaby, J. C., & Linjordet, R. (2018). Feeding frequency influences process performance and microbial community composition in anaerobic digesters treating steam exploded food waste. *Bioresource Technology*, *269*, 276–284. <https://doi.org/10.1016/j.biortech.2018.08.096>
- Terzin, M., Laffy, P. W., Robbins, S., Yeoh, Y. K., Frade, P. R., Glasl, B., ... Bourne, D. G. (2024). The road forward to incorporate seawater microbes in predictive reef monitoring. *Environmental Microbiome*, *19*(1), 1–13. <https://doi.org/10.1186/s40793-023-00543-4>
- Tesch, M., Eikmanns, B. J., De Graaf, A. A., & Sahm, H. (1998). Ammonia assimilation in *Corynebacterium glutamicum* and a glutamate dehydrogenase-deficient mutant. *Biotechnology Letters*, *20*(10). <https://doi.org/10.1023/A:1005406126920>

- Theuerl, S., Klang, J., Heiermann, M., Vrieze, J. De, & De Vrieze, J. (2018). Marker microbiome clusters are determined by operational parameters and specific key taxa combinations in anaerobic digestion. *Bioresource Technology*, 263(April), 128–135. <https://doi.org/10.1016/j.biortech.2018.04.111>
- Tian, G., Xi, J., Yeung, M., & Ren, G. (2020). Characteristics and mechanisms of H₂S production in anaerobic digestion of food waste. *Science of the Total Environment*, 724, 137977. <https://doi.org/10.1016/j.scitotenv.2020.137977>
- Tian, H., Fotidis, I. A., Kissas, K., & Angelidaki, I. (2018). Effect of different ammonia sources on acetoclastic and hydrogenotrophic methanogens. *Bioresource Technology*, 250(November 2017), 390–397. <https://doi.org/10.1016/j.biortech.2017.11.081>
- Tonanzi, B., Braguglia, C. M., Gallipoli, A., Montecchio, D., Pagliaccia, P., Rossetti, S., & Gianico, A. (2020). Anaerobic digestion of mixed urban biowaste: The microbial community shift towards stability. *New Biotechnology*, 55(October 2019), 108–117. <https://doi.org/10.1016/j.nbt.2019.10.008>
- Verma, S. C., & Mahadevan, S. (2012). The ChbG gene of the chitobiose (chb) operon of *Escherichia coli* encodes a chitoooligosaccharide deacetylase. *Journal of Bacteriology*, 194(18), 4959–4971. <https://doi.org/10.1128/JB.00533-12>
- Villanueva-Galindo, E., Pérez-Rangel, M., & Moreno-Andrade, I. (2024). Lactic acid production from different sources of organic solid waste: evaluation of the inoculum type and operational optimization. *Biomass Conversion and Biorefinery*. <https://doi.org/10.1007/s13399-024-05563-9>
- Wang, G., Fu, P., Su, Y., Zhang, B., Zhang, M., Li, Q., ... Chen, R. (2024). Comparing the mechanisms of syntrophic volatile fatty acids oxidation and methanogenesis recovery from ammonia stress in regular and biochar-assisted anaerobic digestion: Different roads lead to the same goal. *Journal of Environmental Management*, 352(13), 120041. <https://doi.org/10.1016/j.jenvman.2024.120041>
- Wang, H., Zhu, X., Yan, Q., Zhang, Y., & Angelidaki, I. (2020). Microbial community response to ammonia levels in hydrogen assisted biogas production and upgrading process. *Bioresource Technology*, 296(September 2019), 122276. <https://doi.org/10.1016/j.biortech.2019.122276>
- Wang, P., Wang, H., Qiu, Y., Ren, L., & Jiang, B. (2018). Microbial characteristics in anaerobic digestion process of food waste for methane production—A review. *Bioresource Technology*, 248, 29–36. <https://doi.org/10.1016/j.biortech.2017.06.152>
- Wei, J., Park, T., Wah, Y., & Yu, Z. (2020). The microbiome driving anaerobic digestion and microbial analysis. In *Advances in Bioenergy* (pp. 1–61). <https://doi.org/10.1016/bs.aibe.2020.04.001>
- Wei, T., & Simko, V. (2021). *R package 'corrplot': Visualization of a Correlation Matrix*. Retrieved from <https://github.com/taiyun/corrplot>

- Wickham, H. (2016). *ggplot2: Elegant Graphics for Data Analysis*. In R. Gentleman, K. Hornik, & G. Parmigiani (Eds.), *Springer Nature* (2nd ed., Vol. 16). New York: Springer-Verlag. <https://doi.org/10.1007/978-3-319-24277-4>
- Wijaya, J., Byeon, H., Jung, W., Park, J., & Oh, S. (2023). Machine learning modeling using microbiome data reveal microbial indicator for oil-contaminated groundwater. *Journal of Water Process Engineering*, 53(January), 103610. <https://doi.org/10.1016/j.jwpe.2023.103610>
- Wingett, S. W., & Andrews, S. (2018). Fastq screen: A tool for multi-genome mapping and quality control. *F1000Research*, 7(0), 1–13. <https://doi.org/10.12688/f1000research.15931.1>
- World Biogas Association. (2021). *Biogas: Pathways to 2030 - Report*. Retrieved from <https://www.worldbiogasassociation.org/biogas-pathways-to-2030-report/>
- Wu, D., Li, L., Peng, Y., Yang, P., Peng, X., Sun, Y., & Wang, X. (2021). State indicators of anaerobic digestion: A critical review on process monitoring and diagnosis. *Renewable and Sustainable Energy Reviews*, 148, 111260. <https://doi.org/10.1016/j.rser.2021.111260>
- Wu, D., Li, L., Zhao, X., Peng, Y., Yang, P., & Peng, X. (2019). Anaerobic digestion: A review on process monitoring. *Renewable and Sustainable Energy Reviews*, 103, 1–12. <https://doi.org/10.1016/j.rser.2018.12.039>
- Wu, D., Li, L., Zhen, F., Liu, H., Xiao, F., Sun, Y., ... Wang, X. (2022). Thermodynamics of volatile fatty acid degradation during anaerobic digestion under organic overload stress: The potential to better identify process stability. *Water Research*, 214(2). <https://doi.org/10.1016/j.watres.2022.118187>
- Wu, D., Liu, H., Xing, T., Xiao, F., Liu, Y., Zhen, F., & Sun, Y. (2024). An integrated evaluation strategy for anaerobic digestion monitoring based on acid-base balance and thermodynamics of volatile fatty acid degradation. *Chemical Engineering Journal*, 486(December 2023). <https://doi.org/10.1016/j.cej.2024.150340>
- Xing, B. S., Han, Y., Wang, X. C., Cao, S., Wen, J., & Zhang, K. (2020). Acclimatization of anaerobic sludge with cow manure and realization of high-rate food waste digestion for biogas production. *Bioresour Technol*, 315, 123830. <https://doi.org/10.1016/j.biortech.2020.123830>
- Xu, F., Li, Y. Y., Ge, X., Yang, L., & Li, Y. Y. (2018). Anaerobic digestion of food waste – Challenges and opportunities. *Bioresour Technol*, 247, 1047–1058. <https://doi.org/10.1016/j.biortech.2017.09.020>
- Xu, J., Shi, Z., Xu, L., Zheng, X., Zong, Y., Luo, G., ... Xie, L. (2024). Recovery capability of anaerobic digestion from ammonia stress: Metabolic activity, energy generation, and genome-centric metagenomics. *Bioresour Technol*, 394(October 2023), 130203. <https://doi.org/10.1016/j.biortech.2023.130203>

- Xu, R., Yang, Z. H., Zheng, Y., Liu, J. B., Xiong, W. P., Zhang, Y. R., ... Fan, C. Z. (2018). Organic loading rate and hydraulic retention time shape distinct ecological networks of anaerobic digestion related microbiome. *Bioresource Technology*, 262(March), 184–193. <https://doi.org/10.1016/j.biortech.2018.04.083>
- Yan, M., Fotidis, I. A., Tian, H., Khoshnevisan, B., Treu, L., Tsapekos, P., & Angelidaki, I. (2019). Acclimatization contributes to stable anaerobic digestion of organic fraction of municipal solid waste under extreme ammonia levels: Focusing on microbial community dynamics. *Bioresource Technology*, 286(April), 121376. <https://doi.org/10.1016/j.biortech.2019.121376>
- Yan, M., Treu, L., Campanaro, S., Tian, H., Zhu, X., Khoshnevisan, B., ... Fotidis, I. A. (2020). Effect of ammonia on anaerobic digestion of municipal solid waste: Inhibitory performance, bioaugmentation and microbiome functional reconstruction. *Chemical Engineering Journal*, 401. <https://doi.org/10.1016/j.cej.2020.126159>
- Yu, D., Wang, T., Liang, Y., Liu, J., Zheng, J., Chen, M., & Wei, Y. (2021). Delivery and effects of proton pump inhibitor on anaerobic digestion of food and kitchen waste under ammonia stress. *Journal of Hazardous Materials*, 416(April), 126211. <https://doi.org/10.1016/j.jhazmat.2021.126211>
- Yu, D., Zhang, J., Chulu, B., Yang, M., Nopens, I., & Wei, Y. (2020). Ammonia stress decreased biomarker genes of acetoclastic methanogenesis and second peak of production rates during anaerobic digestion of swine manure. *Bioresource Technology*, 317(June), 124012. <https://doi.org/10.1016/j.biortech.2020.124012>
- Zamanzadeh, M., Hagen, L. H., Svensson, K., Linjordet, R., & Horn, S. J. (2016). Anaerobic digestion of food waste - Effect of recirculation and temperature on performance and microbiology. *Water Research*, 96, 246–254. <https://doi.org/10.1016/j.watres.2016.03.058>
- Zhang, Hong, Peng, Y., Yang, P., Wang, X., Peng, X., & Li, L. (2020). Response of process performance and microbial community to ammonia stress in series batch experiments. *Bioresource Technology*, 314(174), 123768. <https://doi.org/10.1016/j.biortech.2020.123768>
- Zhang, Hong, Yuan, W., Dong, Q., Wu, D., Yang, P., Peng, Y., ... Peng, X. (2022). Integrated multi-omics analyses reveal the key microbial phylotypes affecting anaerobic digestion performance under ammonia stress. *Water Research*, 213. <https://doi.org/10.1016/j.watres.2022.118152>
- Zhang, Huimin, Elolimy, A. A., Akbar, H., Thanh, L. P., Yang, Z., & Looor, J. J. (2022). Association of residual feed intake with peripartal ruminal microbiome and milk fatty acid composition during early lactation in Holstein dairy cows. *Journal of Dairy Science*, 105(6). <https://doi.org/10.3168/jds.2021-21454>
- Zhang, Le, Loh, K. C., & Zhang, J. (2018). Food waste enhanced anaerobic digestion of biologically pretreated yard waste: Analysis of cellulose crystallinity and microbial

- communities. *Waste Management*, 79, 109–119. <https://doi.org/10.1016/j.wasman.2018.07.036>
- Zhang, Liang, Guo, K., Wang, L., Xu, R., Lu, D., & Zhou, Y. (2022). Effect of sludge retention time on microbial succession and assembly in thermal hydrolysis pretreated sludge digesters: Deterministic versus stochastic processes. *Water Research*, 209(November 2021), 117900. <https://doi.org/10.1016/j.watres.2021.117900>
- Zhang, W., Chen, B., Li, A., Zhang, L., Li, R., Yang, T., & Xing, W. (2019). Mechanism of process imbalance of long-term anaerobic digestion of food waste and role of trace elements in maintaining anaerobic process stability. *Bioresource Technology*, 275, 172–182. <https://doi.org/10.1016/j.biortech.2018.12.052>
- Zhang, W., Li, L., Xing, W., Chen, B., Zhang, L., Li, A., ... Yang, T. (2019). Dynamic behaviors of batch anaerobic systems of food waste for methane production under different organic loads, substrate to inoculum ratios and initial pH. *Journal of Bioscience and Bioengineering*, 128(6), 733–743. <https://doi.org/10.1016/j.jbiosc.2019.05.013>
- Zhang, X., Jonassen, I., & Goksoyr, A. (2021). *Machine Learning Approaches for Biomarker Discovery Using Gene Expression Data* (Vol. 4; H. I. Nakaya, Ed.). Exon Publications. <https://doi.org/10.36255/exonpublications.bioinformatics.2021>
- Zhang, Y., Guo, B., Zhang, L., & Liu, Y. (2020). Key syntrophic partnerships identified in a granular activated carbon amended UASB treating municipal sewage under low temperature conditions. *Bioresource Technology*, 312(February), 123556. <https://doi.org/10.1016/j.biortech.2020.123556>
- Zhao, D., Yan, B., Liu, C., Yao, B., Luo, L., Yang, Y., ... Zhou, Y. (2021). Mitigation of acidogenic product inhibition and elevated mass transfer by biochar during anaerobic digestion of food waste. *Bioresource Technology*, 338(July), 125531. <https://doi.org/10.1016/j.biortech.2021.125531>
- Zhu, X., Campanaro, S., Treu, L., Seshadri, R., Ivanova, N., Kougias, P. G., ... Angelidaki, I. (2020). Metabolic dependencies govern microbial syntrophies during methanogenesis in an anaerobic digestion ecosystem. *Microbiome*, 8(1), 1–14. <https://doi.org/10.1186/s40168-019-0780-9>
- Ziganshin, A. M., Liebetrau, J., Pröter, J., & Kleinstaub, S. (2013). Microbial community structure and dynamics during anaerobic digestion of various agricultural waste materials. *Applied Microbiology and Biotechnology*, 97, 5161–5174. <https://doi.org/10.1007/s00253-013-4867-0>